Formulation of Targeted Drug-Loaded Nanoparticles for Lung Cancer Therapy

Muhammad Taufiq Bin Mohd Jailani

Strathclyde Institute of Pharmacy & Biomedical Sciences

A thesis submitted to the University of Strathclyde in part fulfilment of the regulations for the degree of Doctor of Philosophy.

2020

Copyright Declaration

Signed:

Date: 25th of August 2020

Acknowledgements

I would like to express my thanks and eternal gratitude to my wife Fairuz and family who supported me through this endeavour, physically and mentally.

I would also like to express my appreciation to the staff of Pharmacy Department, Hospital Teluk Intan for nurturing the pharmacist in me.

This thesis is dedicated to my daughters Afiya and Alanna. May this inspire you for greatness in your lives.

Abstract

The use of combination chemotherapy for treatment of lung cancer has been proven to be more effective than single-agent therapy. Such combination, when used in conjunction with nanoparticle carriers has the potential to effectively deliver the therapeutic payload to the cancer sites with minimal side effects. Small scale production method of liposome in laboratory setting such as thin film hydration requires post-processing steps to achieve desired physical characteristics and upscaling such method would prove to be economically unfeasible. Laboratory scale liposome purification methods such as dialysis and ultracentrifugation also suffer from similar limitation in upscaling. These challenges need to be overcame to streamline liposome production from laboratory to commercial scale whilst maintaining the desired liposome characteristics. In this study, liposomal formulations with varying molar ratio of 1,2-Distearoyl-sn-glycero-3-phosphocholine, 1,2-Dipalmitoyl-sn-glycero-3-phosphocholine, 1,2-Distearoyl-sn-glycero-3-phospho-rac-(1-glycerol) and cholesterol were fabricated using microfluidics technique with staggered herringbone mixer. Desired liposomal formulations were obtained by manipulating fabrication characteristics such as total flow rate (TFR) and aqueous-to-lipid flow rate ratio. Selected stable liposomal formulations were then subjected to entrapment of cisplatin and irinotecan, filter centrifugation and tangential flow filtration (TFF) methods, scale-up fabrication process, entrapment efficiency and release studies, lyophilisation and in vitro assay against A549 cells. It was also observed that these stable liposome formulations are suitable for entrapment of both cisplatin and irinotecan and demonstrated higher cytotoxicity against A549 cancer cells in comparison with their free drug counterparts. TFF method was found to be more effective in purification and

concentrating large volume of liposomal suspension. Scaling up fabrication volume exhibited no significant impact on the physical characteristics, entrapment efficiency and entrapped material release characteristics of the liposomes. The results of this study demonstrated the feasibility, scalability and modularity of dual-loaded irinotecan and cisplatin in a liposomal system and also its higher efficacy against A549 cancer cells, paving the way for the use of this liposomal system for lung cancer therapy.

Contents

List of Figures

List of Tables

Abbreviations

9NC	9-nitrocamptothecin
ABS	acrylonitrile butadiene styrene
AFM	atomic force microscopy
CDDP	cisplatin
CHEMS	cholesteryl hemisuccinate
COPD	chronic obstructive pulmonary disease
CPT-11	irinotecan
DCP	dihexadecyl phosphate
DLS	dynamic light scattering
DMPC	dimyristoylphosphatidylcholine
DMSO	dimethyl sulfoxide
DOPE	dioleoylphosphatidylethanolamine
DOTAP	1,2-dioleoyl-3-trimethylammonium-propane
DPPC	1,2-dipalmitoyl-*sn*-glycero-3-phosphatidylcholine

DSPC	1,2-distearoyl-*sn*-glycero-3-phosphatidylcholine
DSPE-PEG_{2000}	distearoylphosphatidylethanolamine-polyethyleneglycol 2000
DSPG	1,2-distearoyl-*sn*-glycero-3-phosphatidylglycerol
EC	etoposide/cisplatin
ED	extensive-stage disease
EGFR	epidermal growth factor receptor
ESEM	environmental scanning electron microscopy
FD	freeze-drying
FRR	flow rate ratio
IC_{50}	half maximal inhibitory concentration
ICD-10	International Statistical Classification of Diseases and Related Health Problems 10th Revision
ICP-MS	inductively coupled plasma mass spectrometry
λ_d	detection wavelength
LD	limited-stage disease
ML	folate-PEG_{2000}-PEG_{5000} liposome

MLV	multilamellar vesicles
MMAD	mass median aerodynamic diameter
MTT	3-(4,5-dimethylthiazol-2-yl)-2,5-diphenyltetrazolium bromide
NL	non-targeted liposome
NMWL	nominal molecular weight limit
NS	normal saline
NSCLC	non-small cell lung cancer
PBS	phosphate-buffered saline
PDI	polydispersity index
PE	phosphatidylethanolamine
PEG	polyethylene glycol
RES	reticuloendothelial system
RT	room temperature
SCLC	small cell lung cancer
SD	standard deviation
SEARO	South East Asia Region

SEM	scanning electron microscopy
SL	non-targeted PEGylated liposome
SLIT	Sustained Release Lipid Inhalation Targeting
T_c	collapse temperature
TEA	triethanolamine
TEM	tunnelling electron microscopy
Tf	transferrin
TFF	tangential flow filtration
TFR	total flow rate
TfR	transferrin receptor
T_g	glass transition temperature
VEGF	vascular endothelial growth factor
WHO	World Health Organisation
WPRO	Western Pacific Region

Chapter 1

General Introduction

1.1 Introduction to lung cancer

Neoplasms, from the Greek word νεοπλάσμα, (neo – new) and (plasma – creation) is a general term for abnormal growth of tissue. This abnormal growth is generally categorized into malignant neoplasm (also widely known as cancer) and benign neoplasm (also known as benign tumour). According to International Statistical Classification of Diseases and Related Health Problems 10th Revision (ICD-10) Version 2015, lung cancer falls under the category of malignant neoplasms of respiratory and intrathoracic organs (C30-C39). This category covers from cancer in the area of nasal cavity and middle ear to ill-defined sites of the respiratory system and intrathoracic organs (World Health Organization, 1992)

1.1.1 Epidemiology

Lung cancer continues to be the most common malignancy for several decades. Current estimate made by GLOBOCAN 2012 placed lung cancer as the most common type of cancer affecting nearly 1.83 million people worldwide with mortality incidence of nearly 1.6 million. While mortality figure has dropped in more developed regions, defined as all regions of Europe plus Northern America, Australia/New Zealand and Japan (627,000 compared with 933,000 in the previous 5 years), it is relatively unchanged in less developed regions, defined as all regions of Africa, Asia (excluding Japan), Latin America and the Caribbean, Melanesia, Micronesia and Polynesia (963,000 compared with 960,000 in the previous 5 years). Significantly more cases are documented in less developed region (1.07 million) than more developed region (758,000) (Ferlay et al., 2013).

It is also documented that lung cancer is the most common cause of mortality from malignancy, accounting for 19.4% (1.59 million) deaths from cancer. In World Health Organisation (WHO) South East Asia Region (SEARO), mortality to incidence ratio is very high at 0.9 (0.03 higher than the worldwide mortality to incidence ratio of lung cancer) and the number of mortalities has increased 43.3% compared to the past 5 years. In WHO Western Pacific Region (WPRO), there is a slight decrease (4.4%) of deaths due to lung cancer compared with previous 5 years. However, mortality to incidence ratio is still among the highest at 0.89, up 0.02 from the overall ratio. In both SEARO and WPRO regions, much higher incidence of lung cancer is detected in males, comprising about 71.6% and 70% respectively (Ferlay et al., 2013). This can be attributed to high use of cigarettes within these two regions which accounts for 56% of total world cigarettes consumption in 2009. From this number, 40% or more males within these regions are smokers (Eriksen, Mackay, & Ross, 2012).

Lung cancer is the third highest number of documented cancer incidence in Malaysia with 4403 documented cases in 2012 after breast and colorectal cancer (Ferlay et al., 2013). It contributed to nearly one-fifth of overall cancer death in Malaysia with very high mortality to incidence ratio of 0.94 (0.07 higher than worldwide mortality to incidence ratio of lung cancer). Higher percentage of lung cancer is also detected in males, comprising of 73.6% from overall lung cancer cases in Malaysia. This figure is significantly higher than worldwide percentage of lung cancer in males, which is 68% from overall lung cancer cases (Ferlay et al., 2013).

1.1.2 Risk factors

The most common risk factor for lung cancer is smoking (Jemal et al., 2011; Siegel, Naishadham, & Jemal, 2013). Exposure to environment tobacco smoke or most

commonly known as second hand smoking is also a by-product of smoking. A meta-analysis study indicated that there is a notable increase in lung cancer risk among people exposed to second hand smoke (Stayner et al., 2007). Multiple carcinogenic agents found in cigarette and tobacco smoke have been linked to lung cancer in humans (Cogliano et al., 2011).

This is a serious public health issue, especially in developing countries or less developed countries. Cigarette consumption in Western Pacific region accounts for 48% of total world consumption in 2009 (Eriksen et al., 2012). In Malaysia, 23.1% of overall adult population smoked tobacco products. From this number, 43.9% of them are males, which is at least 40 times more than females that are currently smoking (1.0%). 20.9% of overall adult population smoked tobacco on daily basis while only 9.5% from them had quit (Institute for Public Health, 2011). This translates to higher degree of exposure to second hand smoke, which caused 162,300 deaths in 2004. Smoking rate among boys aged 13-15 years old is also worryingly high at 36.3% (Eriksen et al., 2012). A UK study in 2013 strongly associated current smoking behaviour of lung cancer patients with an early death (O'Dowd et al., 2014).

It is also documented that lung diseases, such as chronic obstructive pulmonary disease (COPD), emphysema, chronic bronchitis, pneumonia and tuberculosis can be associated with lung cancer risk (Brenner, McLaughlin, & Hung, 2011). There is also evidence that inflammatory process plays a major role in development of lung cancer. People with high level of C-reactive protein which is an inflammation marker are more likely to be associated with higher level of lung cancer risk (Engels, 2008). Environmental and domestic factors also play a role in elevating the risk of having lung cancer. Case study in China associated the use of unventilated coal stove indoor

and cooking oil smoke produced by heating to high temperatures in open woks with higher incidence of lung cancer in non-smoking females (Thun et al., 2008).

1.1.3 Types and pathophysiology

According to WHO, lung cancer is defined into four major types: adenocarcinoma, squamous cell carcinoma, large cell carcinoma and small cell lung cancer (SCLC). Other than SCLC, malignancies of the lung are collectively known as non-small cell lung cancer (NSCLC) (Travis, Brambilla, Muller-Hermelink, & Harris, 2004). NSCLC accounts for 85% of the total lung cancer cases while SCLC makes up the minority at 15%. Among NSCLC, adenocarcinoma is the highest reported type of lung cancer reported at 38.5% of total lung cancer cases, far surpassing squamous cell carcinoma and large cell carcinoma at 20% and 2.9% of total lung cancer cases reported respectively (Dela Cruz, Tanoue, & Matthay, 2011).

Most cases of adenocarcinoma are found among smokers. However, it is also more frequently found lung carcinoma type among non-smokers and women in particular. Adenocarcinomas are commonly found as peripheral nodules (Fig. 1.1). It is also found, albeit less frequently, at central lung as hilar or perihilar masses. As this type of tumour manifests more frequently at peripheral lung, more involvement of pleura and chest wall is expected, and this is seen in about 15% of the cases which is more than any other lung carcinomas. There are several localisation patterns of adenocarcinoma. It can arise as a central or endobronchial tumour. In this pattern, it can form a plaque or polypoid growth with retention of the overlying mucosa. As it progresses further down the bronchiole, the growth will obstruct the lumen of the bronchiole itself. Another pattern of the carcinoma is that it manifests as diffuse pneumonia-like consolidation involving all lobes of the lung. In this case, it is often

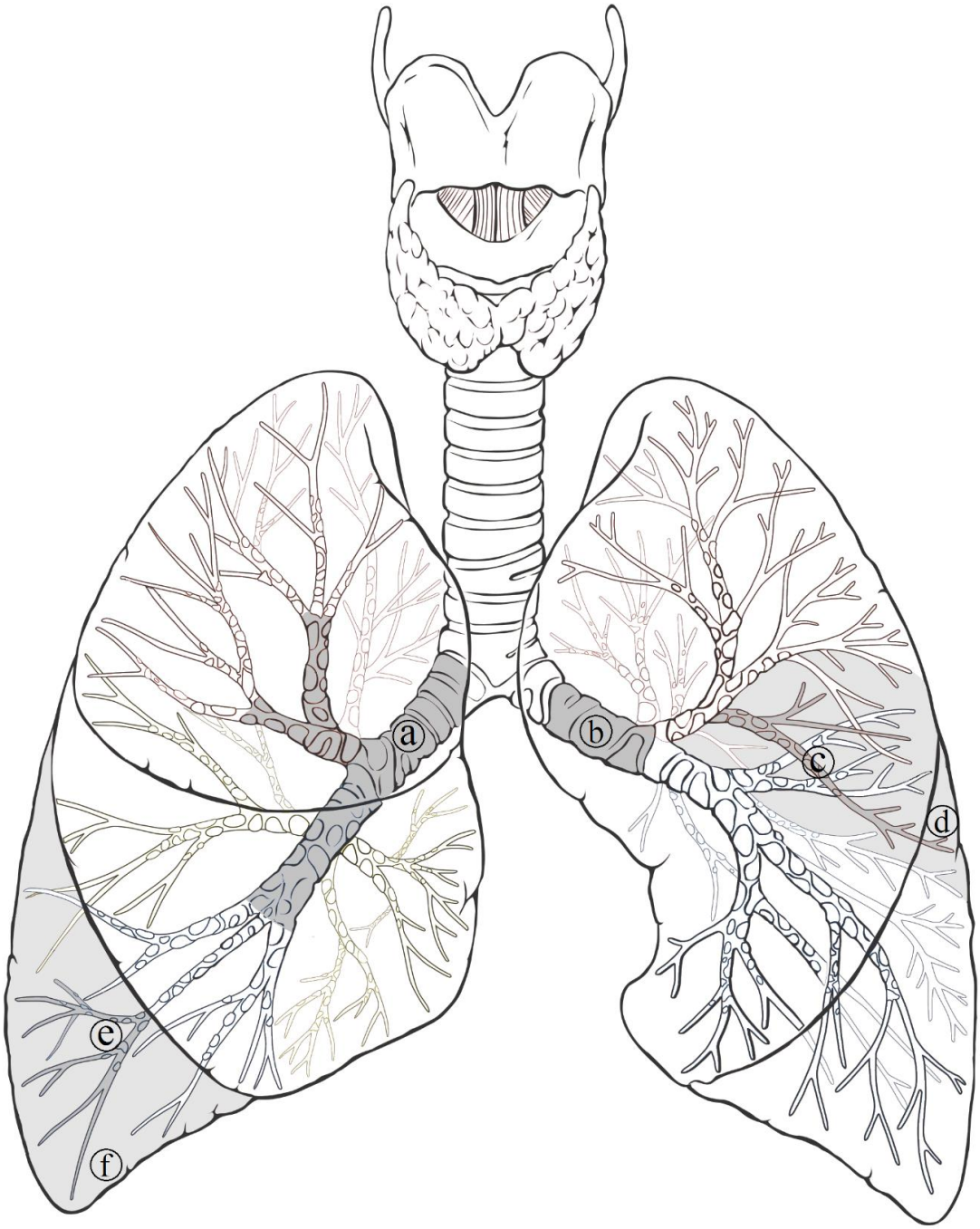

Figure 1.1 Cancer localisation sites in the lung. Squamous cell cancer is commonly originated from central lung site (a), with the minority of adenocarcinoma and large cell carcinoma cases arising from this site. SCLC arises primarily from bronchus (b), with submucosal spread along the bronchi with resultant circumferential compression. Majority of large cell carcinoma and adenocarcinoma originate from peripheral lung site (c), with involvement of pleura (d) and chest wall for the latter. Invasion of pleura by intrabronchiolar squamous cell carcinomas may lead to involvement of diaphragm and chest wall (f).

associated with bronchioalveolar or papillary tumour. As with other tumours, adenocarcinoma spreads commonly via lymphatic and haematogenous routes. In bronchioalveolar adenocarcinoma however, aerogenous spread is also found which is responsible for the growth of the tumour throughout the airways distant from the main growth site. This process of dissemination can account for the spread of adenocarcinoma in the same lobe or even in different lobes (Travis et al., 2004).

More than 90% of squamous cell carcinomas occur in smokers. Exposure to arsenic is also strongly associated with this type of carcinoma (Travis et al., 2004). This tumour can arise at both central and peripheral lung sites. The majority of this tumour is found at central lung which is about two-thirds of the presentation (Fig. 1.1). The rest of the carcinoma cases commonly presented at the peripheral lung. Recent evidence points towards an increase of the tumour presented at the lung periphery and in some cases more than 50%. This type of carcinoma is most commonly found at segmental bronchi and can also affect lobar and mainstem bronchus (Travis, 2011). Squamous cell carcinomas in major bronchi have been found to spread intraepithelial in two distinct patterns which are the “creeping type” and the “penetrating type”. The former spread laterally along the surface epithelium which is responsible for the bronchial mucosa while the latter form small polypoid mucosal lesion with evidence of downward spread of the tumour. In peripheral squamous cell carcinoma, the tumour form either solid intrabronchiolar nodule or intraepithelial extension or both. Advanced stage of the disease may involve chest wall or diaphragm by the invasion of the tumour cells through the pleura (Travis et al., 2004).

Large cell carcinoma is the less common type of tumour in the classification of NSCLC. In most of the cases it is found in the peripheral lung (Fig. 1.1), although this

tumour is also known to develop from central lung site (Travis, 2011). In peripheral lung site, involvement of pleura and chest wall is common (Travis et al., 2004). Under examination, this tumour presents as large necrotic mass. Distinguishing large cell carcinomas from other types of lung cancer is done by excluding any presence of squamous cell or glandular differentiation (Travis, 2011).

The majority of small cell lung carcinomas present as perihilar mass. This type of carcinoma typically arises from peribronchial site with involvement of bronchial submucosa and peribronchial tissue (Fig. 1.1). Bronchial obstruction can occur as the result of circumferential compression of the bronchus (Travis, 2011). This is due to the spread of tumour along the submucosal layer of the bronchi (Travis et al., 2004). Extensive metastases of lymph node are commonly found in this type of tumour. In these cases, extensive necrosis is also found within the tumour mass itself. In advanced stage of this type of tumour, the bronchial lumen itself can be compressed and blocked by tumour mass in the lymph node pressing on the bronchus (Travis, 2011).

WHO introduced a newer classification of lung tumours in 2015 (Travis et al., 2015) that afforded a greater emphasis on immunohistochemistry and oncogenic expression of the tumours, leading to changes in the original classification of some of the tumours from the 2004 version (Travis et al., 2004).

Utilising immunohistochemistry allows reclassification of poorly differentiated carcinoma under light microscopy. Carcinoma expressing TTF-1 and/or Napsin A markers are diagnosed as solid adenocarcinoma (Travis et al., 2015) while those expressing markers such as p40, CK5/6 and p63 (Bishop et al., 2012) can be classified under non-keratinising squamous cell carcinoma.

Comprehensive molecular profiles of lung cancer identified by The Cancer Genome Atlas have been useful in determining the genetic mutations commonly occurring in certain subtypes of lung carcinoma. Adenocarcinoma, for example, has been found to have 18 statistically significant genetic mutations including but not limited to *TP53*, *KRAS*, *KEAP1*, *STK11* and epidermal growth factor receptor (*EGFR*) (Collisson et al., 2014). Squamous cell carcinoma on the other hand has demonstrated 11 statistically significant genetic mutations including but not limited to *TP53*, *CDKN2A*, *PTEN*, *PIK3CA* and *KEAP* (Hammerman et al., 2012). These findings are pertinent for development of anti-cancer agents targeting specifically for these genetic mutations to improve efficacy whilst simultaneously mitigate side-effects commonly associated with chemotherapy.

1.1.4 Conventional treatment modalities

Different staging systems are used in SCLC and NSCLC. In SCLC, there are two stages which are limited-stage disease (LD) and extensive-stage disease (ED). The use of chemotherapy is the mainstay for both stages. The addition of radiation therapy to chemotherapy during LD improves overall survival rate. Combinations of chemotherapy agents during ED are correlated with higher response rate to the treatment. However, it does not improve the survival odds. About one in every three patients diagnosed with SCLC present with LD. At this stage, higher response can be expected to the treatment which is using combination chemotherapy. The majority of the patients, however, present with ED which put the median survival between 8-20 months, depending whether the disease has reached metastatic stage or not. Refusal of treatment in metastatic disease has even more dire consequences with median survival of 5 weeks (Kurup & Hanna, 2004). Evidence has shown that four to six cycles of

etoposide/cisplatin (EC) combination remains the most effective for first-line treatment of both LD and ED with complete response rate over 20% in non-Asian, fit and ED patients. In Asian patients, however, the same response rate can be seen with the chemotherapy combination of irinotecan and cisplatin with the same number of treatment cycles. The use of irinotecan in the combination chemotherapy is advantageous in term of less severe anaemia, neutropenia and thrombocytopenia while also causing more severe vomiting and diarrhoea (Xu et al., 2018). Data from meta-analyses demonstrate that by using carboplatin in lieu of cisplatin in EC, survival rate is not affected but it is an option for oncologists when patients can no longer tolerate side-effects of cisplatin (van Meerbeeck, Fennell, & De Ruysscher, 2011).

Staging system for primary tumour of NSCLC starts from occult carcinoma up to stage IV which consists of primary tumour plus metastases to regional lymph nodes and distant sites. Several treatments options exist for NSCLC which are surgical resection, chemotherapy and radiotherapy. These options are available to the patients depending on the size, location of the tumour and also whether the tumour had metastasized (Goldstraw et al., 2011). Chemotherapy remains to be the main treatment modality for NSCLC. Clinical guidelines recommend the use of platinum-based doublet for fit patients. The most common agents used in this combination are cisplatin/gemcitabine and cisplatin/pemetrexed. Recent evidence pointed out the advantage of selection of therapy based on histologic subtype (Scagliotti et al., 2009). Patients suffering from non-squamous cancers benefit better from the use of cisplatin/pemetrexed combination (median survival of 11.8 months) compared with patients with squamous cancer (median survival of 9.8 months). Therefore cisplatin/gemcitabine combination is preferred in patient with squamous cancer

(median survival of 10.8 months) (Scagliotti et al., 2009). Growing interest in molecularly targeted drugs has yielded several new chemotherapy agents. One of such agents, bevacizumab, has shown promise in showing better survival rate when used in combination with paclitaxel/carboplatin for patients with non-squamous carcinoma (median survival of 12.3 months) (Sandler et al., 2006). Conventional treatment guidelines for first-line chemotherapy recommend a maximum of 6 cycles due to debilitating side effects of platinum-based doublet. Recent data from clinical trial focusing on the use of pemetrexed as single agent maintenance therapy in stable or responsive non-squamous NSCLC patients after undergoing four cycles of platinum-based doublet chemotherapy showed significant improvement in survival rates (median survival of 15.5 months) with less side effects which are commonly associated with the full 6 cycles of platinum-based doublet chemotherapy (Ciuleanu et al., 2009).

The usage of platinum-based chemotherapy agents such as cisplatin, carboplatin and oxaliplatin is quite common for cancer treatment in Malaysia. The average dose per treatment cycle for them is 130 mg, 500 mg, and 150 mg respectively. Carboplatin is the most widely used, in term of total dosage/1000 population, with 0.720 in 2009 and increasing to 2.015 in 2010 followed by cisplatin with 0.125 in 2009 and increasing to 0.259 in 2010 (Pharmaceutical Services Division and Clinical Research Centre Ministry of Health Malaysia, 2014). Oxaliplatin is the least used with 0.142 total dosage/1000 population in 2009 and decreasing to 0.053 in 2010. There is not much difference between public sector usage of cisplatin between the year 2009 and 2010 (0.098 and 0.093 respectively, in term of total dosage/1000 population). However, marked increase can be seen in private sector usage of cisplatin and carboplatin between the same years (0.138 increment for cisplatin and 1.59 increment

for carboplatin, in term of total dosage/1000 population). This can be attributed to their departure from oxaliplatin usage which showed a sharp drop to 0.001 total dosage/1000 population in 2010 from 0.101 in the previous year. The usage of irinotecan is much less compared to the platinum-based agents. The average dose per treatment is 310 mg with a slight increase in usage in 2010 compared with 2009 (0.034 total dosage/1000 population and 0.022 respectively) (Pharmaceutical Services Division and Clinical Research Centre Ministry of Health Malaysia, 2014).

As with other chemotherapy agents, cost can be one of the limitations of their usage. Average price of drug dose per treatment cycle is manageable for cisplatin and carboplatin at MYR188.50 and MYR401.11 respectively while both oxaliplatin and irinotecan are comparably higher at MYR4000.05 and MYR4820.5 respectively (Pharmaceutical Service Division Ministry of Health Malaysia, 2015). This might contribute to their usage limitation even though they can be more effective with less side effects compared with their older counterparts.

1.2 Current treatment approach to lung cancer

In the recent decade, several new anti-cancer agents have been approved to be used for chemotherapy. The introduction of new agents coupled with revised chemotherapy cycle tailored to specific patients based on histological screening improved lung cancer survival rate over the years. These new agents, ranging from analogues of conventional chemotherapy agent such as topotecan to molecularly targeted agents such as EGFR inhibitors (gefitinib) and vascular endothelial growth factor (VEGF) inhibitors (bevacizumab) share most of the common problems plaguing the conventional chemotherapy, including adverse reactions which limit the

effectiveness of the chemotherapy itself due to deterioration of patient's quality of life (Ramalingam, Owonikoko, & Khuri, 2011).

To alleviate these problems and to some extent overcome them altogether, developments in the field of controlled and targeted release mechanisms have been pursued. Some of the products of these developments have shown good promise during in vitro testing in effectively delivering the anti-cancer drugs directly to the cancer site either by active or passive targeting mechanism while incorporating a minuscule amount of the drugs in the delivery system itself, thus reducing the side-effects of the drugs (Mura, Bui, Couvreur, & Nicolas, 2015). This method of drug delivery is not only developed to be utilized in lung cancer therapy, but also have been adapted for other kinds of drugs such as intravenous liposomal cisplatin (LipoPlatin®). This strategy mitigates the side-effects of cisplatin which hamper the therapeutic objectives because treatment has to be stopped due to decreasing patient's quality of life.

1.2.1 Entrapment of anti-cancer drugs

Entrapment of drugs in liposomes has been done over several decades involving hundreds of antimicrobials, peptide hormones, anti-cancer and many other therapeutic agents (Bulbake, Doppalapudi, Kommineni, & Khan, 2017; Tiwari et al., 2012). The biocompatibility and the flexible nature of liposomes have been useful in producing various drug-loaded derivatives of liposomes with desirable characteristics. Since its discovery in 1965, liposomes have been used in numerous drug delivery systems such as Doxil® (liposomal doxorubicin), DaunoXome® (liposomal daunorubicin) and MiKasome® (liposomal amikacin). Both in vitro and in vivo applications have shown remarkable results in enhancing therapeutic efficacy due to passive accumulation of the drug at the target site, active targeting by ligand

attachment, improved bioavailability to the target site by incorporating stealth ligands to the particle surface and minimisation of drug toxicity by low systemic exposure to the drug (Samad, Sultana, & Aqil, 2007).

Delivery of anti-cancer drug via inhalation has been explored by using cisplatin entrapped in liposomes for treatment of patient with lung carcinoma. Findings of the experiment are very promising with the drug well tolerated by patients, no evidence of common toxicities of cisplatin and very low platinum level found in plasma. 12 patients out of 17 enrolled in the trial had their tumour stabilized after the treatment (Wittgen et al., 2007). Other study evaluated the delivery and safety of inhaled liposomal 9-nitrocamptothecin (9NC) found that 3 out of the 6 patients suffering from lung cancer enrolled in the trial demonstrated tumour stabilisation. No haematological toxicity is found in all of the test subjects throughout the study even though plasma levels of 9NC detected in the subjects are the same as observed in oral delivery of the drug (Verschraegen et al., 2004).

There are several novel formulations of liposomal cisplatin that can be explored and used within the scope of this project. The most favourable among these is by using combination of 1,2-distearoyl-*sn*-glycero-3-phosphatidylcholine (DSPC), 1,2-dipalmitoyl-*sn*-glycero-3-phosphatidylcholine (DPPC), 1,2-distearoyl-*sn*-glycero-3-phosphatidylglycerol (DSPG) and cholesterol (Tardi et al., 2009). Current evidence suggests that the combination of these phospholipids in molar ratio of 35:35:20:10 produced liposomes with mean diameter of 110 nm, suitable to be used for entrapment of both cisplatin and irinotecan and maintained drug entrapment at ~98% in storage of -20°C (Tardi et al., 2009). Entrapment of cisplatin is achieved by heating the mixture of drug and empty liposomes solution to 60°C for 1 h in the presence of ethanol to

enhance cisplatin uptake. Entrapment of irinotecan using this method requires the lipids to be dissolved in 10 mM sodium gluconate/150 mM triethanolamine (TEA) in pH 7 as the TEA will be entrapped inside the liposomes first. Drug entrapment is then achieved by charge neutral exchange process with the TEA inside the liposomes (Dicko, Tardi, Xie, & Mayer, 2007). While this study mentions the percentage of drug entrapment after storage, it does not mention the entrapment efficiency of the liposomal cisplatin or irinotecan. Further study should be conducted to determine this parameter as it will determine the overall cost-effectiveness of the formulation.

Another formulation of liposomal cisplatin requires the simple combination of phosphatidylethanolamine (PE) and cholesterol with weight ratio of 1.6:0.4 (Hwang, Lee, Hua, & Fang, 2007). The formulation employs thin film hydration method with the addition of deoxycholic acid to stabilize the PE bilayers. Cisplatin liposomes produced with this formulation have mean size of 95.6 nm and zeta (ζ) potential of -54.9 mV. More importantly, the entrapment efficiency is fairly high at 70%. The in vitro cisplatin release profile of the liposomes is significantly lower than control sample albeit the release itself is stable over a prolonged period of time with no initial burst release. Cytotoxicity assay performed with this liposomal cisplatin sample showed strong initial inhibition of cell proliferation at 12 h compared with free cisplatin as control and slightly higher effect was observed at 24 h (Hwang et al., 2007). There are several crucial pieces of information not available in this study such as the suitable storage condition and stability of the liposomes. These are important as the nature of the liposome itself could change during the course of the study and may affect the outcome.

Another study describes a formulation of pH-sensitive liposomal cisplatin consisting of dioleoylphosphatidylethanolamine (DOPE), cholesteryl hemisuccinate (CHEMS), and distearoylphosphatidylethanolamine-polyethyleneglycol 2000 (DSPE-PEG_{2000}) with molar ratio of 5.7:3.8:0.5 (Junior et al., 2007). The cisplatin liposomes are prepared using the thin film hydration method with a lipid concentration of 40 mM, yielding liposomes with mean size of 445.3 nm, polydispersity index (PDI) of 0.6 and entrapment efficiency of 18.6%. The liposomes were then subjected to extrusion to produce monodispersed liposomes with mean diameter of 174 nm and ζ-potential of 1.67 mV. The extrusion process did not affect the entrapment efficiency of the liposomes. A stability study showed that 30% cisplatin is lost from the liposomes in both mouse plasma (pH 7.4) and normal saline (NS) (pH 6.5) at 37°C over 30 min. This is attributed to the temperature of the solution and not caused by the instability of the liposome itself. The cytotoxicity assay result for the liposomal cisplatin is specific. Significant cell proliferation inhibition by the liposomal cisplatin is seen in A549 (human lung cancer cell line) compared with free cisplatin but in A431 (human cervix squamous carcinoma cell line) the liposomal cisplatin is less effective than free cisplatin (Junior et al., 2007). This result is favourable to this project due to its specificity in lung cancer cell inhibition. However, the entrapment efficiency is quite low at 18.6%. In order for the formulation to be cost-effective and efficacious, entrapment efficiency should be increased. However, the actual optimal entrapment efficiency for the specific formulation that will be used for this project would have to factor in the effective dose of the anti-cancer drug itself, the cost of fabrication method of the liposomes and the optimization process itself. The stability study done in this liposome formulation is not sufficient. The sample was only subjected to 37°C

incubation for 30 min, therefore further study should be done to explore the effect of long-term storage in different temperature and medium to obtain the optimal storage condition. There was no in vitro test done to determine the cisplatin release rate from the liposomes. This should be carried out as the release rate plays a major role determining the effective dose of cisplatin delivered to the cancer cells.

In order to improve cell uptake, the mean diameter size of the liposomes should be in the range of 90 – 200 nm, with the maximal uptake occurring for nanoparticles of 100 nm in size (Win & Feng, 2005). A study on the cell uptake of gold nanoparticles has shown that the optimal size for cell uptake is nanoparticles of 98.1 nm in size (Yang et al., 2007) which is in line with the result of the aforementioned study. There are several interactions between the nanoparticles and cells surface that play a major role in determining the optimal size for the cell uptake of the nanoparticles such as membrane tension and adhesion strength (Xu et al., 2012). This project also aims to determine the optimal anti-cancer agents-loaded liposomes size for the cell uptake.

While these formulations are favoured to be used in this project due to its suitability for entrapment of cisplatin, several challenges need to be addressed first in order for these formulations to be viable. One of the key challenges is the method of production. All of the mentioned studies employed thin film hydration method and followed by extrusion to remove multilamellar vesicles (MLV) and reduce liposome size in some of them. Thin layer film hydration method is suitable for producing laboratory scale sample, but it is not possible to scale up the production process to create large, uniform and reproducible samples. The method itself depends on a number of variables that may affect the characteristics of the end product which cannot be effectively controlled. For these reasons, this project will utilise microfluidics

method. The advantages of this method are the production of the liposomes can be scaled up and the production variables can be maintained to produce large, uniform and reproducible samples. This is pertinent to the continuous manufacturing process, in which large volume of uniform end products can be expected out of an uninterruptible manufacturing line.

1.2.2 Liposome characterisation techniques

Physical characterisation, particularly the size of the produced liposomes is important in order to obtain liposomes within the desired size range. As mentioned beforehand, to achieve the optimal uptake by cancer cells, the liposomes should be in the range of 90 – 200 nm. There are several methods that can be employed in order to determine the size of the liposomes, namely dynamic light scattering (DLS), atomic force microscopy (AFM), scanning electron microscopy (SEM) and tunnelling electron microscopy (TEM). The principle behind DLS method is fairly simple; a beam of light is emitted into the sample and the particles within the sample will cause the beam of light to be scattered. The intensity of the scattered light is then measured from a specific angle from the incident beam. This method is considered suitable for determining particle size from nanometres up to a few microns range. DLS method also allows relatively quick size determination of hundreds of thousands to millions of liposomes. This is important in order to obtain quantitatively significant data in relation to the total number and size range of liposomes within a specific sample. This aspect makes DLS more advantageous compared with other sizing methods.

Other methods mentioned previously utilise optical imaging of the sample. SEM and TEM utilise a focused beam of electrons directed to sample. In SEM, this beam of electrons is directed to the specimen in a raster scan pattern. The electrons

interact with the atoms of the sample, producing secondary electrons which are detected by secondary electron detector. This allows detailed resolution of the sample's surface as the number of secondary electrons detected would vary according to the topography of the sample's surface.

TEM on the other hand, transmit the beam of electrons through ultrathin sample. The electrons interact with the material of the sample as they pass through the sample, modifying the resultant image which is magnified and focused on an imaging device. The working principle of TEM is similar to light microscopy except for the utilisation of electron beam instead of visible light. This allows higher resolution image to be obtained as electron has smaller wavelength than visible light. As opposed to SEM, TEM produces images with no information on topographical surface of the specimen.

AFM differs from the other methods in this regard, as it utilises physical contact or interaction with the sample in order to obtain the image. This imaging process is achieved using nanometre sized probe mounted on a flexible cantilever with a specific spring constant oscillating in a known frequency while scanning the topography of the sample mounted on mica or glass surface. A laser beam is used to determine the distance between the cantilever tip and the surface of the mica or glass stage by measuring the reflected laser beam from the tip using a photodiode array detector. Passing over the surface of the sample causes deflection of the cantilever tip, which causes a change to the distance between the tip and the photodiode array detectors. A feedback mechanism interprets this change and adjusts to maintain the distance of the tip, oscillation amplitude or the cantilever deflection depending on the scanning mode. The AFM is useful in term of determining the mechanical strength of

liposome. While it is also useful in determining the shape and size of liposome, care must be taken to ensure that sample immobilisation on the stage's surface does not affect the nature of the liposome itself and the probe's scanning oscillation force does not alter the sample (Edwards & Baeumner, 2006).

1.3 Thesis objectives and structure

This thesis aims to produce scalable liposome formulation loaded with irinotecan (CPT-11) and cisplatin (CDDP) for lung cancer therapy. Production of such liposomes will utilise a fabrication method that allows for modifications to be made on the process parameters in order to achieve the ideal physical characteristics of the liposomes such as size of 90 – 200 nm with PDI < 0.3, anionic and stable. The chosen formulations will be loaded with standalone CPT-11 and CDDP and combination of both agents. The loaded liposomes will then be subjected to purification processes in order to gain an insight on the effectiveness of such processes and their effects on the liposomes. Physical characteristics, stability and entrapment efficiency of the liposomal systems will also be assessed. The liposomes will also be subjected to a lyophilisation process in an attempt to improve shelf-life of the product. The effect of such process will also be studied. *In vitro* analysis of the free drugs, blank liposomes, CPT-11/CDDP standalone and combination liposomes will also be studied against A549 cancer cells in order to establish their cytotoxicity.

Objective 1: Design stable liposome formulations with desired physical characteristics and create CDDP-loaded liposomes.

In chapter 2, several liposome formulations will be fabricated, and their physical characteristics and morphology assessed. Stability study will be carried out on the liposomes over the course of 28 days. Chosen liposome formulations will be loaded with CDDP and their physical characteristics assessed and compared with blank liposomes. Liposome purification will be carried out using filter centrifugation method followed by encapsulation efficiency analysis and drug release study.

Objective 2: Scale-up fabrication of loaded liposomes and analyse and compare the characteristics of such liposomes with their scaled-down counterparts.

In chapter 3, dye-loaded liposomes of chosen formulations will be fabricated in small- and large-scale productions. Liposomal systems from both production scales will be purified using filter centrifugation and subsequently compared in terms of physical characteristics, entrapment efficiency and release profile.

Objective 3: Formulate and analyse standalone and combination-loaded CPT-11 and CDDP liposomes and compare between purification processes of filter centrifugation and TFF.

In chapter 4, blank, standalone and combination-loaded CPT-11 and CDDP liposomes will be fabricated using chosen formulations and subsequently analysed in terms of physical characteristics and stability over the period of 28 days. The loaded liposome

will be purified using filter centrifugation and TFF methods. Drug content analysis for both CPT-11 and CDDP will also be carried out.

Objective 4: To lyophilise and subsequently study the morphology of the liposomes and analyse the cytotoxicity of the blank, free drugs, standalone and combination CPT-11 and CDDP loaded liposomes.

In Chapter 5, freeze-drying method will be employed in order to lyophilise the liposomal suspension and its effects on the liposomes will be studied. Morphology study will be carried out on blank and loaded liposomes to directly visualise the liposomes using AFM and SEM. *In vitro* study of the liposomes will be carried out to assess the cytotoxicity of the blank, standalone and combination-loaded liposomes and compared with free drugs against A549 cancer cells.

Objective 5: To draw clear conclusions from the overall project and make recommendations for future work.

Chapter 2

Fabrication, Characterisation, Purification and Release Study of Blank and Cisplatin-loaded Liposomes

2.1 Introduction

Microfluidics technology utilising flow focusing is one of the most suitable techniques for producing liposomes on a large scale (Thiele, Steinhaus, Pfohl, & Förster, 2010). The flow focusing method is achieved using a uniform flow of phospholipids in alcohol solution within a central microchannel intersected with microchannels carrying aqueous solution flow from either side of the central microchannel (Fig. 2.1a). The resultant alcohol flow is compressed by the aqueous flow pressure, narrowing the alcohol flow and more importantly, producing a concentration gradient along the compressed alcohol flow. As the alcohol solution becomes diluted by the aqueous solution, the phospholipids in the alcohol solution spontaneously self-assemble into liposomes once the solution is diluted past a critical concentration (Jahn, Vreeland, Gaitan, & Locascio, 2004). Manipulation of fabrication parameters such as alcohol-to-aqueous volumetric flow rate and ratio within the microfluidics device itself allows fine-tuning of the produced liposomes size. This is crucial in order to achieve specific size of liposomes even when using a broad range or possibly a mixture of phospholipids and cholesterol (Jahn et al., 2010; Jahn, Vreeland, DeVoe, Locascio, & Gaitan, 2007).

Several liposome fabrications have been demonstrated using the microfluidics method (Carugo, Bottaro, Owen, Stride, & Nastruzzi, 2016b; Damiati, Kompella, Damiati, & Kodzius, 2018). One of the studies used 1,2-dimyristoyl-*sn*-glycero-3-phosphocholine (DMPC), cholesterol and dihexadecyl phosphate (DCP) dissolved in isopropyl alcohol in a molar ratio of 5:4:1 as the lipid mixture and phosphate-buffered saline (PBS) at pH ≈ 7.4 as aqueous buffer. The fabrication utilised two different designs of microchannels. The first design has two oblique side channels (65 μm wide)

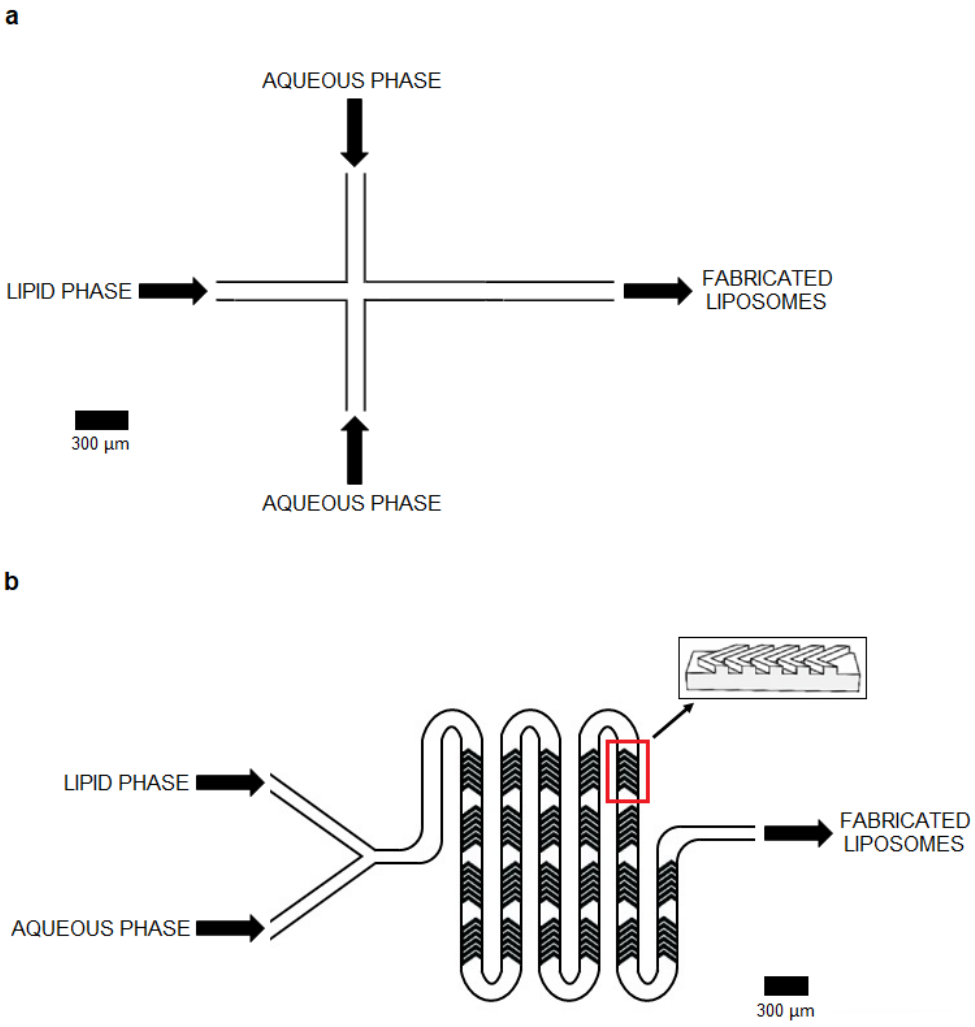

Figure 2.1 Basic principle of microfluidics technology utilising (a) flow focusing method and (b) staggered herringbone mixer (SHM) in fabrication of liposomes. Liposomes are created in the mixing channel when the lipid phase is diluted past the critical concentration by the aqueous buffer. Scale on the image is applicable to the width of the channels.

intersecting the central channel (42 µm wide) at an angle of 45° with all channels at 120 µm deep and the mixing channel at 65 µm wide and 10 mm long. The second design has all the channels at 36 µm deep and 10 µm wide with the mixing channel of 10 mm long. The two oblique side channels intersect the central channel at an angle of

90° (Jahn et al., 2010). The authors studied the effect of aqueous-to-lipid flow rate ratio (FRR) and volumetric total TFR on size and size distribution of the liposomes. They found that by using higher FRR, smaller sized liposomes can be achieved which is in line with findings of more recent research (Shah et al., 2019). More importantly, using constant total flow velocity, approximately similar sized liposomes can be produced using the 65 µm channel device using double the value of FRR used with the 10 µm channel device. This provides some insight on the correlation of FRR and the mixing channel size with the size of liposomes produced.

Utilisation of larger sized microchannel might mitigate some of the problems associated with the use of smaller sized microchannel such as clogging. Using the 65 µm channel device at higher FRR, changes in TFR (25 µL min^{-1}, 50 µL min^{-1} and 100 µL min^{-1}) have subtle effect on both size and size distribution of the liposomes. However, at lower FRR, changes in TFR affect both size and size distribution of the liposomes greatly. As demonstrated with FRR = 19, increasing the TFR to 100 µL min^{-1} increases the size of the liposomes and narrows the size distribution. Increasing the TFR in this manner has a limitation, as using TFR greater than 200 µL min^{-1} resulted in bimodal size distribution (Jahn et al., 2010).

Another study utilised DPPC, DSPC, cholesterol and DCP in some of the liposome formulations to scrutinise the effect of temperature on the size and size distribution of the fabricated liposomes (Zook & Vreeland, 2010). Both DPPC and DSPC have relatively high transition temperatures of 41°C and 55°C respectively. Using the molar ratios of phospholipids:cholesterol:DCP of 5:4:1, it was found that the closer the fabrication temperature to the transition temperature of the phospholipids, the smaller the size of the liposomes produced. According to the

authors, PDI of the produced liposomes increases with increasing liposome size, and the latter can be caused by the fabrication temperature or FRR. Interestingly, liposomes fabricated using DPPC, cholesterol and DCP were found to be more uniform in size compared with liposomes fabricated from DSPC, cholesterol and DCP (Zook & Vreeland, 2010).

Microfluidics technique for nanoparticles fabrication offers new possibilities in terms of liposome characteristics manipulation and production scale (Damiati et al., 2018; Thiele et al., 2010). This is an advantage over the thin film hydration method due to the absence of postprocessing (Ong, Chitneni, Lee, Ming, & Yuen, 2016). However, this technique is limited in its efficiency of liposome production due to liposome formation occurring only on the fluids interface (Jahn et al., 2010). This slow, uniaxial and diffusive mixing, requires a long microchannel to be achieved completely in which the length is linearly related to the Péclet number of the fluids being mixed (Stroock et al., 2002). Incorporation of SHM (Fig. 2.1b) revolutionises such technique by introducing an induced chaotic flow within the microfluidics system (Stroock et al., 2002). This chaotic flow increases the surface area of the boundary layer, homogenising the aqueous and lipid phases in a more efficient way and therefore increasing the liposome yield.

Another liposome formulation utilising the microfluidics technique with SHM method with the use of benchtop NanoAssemblr™ instrument (Precision NanoSystems Inc.) utilised DOPE and 1,2-dioleoyl-3-trimethylammonium-propane (DOTAP) dissolved in ethanol in equal molar ratio to form the lipid mixture and Tris buffer (10 nM; pH 7.4) as aqueous buffer (Kastner et al., 2014). Several buffer-to-solvent FRR (5:1, 3:1 and 1:1) and TFR (0.5 mL min^{-}1, 1.0 mL min^{-1}, 1.5 mL min^{-1}

and 2.0 mL min^{-1}) were used within the scope of this study to examine their effects of the size and size distribution of the resultant liposomes. In agreement with previous studies (Jahn et al., 2010; Obeid, Gebril, Tate, Mullen, & Ferro, 2017; Zook & Vreeland, 2010), increasing the FRR caused reduction in liposomes size while changing TFR value has minimal effect on the size. It is interesting to note that in this study, increasing FRR caused PDI to increase as well to a maximum of 0.5 with TFR of 1.0 mL min^{-1} (Kastner et al., 2014). It is pertinent for the scope of this project to determine the most suitable FRR and TFR for the liposome fabrication in order to obtain stable liposomes of a specific size range while keeping the PDI as low as possible.

There are several novel formulations of liposomal cisplatin that can be explored and used within the scope of this project. The most favourable among these is by using a combination of DSPC, DPPC, DSPG and cholesterol (Tardi et al., 2009). Current evidence suggests that the combination of these phospholipids and cholesterol in molar ratio of 35:35:20:10 respectively produced liposomes with mean diameter of 110 nm, possible to be used for entrapment of both CPT-11 and CDDP and maintained drug entrapment at ~98% in storage at -20°C (Tardi et al., 2009).

In this study, fabrication of both blank and CDDP-loaded liposomes was carried out using microfluidics technique with SHM method. Various combinations of DSPC, DPPC, DSPG and cholesterol molar ratios were tested as well as manipulations of fabrication parameters such as FRR and TFR. Physical characteristics and stability of the resultant liposomes were then determined. Selected CDDP-loaded liposome formulations were then measured in terms of entrapment efficiency and eventually the CDDP release characteristics.

2.2 Materials

DSPC, DPPC, DSPG and cholesterol (Fig. 2.2) were used in the lipid phase as liposome components. Ethanol (>99.8% purity) was used as solvent for lipid phase. PBS tablets and sodium chloride (≥99.5% purity) were used with deionised water (Millipore Direct-Q, 18.2 MΩ•cm at 25 °C) to create a buffer solution (0.01 M phosphate buffer, 0.0027 M potassium chloride, 0.137 M sodium chloride, pH 7.4 at 25 °C) and 0.9% NS respectively. CDDP (≥99.9% purity) was used as the entrapped material. All materials were obtained from Sigma-Aldrich (Dorset, UK) unless stated otherwise.

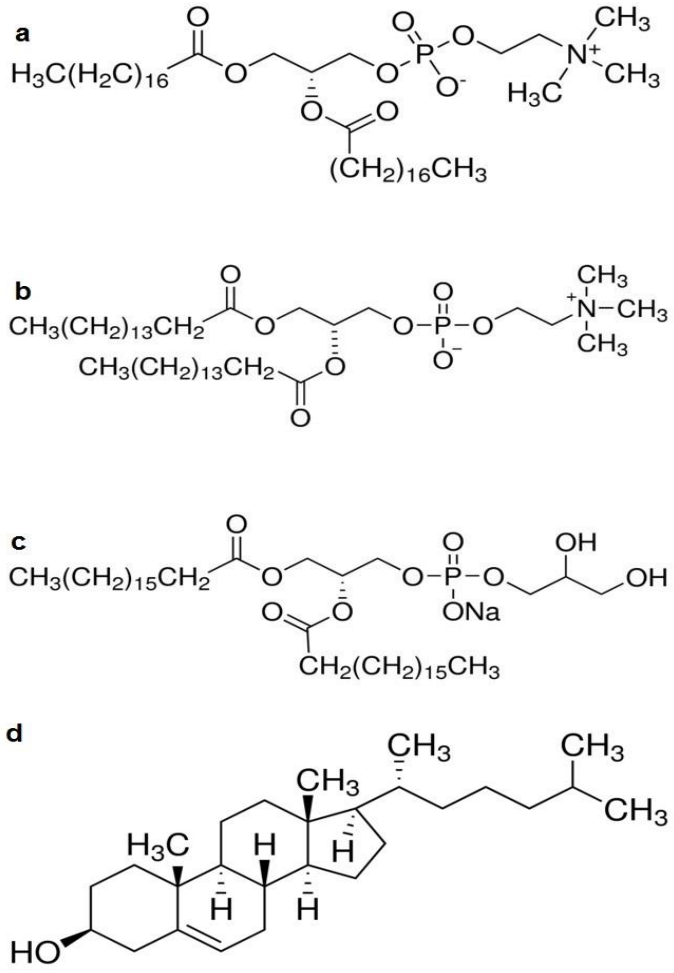

Figure 2.2 Chemical structure of the phospholipids; (a) 1,2-Distearoyl-sn-glycero-3-phosphocholine (DSPC) (b) 1,2-Dipalmitoyl-sn-glycero-3-phosphocholine (DPPC), (c) 1,2-Distearoyl-sn-glycero-3-phospho-rac-(1-glycerol) (DSPG) and (d) cholesterol.

2.3 Methods

2.3.1 Blank liposome fabrication

Molar ratio of the phospholipids and cholesterol used for the fabrication of liposomes in this study is based from previous study (Tardi et al., 2009) with several modifications implemented in order to obtain liposomes of desirable physical characteristics. Fig. 2.2 shows the chemical structure of the constituent phospholipids and cholesterol and Table 2.1 details all the molar ratios of all phospholipids and cholesterol used for this study. The variation in each of the constituent phospholipids and cholesterol are to study the effect of the variation itself and the effect of increasing molar ratio of cholesterol in the formulation.

Table 2.1 Molar ratio of each phospholipids (DSPC, DPPC and DSPG) and cholesterol of the liposome formulations.

Formulation	Phospholipids			Cholesterol
	DSPC	DPPC	DSPG	
1	35	35	20	10
2	45	45	0	10
3	45	0	45	10
4	0	45	45	10
5	25	25	20	30
6	20	20	20	40
7	20	20	10	50

Liposomes fabrication was achieved using microfluidics technique with SHM method. Briefly, spontaneous self-assembly of liposomes is achieved when phospholipid in alcohol solution is diluted with a buffer solution past the critical concentration along the concentration gradient of the phospholipid mixture turbulent flow produced by the SHM inside the microchannel.

Firstly, 20 mg ml^{-1} stock solutions for each of the phospholipids and cholesterol in ethanol were made. DPPC stock solution was prepared by mixing the phospholipid in ethanol at room temperature (RT). DSPC and cholesterol stock solutions were prepared by heating the mixtures at 40°C and vortexing for 10 mins. DSPG stock solution was prepared by heating the mixture at 70°C and sonicating for 30 mins.

Appropriate volume of each stock solution was then mixed with ethanol to make up 500 µl lipid phase for each of the formulation as in Table 2.2. Each of the lipid phase solution was then mixed with 1.5 ml 0.01 M PBS solution in Benchtop NanoAssemblr™ (Precision Nanosystems Inc., Vancouver, Canada) set at 70°C with FRR of 3:1 and TFR of 12 ml min^{-1}. The resultant liposome formulations were mixed with an additional 1.5 ml of PBS solution and allowed to cool down to RT for 2 h before further analysis.

The procedure was then repeated for formulation 1, 5, 6 and 7 with variations of FRR and TFR combinations as stated in Table 2.3 to study the effect of both parameters on the size and stability of the formulations.

Table 2.2 Volume of ethanol, phospholipids and cholesterol stock solutions in µl needed for 500 µl lipid phase of each of the formulation.

Formulation	Phospholipids (µl)			Cholesterol (µl)	Ethanol (µl)
	DSPC	DPPC	DSPG		
1	94.4	87.7	54.7	13.2	250.0
2	122.7	114.0	0.0	13.3	250.0
3	117.8	0.0	119.4	12.8	250.0
4	0.0	113.2	123.5	13.3	250.0
5	75.1	69.8	60.9	44.1	250.0
6	63.8	59.2	64.6	62.4	250.0
7	68.3	63.5	34.6	83.6	250.0

Table 2.3 FRR and TFR combinations studied for liposome fabrication in all formulations. Check mark (✔) denotes FRR and TFR combination used while cross mark (✘) denotes unused FRR and TFR combinations.

TFR (ml min^{-1})	FRR		
	1:1	3:1	5:1
0.5	✔	✔	✔
4	✔	✔	✔
12	✘	✔	✘
16	✔	✔	✔

2.3.2 Fabrication of cisplatin-loaded liposome

Formulation 5 and 7 were selected as the liposome formulation to be loaded with CDDP based on the physical characteristics and stability results of the blank liposomes. The liposome production method is as described previously. Briefly, 500 µl of lipid phase solution from each formulation was mixed with 1.5 ml of 1.5 mg ml^{-1} CDDP in NS solution in Benchtop NanoAssemblr™ set at 70°C with FRR of 3:1 and TFR of 0.5 and 12 ml min^{-1}. The liposomal solutions were then mixed with an additional 1.5 ml of NS solution afterwards and allowed to cool down to RT for 2 h before further analysis.

2.3.4 Liposome characterisation and stability study

Particle size and zeta potential analysis of the liposomes were determined using Zetasizer Nano ZS (Malvern Instrument, Malvern, UK). Liposome suspensions were diluted to concentration of 1% v/v using their respective blank aqueous media. The samples were then placed in a folded capillary zeta cell and measured in DLS mode at 25°C and 173° Non-Invasive BackScatter angle using light source of 633 nm wavelength to determine the average particle size and PDI. PDI of < 0.5 is considered as monodisperse in this study. ζ-potential value was obtained using electrophoretic light scattering method and calculated using Smoluchowski model. All measurements were performed in triplicate.

Stability study for the blank liposome formulation was carried out by measuring particle size and PDI at set intervals within 28 days. The samples were kept in 4°C during the whole period of stability study.

AFM method was used for morphology study of the liposomes using the Dimension Bio FastScan AFM (Bruker-Nano). AFM images were obtained at 7 days after fabrication. 5µl of liposome sample from each formulation was placed on the surface of freshly cleaved mica and air-dried for 30 min. AFM imaging was carried out by scanning the mica surface in air under room conditions with the instrument operating under peak force with ScanAsyst mode. The images obtained were analysed using NanoScope Analysis ver. 19.

2.3.5 Liposome purification

CDDP-loaded liposomes were purified from unentrapped drug using filter centrifugation. 4 ml of diluted liposomal solution was added into Amicon® Ultra-4 centrifugal filter (Merck Millipore, UK) with 100 kDa Nominal Molecular Weight Limit (NMWL) and centrifuged using HERMLE Z 323 K centrifuge (HERMLE Labortechnik GmbH, Germany) with fixed angle rotor at 5000 x*g* and 4°C for 1 h.

Three centrifugation runs were performed, and the filtrate was collected at the end of each centrifugation run and NS was added to the concentrated liposome suspension with volume equivalent to the collected filtrate. One final centrifugation run was then carried out to concentrate the liposome suspension to 250 µl or lower.

The concentrated liposome suspension was then recovered from the centrifugal filter for entrapment efficiency determination and release study. The filtrate from each centrifugation run was then combined to determine the amount of unentrapped drug for use of entrapment efficiency determination.

2.3.6 CDDP content and entrapment efficiency determination

CDDP content in all samples was analysed using Agilent 7700 Series Inductively Coupled Plasma Mass Spectrometry (ICP-MS) (Agilent, US). Platinum 195 isotope was selected for quantitative determination along with bismuth 209 isotope as internal standard.

Samples containing CDDP were diluted to desired concentration to make up 10 ml solutions in 2% HNO_3 for the analysis. Platinum standard curve was obtained from a series of solutions diluted from PlasmaCAL platinum calibration standard solution for ICP-MS (SCP Science, Canada).

Entrapment efficiency was calculated using a method mentioned previously (Tomoko & Fumiyoshi, 2005).

$$Entrapment\ efficiency\ (\%) = \frac{CDDP_{total} - CDDP_{free}}{CDDP_{total}} \times 100$$

where $CDDP_{total}$ is amount of CDDP in the initial volume of stock solution in the aqueous phase used during the liposome fabrication step and $CDDP_{free}$ is the amount of unentrapped CDDP collected after the liposome purification step.

2.3.7 Release study

Concentrated CDDP-loaded liposome suspension from formulation 5 was filled into dialysis tube (Sigma-Aldrich) with molecular weight cut-off of 14 kDa and immersed in 10 ml of NS acting as release medium at 4°C to represent storage temperature and 37°C to represent normal human physiological temperature. Release study samples at 37°C were placed on a tilting platform set at 15 rpm. 2 ml aliquot was taken from the release medium at specific time intervals and immediately replaced with fresh NS of the same volume.

The release study was carried out over a total period of 72 h. The liposome suspension was recovered from the dialysis tube at the end of the release study. Both the liposome suspension and the aliquot were stored in 4°C prior to analysis. CDDP content in both remaining liposome suspension and the aliquot was analysed using ICP-MS as stated above.

2.3.8 Statistical analysis

Unless stated otherwise, all measurements were performed in triplicate from independent samples and *t*-test statistical analysis was carried out on using Minitab version 17.1.0. Results are expressed in mean ± standard deviation (SD). Significance was defined as $p < 0.05$ (marked with *), $p < 0.01$ (marked with **) and $p < 0.001$ (marked with ***). No significance was defined as $p > 0.05$ (marked with n.s).

2.4 Results and Discussion

2.4.1 Liposome fabrication

The specific ratio of phospholipids and cholesterol in Formulation 1 (**Error! Reference source not found.**) obtained from literature was emulated in this study due to its favourable characteristics of being able to effectively encapsulate both cisplatin and irinotecan (Tardi et al., 2009), the two drugs that are also the focal points of this project. The modifications of the molar ratios of constituent phospholipids were introduced since this study uses microfluidics technique with SHM as the method of liposome fabrication as opposed to thin-film hydration method of the original study. Adaptation of a previous study (Bruglia, Rotella, McFarlane, & Lamprou, 2015) regarding effect of cholesterol on the stability of liposomes was introduced by several alterations in the molar ratio of phospholipids and cholesterol for Formulations 5, 6 and 7 (70:30, 60:40 and 50:50 respectively).

DPPC dissolved readily in ethanol at RT at the required concentration. While DSPC and cholesterol stock solutions required low heating to fully solubilise the materials, but no precipitation was observed on both solutions when left at RT and therefore deemed as stable. DSPG however, did not readily dissolve in ethanol in the required concentration for the stock solution.

Table 2.1 Solubility profiles of phospholipids and cholesterol used in this study. Solubility of cholesterol in ethanol was measured at 27°C using radiolabel assay method.

Material	Solvent	Solubility (mg ml^{-1})	Reference
DSPC	Ethanol	25	(Cayman Chemical, 2013b)
DPPC	Ethanol	30	(Cayman Chemical, 2013a)
DSPG	Chloroform	2	(Cayman Chemical, 2013c)
Cholesterol	Ethanol	23.7	(Flynn et al., 1979)

As shown in Table 2.1, DSPC, DPPC and cholesterol are fairly soluble in ethanol. DSPG is sparingly soluble in a non-polar solvent such as chloroform and demonstrated very low solubility in water (Engblom, Miezis, Nylander, Razumas, & Larsson, 2001). This posed a problem during the initial mixing of the lipid phase for the liposome fabrication. The high temperature required to solubilise DSPG in ethanol renders the solution unstable when removed from the water bath for the mixing process. Moreover, at this temperature, ethanol evaporates fairly quickly when it is being transferred hence altering the concentration of DSPG in the stock solution. The effect is more prominent especially when very low volumes were used (52 – 130.5 µl) from the stock solution.

Several steps were taken during the lipid phase mixing process in order to mitigate this problem. Firstly, required volumes of DSPC, DPPC and cholesterol stock solutions were mixed first with ethanol. Required volume of DSPG stock solution was then pipetted into the corresponding mixture from the previous step to finalise the lipid phase whilst keeping the stock solution in the water bath at 70°C. During this step, the DSPG stock solution was pipetted in and out for a few times in the solution in order to equilibrate the temperature between the solution itself and the pipette tip. This is to minimise the formation of DSPG precipitates on the inside surface of the pipette tip which could lead to inaccuracy in the actual amount of DSPG mixed in the lipid phase solution.

Microfluidics technique with SHM was chosen as the method of choice for liposome fabrication due to its speed and uniformity in nanoparticle production and potential for industrial scale application (Obeid, Gebril, et al., 2017). Due to the high temperature required to solubilise DSPG in the lipid phase, the fabrication process was carried out in 70°C to prevent the phospholipid from precipitating out during the process. The heating was achieved using a heating block and a temperature controller attached to the Benchtop Nanoassemblr™. However, in this case, the utilisation of the heating block effectively lowers the volume of liposome suspension that can be produced in a single run due the small diameter of one of the slots in the heating block that can only accommodate a 1 ml syringe (4.78 mm in diameter).

CDDP loading into the liposomes was achieved by using 1.5 mg ml^{-1} CDDP in NS solution as the aqueous phase during the fabrication process. NS was chosen as the aqueous solvent in lieu of PBS due to its ability to stabilise CDDP in aqueous solution by preventing substitution of chlorine ions with hydroxide ions (Karbownik et al.,

2012) in comparison with PBS which is not very efficient in preventing the substitution process (Davies, Berners-Price, & Hambley, 2000).

Additional aqueous solvent was added to the liposome suspension post fabrication in order to mitigate the effects of ethanol on the liposomes. Similar technique have been employed elsewhere to this end (Obeid, Khadra, Mullen, Tate, & Ferro, 2017). Studies have suggested that the presence of ethanol, especially in higher concentration (Frischknecht & Frink, 2006), increases lipid bilayer membrane permeability (Komatsu & Okada, 1997), fluidity (Chin & Goldstein, 1977) and lateral mobility (Shao-Yu, Bing, Jacobson, & Sulik, 1996). It has been suggested that the ordering of hydrocarbon chains in the vicinity of glycerol backbone decreases in larger concentration of ethanol and the area per lipid increases due to ethanol binding in the lipid headgroup region therefore increasing permeability of the membrane (Patra et al., 2006).

2.4.2 Blank liposome characterisation and stability study

Size and size distribution of liposomes are some of the important aspects in determining the end result and robustness of a fabrication process and also suitability of the liposomes to be used for a specific purpose. This project in particular, focuses on production of liposomes with size range of 90 – 200 nm in order to optimise cell internalisation of the liposomes as discussed previously (Win & Feng, 2005).

DLS is one of the methods for measuring nanoparticles size as demonstrated by previous studies (Fischer & Schmidt, 2016) (Obeid, Gebril, et al., 2017). Correct dilution of the liposome samples is important in order to obtain robust and repeatable results (Surianarayanan, Shivakumar, Vegesna, & Srivastava, 2016). In this

experiment, the value used to describe particle size is Z-average. Z-average is defined as the harmonic intensity average particle diameter in ISO 22412:2017 and the most stable parameter produced by DLS method. Z-average values are comparable when the samples are monomodal, monodispersed, spherical in shape and contained in a suitable dispersant, all of which are suitable for this study.

PDI is a dimensionless number obtained from a simple two-parameter fit to the cumulants analysis. It is a useful indicator in determining the liposome size distribution in the solution and to a certain extent, the form and stability of the liposome itself as changes in PDI during storage suggest lack of stability (Wolfram et al., 2014). Very low number indicates highly monodispersed particles which in this study, indicates stable and uniformly sized particles. High value of PDI indicates inherent instability of the particles in the solution, arising either from failure of uniform particle formation during the fabrication process or formation of liposome aggregates which ultimately becomes unsuitable for analysis with DLS method.

ζ-potential is the measure of repulsive/attractive charge magnitude of particles in a colloidal system. This parameter is useful in predicting the stability of the system, in which a system with high positive or negative value of ζ-potential is likely to be stable due to the electrostatic repulsion between the particles. This repulsive force prevents flocculation of the particles, hence contributing to the stability of the colloidal system (Joseph & Singhvi, 2019).

Table 2.2 Size and PDI of blank liposomes fabricated using Formulation 2, 3 and 4 with FRR of 3:1 and TFR of 12 ml min^{-1} immediately post-production.

	Size (nm)	PDI
Formulation 2	1175.0	1
Formulation 3	342.0	0.554
Formulation 4	220.2	0.547

Formulation 1, 5, (Fig. 2.3) 6 and 7 (Fig 2.4) were found to produce stable liposomes using the initial FRR of 3:1 and TFR of 12 ml min^{-1}. As shown in Table 2.2, Formulation 2, 3 and 4 on the other hand produced polydispersed (PDI = 1, 0.554 and 0.547 respectively) and large liposomes (1175, 342.0 and 220.2 nm respectively). These liposomes were found to be unstable on the following days post fabrication due to presence of precipitates in the solution and therefore the formulations were deemed unsuitable to be used for further experiments involving variations in FRR and TFR during fabrication process.

The smallest liposomes (~60 nm) were produced using formulation 6 and 7 using TFR of 4 and 16 ml min^{-1} respectively and FRR of 5:1 (Fig. 2.4). Both of these liposomes are significantly smaller than their counterparts produced using higher FRR of 3:1. This suggests that higher FRR is correlated to lower particle size and is in accordance to previous studies (Jahn et al., 2010; Jahn et al., 2007; Obeid, Gebril, et al., 2017). This effect is prominent in formulation 1 (Fig. 2.3a), where the difference in liposomes sizes is in the magnitude of ~80 nm. Using a much lower FRR of 1:1 on the other hand, yielded very large or unstable particles. The only stable liposome

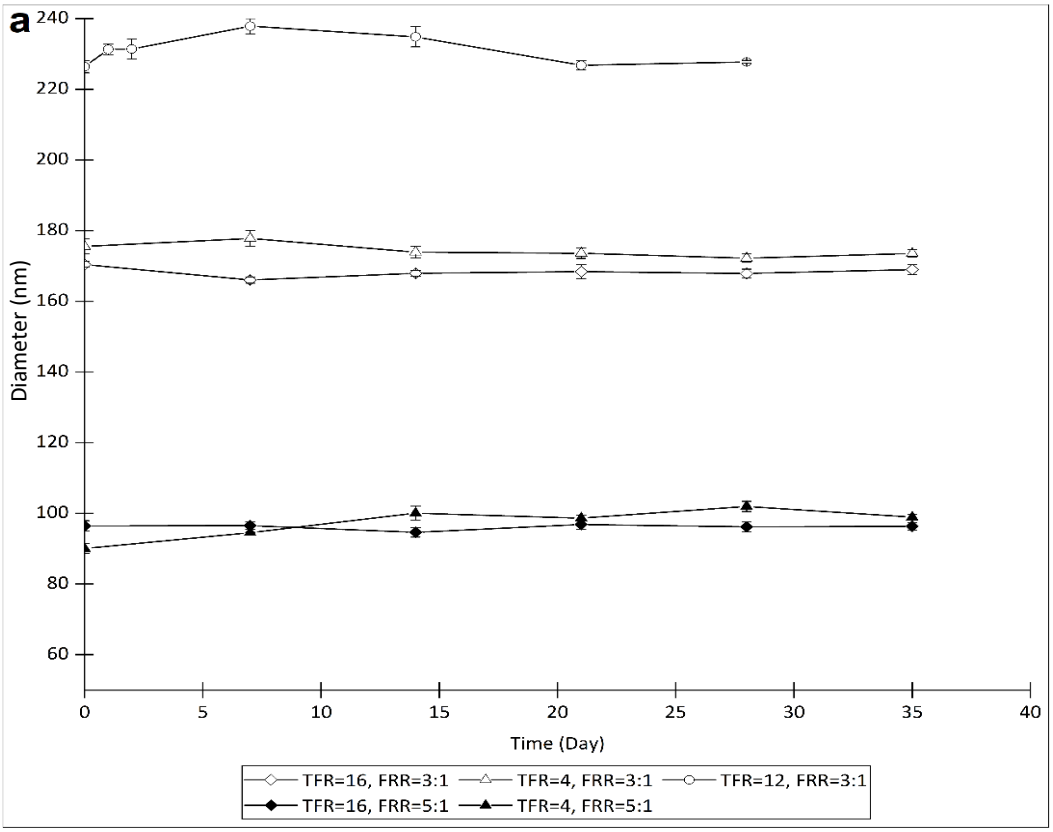

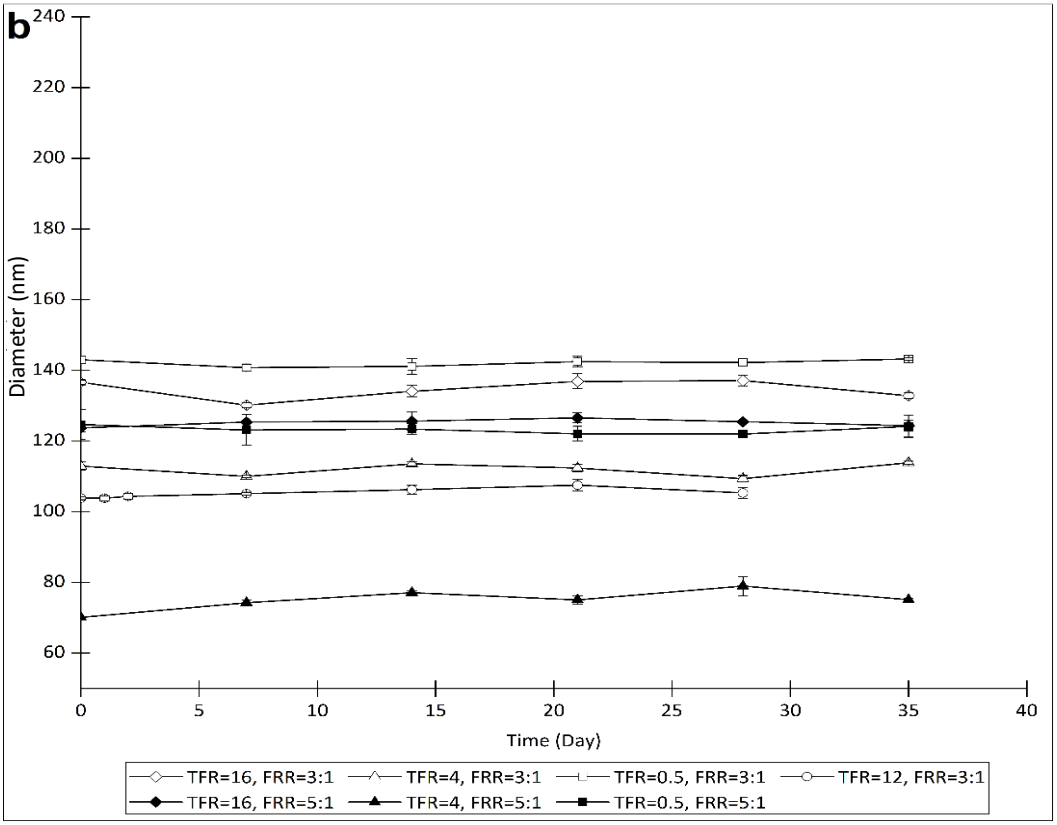

Figure 2.3 Liposome size of (a) Formulation 1 and (b) Formulation 5 produced using combinations of various TFR and FRR measured over 35 days. Mean ± SD shown are from three independent measurements.

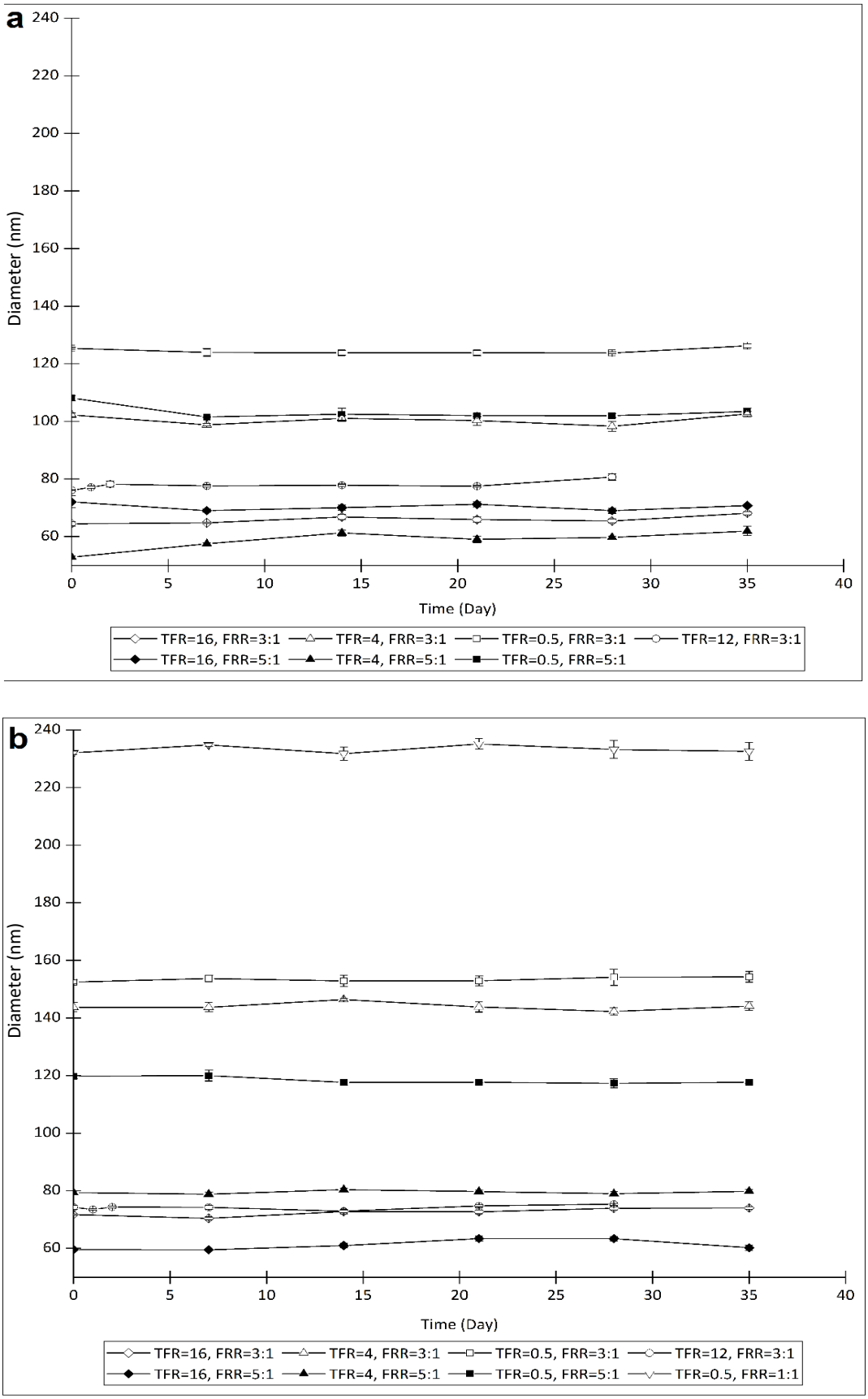

Figure 2.4 Liposome size of (a) Formulation 6 and (b) Formulation 7 produced using combinations of various TFR and FRR measured over 35 days. Values shown are means ± SD from three independent measurements.

produced with this FRR is by using formulation 7 and TFR of 0.5 ml min^{-1}, albeit a significantly larger size of ~235 nm.

In general, TFR effect on the particle size of produced liposomes is minimal. While some observations show that higher TFR yielded smaller particles when the same FRR was used (Fig. 2.4b), other formulations yielded mixed results with TFR of 4 ml min^{-1} predominantly produced the smallest particles for each formulation (Fig. 2.3b & 2.4a).

Size distribution varies across the formulations within the same FRR and TFR ranges. The smallest distribution was achieved using formulation 6 (60 – 123 nm) within TFR range of 4 and 16 ml min^{-1} and FRR of 3:1 and 5:1 (Fig. 2.4a). This suggests relative robustness of formulation 6 under different fabrication conditions and might be useful when drug entrapment process requires these variations in order to optimise the entrapment efficiency.

As demonstrated by PDI values in Table 2.6, the liposomes produced using formulation 1, 5, 6 and 7 are monodisperse across the range of TFR and FRR save for formulation 1 at TFR of 0.5 ml min^{-1}. The latter was found to be highly polydisperse immediately after fabrication and unstable 24 h post fabrication.

It was observed that increasing TFR led to reduced PDI values for both FRR of 5:1 and 3:1 (Fig. 2.5). This effect was prominently demonstrated by all formulations when FRR of 5:1 was used (Fig. 2.5b), showing very significant ($p < 0.01$) decrease in PDI when TFR was increased from 0.5 ml min^{-1} to 16 ml min^{-1}. Similar finding was observed when FRR of 3:1 was used instead (Fig. 2.5a), except for formulation 7 in which the decrease in PDI is not significant when TFR was increased.

Table 2.3 PDI of liposomes produced using formulation 1, 5, 6, 7 and combinations of various TFR and FRR. Values shown are means ± SD from three independent measurements on set intervals over 35 days. * = means ± SD from three independent measurements on day 0.

TFR (ml min^{-1})	16		12	4		0.5	
FRR	3:1	5:1	3:1	3:1	5:1	3:1	5:1
Formulation 1	0.062 ±0.015	0.088 ±0.073	0.227 ±0.005	0.177 ±0.015	0.125 ±0.028	0.693 ±0.075*	0.640 ±0.047*
Formulation 5	0.122 ±0.044	0.043 ±0.022	0.090 ±0.022	0.083 ±0.015	0.114 ±0.029	0.165 ±0.008	0.289 ±0.022
Formulation 6	0.069 ±0.017	0.083 ±0.029	0.143 ±0.005	0.099 ±0.014	0.125 ±0.031	0.167 ±0.014	0.223 ±0.010
Formulation 7	0.156 ±0.013	0.141 ±0.038	0.069 ±0.016	0.102 ±0.008	0.126 ±0.006	0.160 ±0.009	0.177 ±0.003

Table 2.4 ζ-potential of liposomes, in mV, produced using formulation 1, 5, 6, 7 and combinations of various TFR and FRR. Values shown are means ± SD from three independent measurements on set intervals over 35 days. * = means ± SD from three independent measurements on day 0.

TFR (ml min^{-1})	16		12	4		0.5	
FRR	3:1	5:1	3:1	3:1	5:1	3:1	5:1
Formulation 1	-25.53 ±1.28	-22.61 ±3.34	-26.25 ±1.43	-26.08 ±0.62	-21.86 ±1.21	-27.50 ±2.17*	-26.5 ±1.21*
Formulation 5	-33.44 ±3.44	-28.14 ±4.04	-18.03 ±1.60	-29.61 ±2.15	-19.89 ±2.33	-28.23 ±1.04	-27.56 ±0.95
Formulation 6	-24.07 ±1.56	-25.50 ±2.05	-25.03 ±1.14	-31.87 ±1.59	-23.10 ±2.28	-24.98 ±1.43	-30.00 ±1.73
Formulation 7	-25.13 ±1.46	-24.97 ±2.60	-21.23 ±0.87	-14.88 ±1.13	-23.66 ±2.57	-18.96 ±0.75	-23.88 ±0.77

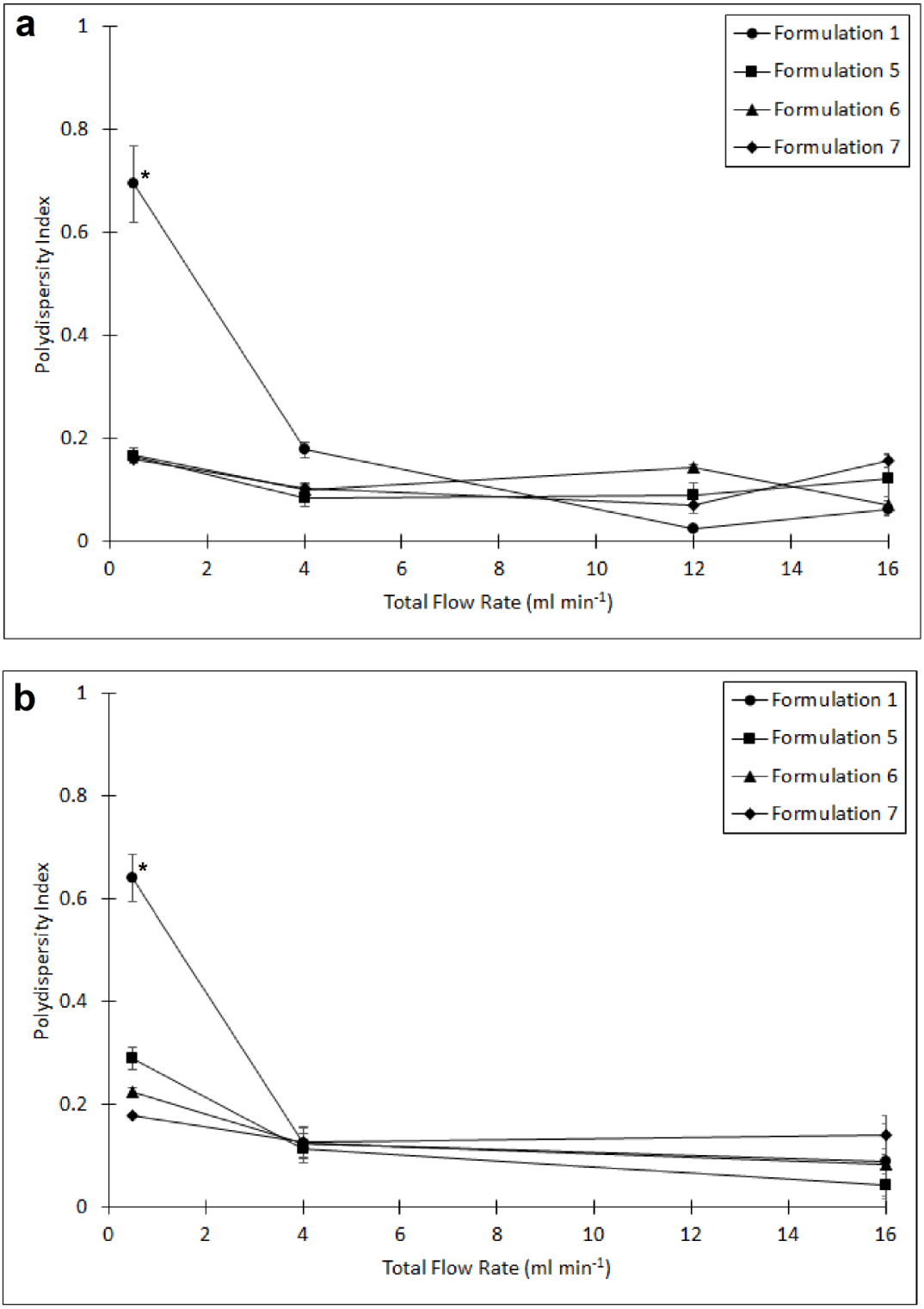

Figure 2.5 PDI of formulation 1, 5, 6 and 7 as a function of TFR and at FRR of (a) 5:1 and (b) 3:1. Values are means ± SD of three independent measurements on set intervals over 35 days. * = means ± SD of three independent measurements post fabrication.

It was also observed that at FRR of 5:1 and TFR of 0.5 ml min^{-1} the PDI of the formulations is decreasing in the following order: 1, 5, 6, and 7. It is likely that this decrease in PDI was influenced by the increase of cholesterol molar ratio in the formulations.

These findings contradict the result of a previous study by (Kastner et al., 2014) from the standpoint of TFR effect on PDI. The difference in the findings merits further research into the effect of TFR on PDI of liposome formulations with varying lipid constituents and molar concentration of each of the constituent.

ζ-potential measured from all the formulations across the ranges of FRR and TFR is detailed in Table 2.7. ζ-potential of -30 mV is considered optimum for a stable nanodispersion (Samimi, Maghsoudnia, Eftekhari, & Dorkoosh, 2019). The results show that all the particles are anionic in nature, due to phosphatidylglycerol headgroup in DSPG (Brown & Conboy, 2015), with the ζ-potential ranging from -14.88 ± 1.13 to -30.00 ± 1.73 mV. These anionic liposomes are preferable over cationic liposomes due to the latter being more cytotoxic to cells by causing membrane disruption (Fröhlich, 2012) and less stable during storage (Balazs & Godbey, 2011). The mechanism of anionic nanoparticles cytotoxicity is largely via apoptosis (Petushkov, Intra, Graham, Larsen, & Salem, 2009). Cationic liposomes, however, are taken up by non-phagocytic cells more than their anionic counterparts (Tomita, Rikimaru-Kaneko, Hashiguchi, & Shirotake, 2011). There are some downsides in the use of anionic liposomes, notably among those is the leakage of the entrapped material post exposure to human low-density lipoproteins in the serum (Comiskey & Heath, 1990). However, the leakage can be minimised by the use of DSPG and reducing the molar percentage of phosphatidylglycerol in the formulation (Comiskey & Heath, 1990). In the interest of

the aim of this project, anionic liposomes were chosen in order to minimise the cytotoxicity of the formulation itself to healthy cells, thus improving the overall outcome of the therapy in relation to minimising side effects of the therapeutic agents themselves.

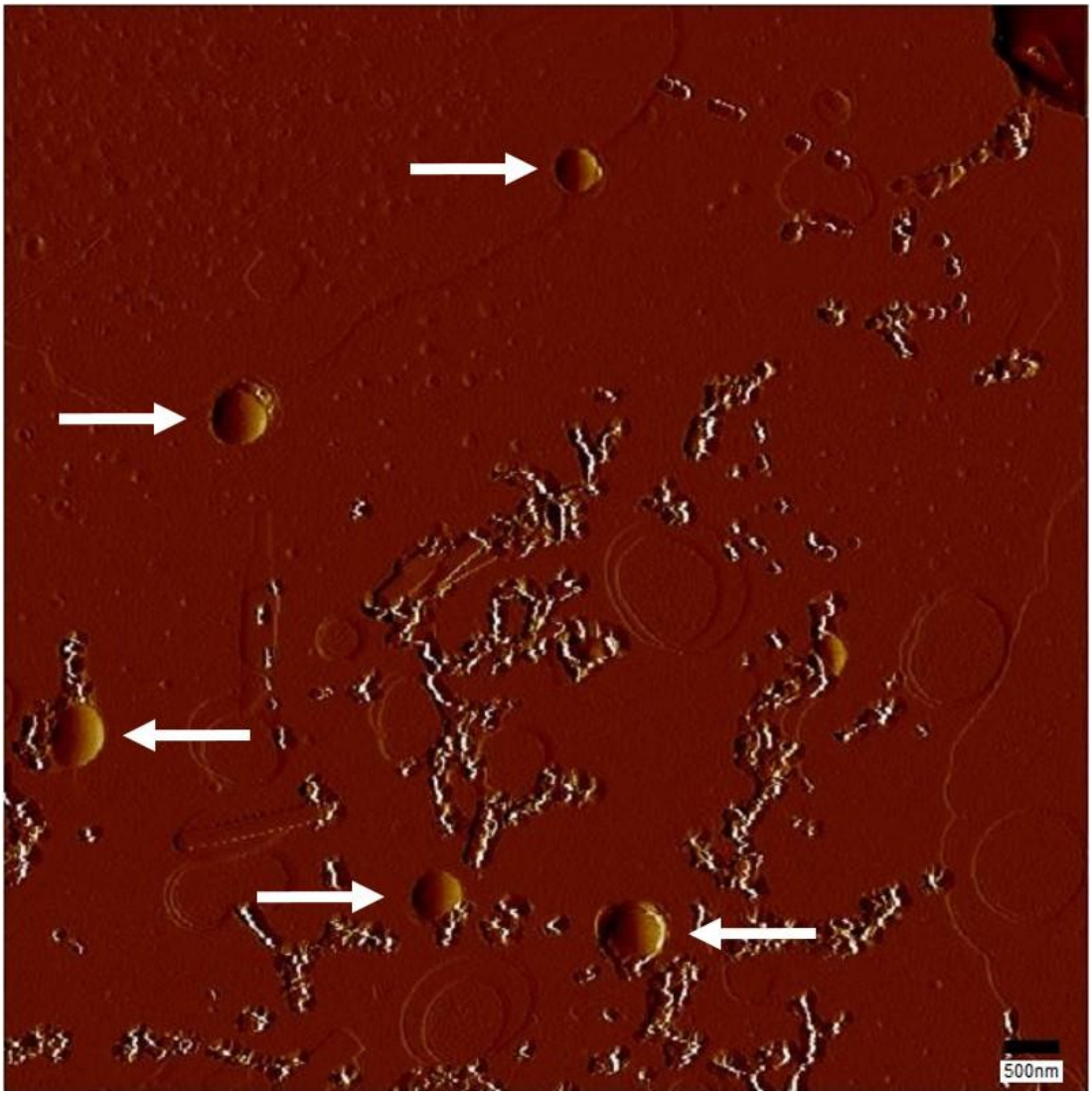

Figure 2.6 AFM image of liposome sample from Formulation 6, 7 days after fabrication. White arrows indicate individual liposomes within the image.

The AFM method is employed in order to directly measure the individual size of the liposomes. As mentioned previously, this method is particularly useful in this regard due to its utilisation of nanometre sized probe which provided high resolution image of the sample at around 0.1 nm. As shown in Fig. 2.6, individual liposomes can

be seen in the image and their sizes can be determined quickly. The size of liposomes in this image ranges from 406.25 nm to 531.25 nm.

There are several limitations in using the AFM to measure the size of liposomes in a sample. Firstly, suitable sample immobilization method must be employed in order to preserve the liposomes natural form on the mica surface (Edwards & Baeumner, 2006). This is including, but not limited to, duration of sample drying on the mica surface and concentration of the sample used with this method. It is important to note that the above parameters are also dependent on the lipid compositions, liposomes sizes and buffer compositions (Edwards & Baeumner, 2006).

As demonstrated in Fig. 2.6, the size range of the liposomes in Formulation 6 determined using the AFM method is very different from the size range of the same formulation measured using the DLS method which is within a narrow range of 78 nm to 80 nm. This can be attributed to deformation of the liposomes on the mica surface, as reported in previous findings (Liang, Mao, & Ng, 2004; Ruozi, Tosi, Forni, Fresta, & Vandelli, 2005; Ruozi, Tosi, Leo, & Vandelli, 2007).

Deformation of the liposomes were reported previously due to adsorption of liposomes on the mica surface. The liposomes in these studies were found to form planar bilayers on top of the mica surface. In one of the studies, the authors observed that one of the liposome samples formed flat disks as soon as 5 – 6 min following deposition (Ruozi et al., 2005). As the formation of the planar bilayers are directly correlated with longer drying time, it can be concluded that soft materials such as liposomes are very vulnerable to collapse when the buffer medium supporting their spherical shape evaporates (Ruozi et al., 2005).

Another study outlined the possibility that larger sized liposomes might rupture upon adsorption on the mica surface. The authors stated that larger sized liposomes are more liable for rupture upon adsorption, forming large flat disks when observed under the AFM. They also mentioned that smaller sized liposomes below certain critical sizes are less prone to rupture upon adsorption, and in their case the critical size ranges between 40-60 nm (Liang et al., 2004). It is also possible that these flat bilayers were placed on top of each other (Ruozi et al., 2005), making it nearly impossible to distinguish one liposome from another and rendering them useless to be used in size determination of the liposomes in the sample.

It is also discovered that using AFM in contact mode can cause deformation of the liposomes due to direct transfer of force from the probe tip to the sample (Ruozi et al., 2005). AFM in non-contact mode can also induce liposome deformation. The transfer of force between the vertical oscillations of the probe tip to the liposome surface through the medium caused concave shaped depression on the liposome surface after 2 h of scanning (Ruozi et al., 2007).

With regard to this project specifically, using DLS to determine the size of the liposomes is more suitable due to the requirement of the liposomes to be suspended in an aqueous buffer solution. Furthermore, obtaining the quantitative data on the size and size distribution of the liposomes is more important in order to determine the effect of fabrication parameters and the type of formulation used on the end product. However, the AFM analysis did provide some insight on the morphology of the liposomes which cannot be obtained via DLS analysis.

Table 2.5 Physical characteristics of CDDP-loaded liposomes produced from formulation 5 and 7 with FRR of 3:1, immediately post fabrication. The results are mean ± SD from three independent measurements.

	Size (nm)		PDI		Zeta potential (mV)	
TFR (ml min^{-1})	0.5	12	0.5	12	0.5	12
Formulation 5	125.90 ±1.31	107.97 ±0.83	0.19 ±0.005	0.05 ±0.015	-27.37 ±0.56	-26.95 ±1.35
Formulation 7	137.50 ±1.45	78.55 ±0.12	0.19 ±0.010	0.10 ±0.009	-25.93 ±1.32	-20.70 ±0.57

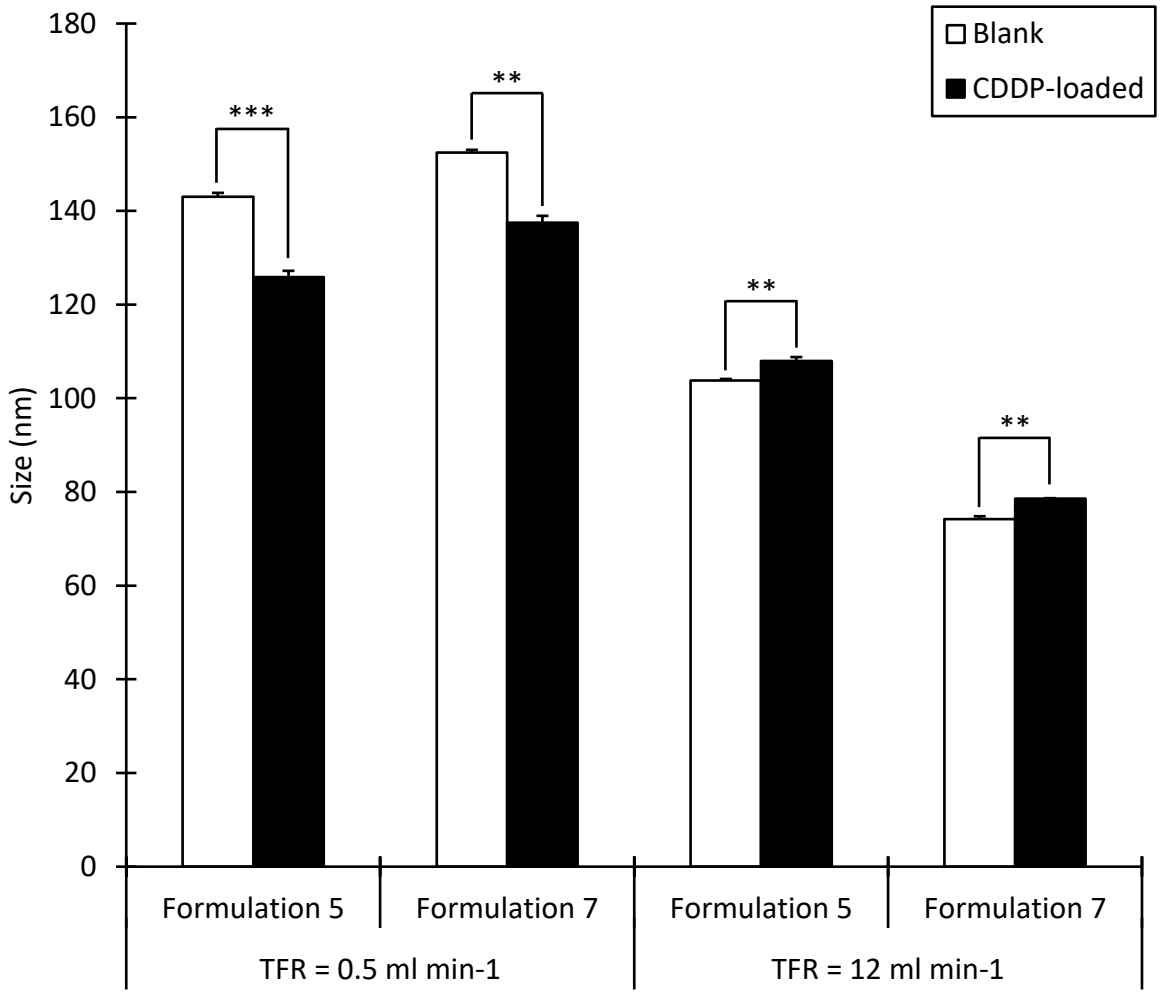

Figure 2.7 Size comparison of blank and CDDP-loaded liposomes produced from formulation 5 and 7, TFR of 0.5 and 12 ml min^{-1} and FRR of 3:1 measured immediately post fabrication. Results shown are means ± SD from three independent measurements. *** = $p < 0.001$. ** = $p < 0.01$.

2.4.3 CDDP-loaded liposomes characterisation

CDDP-loaded liposomes were fabricated using formulation 5 and 7 and analysed afterwards to determine the physical characteristics. They demonstrated high degree of stability and favourable physical characteristics in terms of size, PDI and zeta potential to be used within the scope of this study. Slight variations were introduced in the TFR of the fabrication process but the FRR was kept constant at 3:1. The results show that higher TFR of 12 ml min^{-1} produced smaller and less polydispersed liposomes for both formulations (Table 2.8). It is also worth noting that by increasing molar ratio of cholesterol and decreasing molar ratio of phospholipids in formulation 7 when compared with formulation 5, a decrease in size was observed in the resultant particles, suggesting influence of molar ratio of constituent components of a formulation on that parameter. All liposomes produced were anionic, in line with the previous observation on their blank counterparts.

Size comparison was carried out between blank and CDDP-loaded liposomes. Both types of liposomes fabricated using formulations 5 and 7 exhibited significantly different sizes. When the lower TFR was used, CDDP-loaded liposomes were found to be smaller than the blank liposomes for both formulations 5 and 7, -17.1 nm and -14.9 nm respectively. The opposite occurred when the higher TFR was used, with the size difference of +4.2 nm for both formulations (Fig. 2.7). Lower PDIs were also observed both formulations when the higher TFR was used. These differences seem to be influenced by the interaction between the aqueous solution and TFR used during the fabrication process. The mechanism behind this phenomenon is not fully understood and warrants further studies. The overall size differences between the blank and CDDP-loaded liposomes, while statistically significant, has minor effect on the

function of the liposomes themselves as they still fall within the range of optimal particle size for cell uptake as mentioned previously (Win & Feng, 2005). Comparable study have been carried out previously on fabrication of niosomes using different aqueous media, yielding nanoparticles with varying physical characteristics (Obeid, Khadra, et al., 2017). TFR of 12 ml min^{-1} and FRR of 3:1 were ultimately chosen as the fabrication parameters for the subsequent drug-loaded liposomes production due to the size, stability and lower size variation between the blank and drug-loaded products.

2.4.4 Liposome purification

Filter centrifugation was chosen for liposome purification method over ultracentrifugation to prevent structural damage to the liposomes. It was reported that ultracentrifugation caused damage to liposomes and subsequently loss of the entrapped material (Heeremans et al., 1995). Filter centrifugation on the other hand, runs at much lower centrifugal force and therefore exerts less force on the liposomes, avoiding membrane rupture. The loss of the entrapped materials is particularly concerning since the extent of the loss is unknown and it can affect entrapment efficiency.

Centrifugation is known to generate heat during the process and can adversely affect heat-labile materials. The purification process was carried out at 4°C in order to minimise physical disruption of liposomal membrane (Du Plessis, Ramachandran, Weiner, & Müller, 1996; Moh'd Atrouse, 2002) and possible loss of entrapped CDDP from the liposomes due to exposure to higher temperature. However, this lower centrifugation temperature poses a problem to the filtration process. Arrhenius type of relation governs temperature influence on membrane permeation of a solution (Nilsson, Trägårdh, & Östergren, 2008). Lower temperature affects filtration process

by reducing water flux across filtration membrane (Ben Amar, Saidani, Deratani, & Palmeri, 2007) and increasing retention rate of solutes at a constant pressure and flux (Snow, de Winter, Buckingham, Campbell, & Wagner, 1996), resulting in reduced filtration rate.

This reduction in filtration rate increases the overall time required to filter and concentrate the liposome suspensions. While the initial three centrifugation runs were capped at 1 h per run and the filtrate collected was replaced with the fresh NS, the final centrifugation runs were intended for filtration and ultimately concentration of the liposome suspension itself. These last runs were particularly long, in some cases up to 3.5 h.

2.4.5 CDDP content and entrapment efficiency determination

Platinum is one of the rarest elements found in earth crust with an abundance of 0.005 ppm (American Society for Testing Materials, 1958). ICP-MS detects platinum in the CDDP molecule and measures the concentration accordingly. This instrument was chosen for CDDP quantification due to its speed, sensitivity to an extremely low concentration (detection limit of platinum up to 4.2 ng l^{-1}), resistance against effects of sample degradation and relative simplicity in sample preparation. The samples were prepared in 2% HNO_3 to facilitate ionisation of platinum and the subsequent detection of the isotope. The rarity of the element also makes it an excellent candidate for analysis using ICP-MS as it reduces the probability of environmental contamination of the samples to virtually zero. Quantification of CDDP in NS stock solution used for the aqueous phase in the fabrication process yielded 97% recovery when compared with theoretical value.

CDDP-loaded liposomes from formulation 5 and 7 were tested for CDDP content post purification step to determine the entrapment efficiency of the fabrication process. The entrapment efficiency quantification method is also called an indirect method (Khoshneviszadeh, Fazly, Housaindokht, Ebrahim, & Rajabi, 2016) with a few modifications. On the other hand, quantifying the CDDP content from the purified liposomes is called a direct method. In this experiment, indirect method was chosen over direct method in measuring the entrapment efficiency due to the limitation imposed when filter centrifugation method is used for purification of liposomes, in which it is virtually impossible to fully recover the purified liposomes from the filter. This limitation might introduce an unknown variation in the CDDP quantification which would adversely affect the accuracy of entrapment efficiency value.

Table 2.6 Entrapment efficiency of liposomes produced from formulations 5 and 7 using FRR and TFR of 3:1 and 12 ml min^{-1} respectively. Results shown are means ± SD from three independent samples. * = CDDP content in concentrated liposome suspensions.

	Entrapment efficiency (%)	CDDP concentration* (mg ml^{-1})
Formulation 5	19.54 ± 4.35	1.14 ± 0.25
Formulation 7	23.86 ± 4.65	1.39 ± 0.27

The entrapment efficiency for both formulations were found to be between 19.54 – 23.86% with no significant difference between them (Table 2.9). This is comparable to a previous study pertaining liposomal cisplatin prepared using thin-film hydration method which yielded entrapment efficiency value of 18.5 – 25.9% (Catanzaro et al., 2018). Another study utilising reverse-phase evaporation method for fabrication of liposomal cisplatin yielded lower cisplatin entrapment efficiency of 8.31% in comparison with this study (Toro-Cordova et al., 2018). It has been pointed

out that there is a lack of systematic comparison pertaining entrapment efficiency for liposomes produced using microfluidics method (Carugo, Bottaro, Owen, Stride, & Nastruzzi, 2016a). CDDP concentration of the concentrated liposome suspension in the result reflects the potential of concentrating the liposome suspensions post purification. Filtering out the aqueous solvent increases the concentration of liposomes and subsequently the CDDP in the solution. However, instability can be induced when the liposome suspension is too concentrated, in which the repulsive charge between the particles is unable to prevent flocculation and might lead to membrane fusion and breakdown, subsequently releasing the entrapped drug.

In this experiment, it was found that concentrating CDDP-loaded liposomes solution by reducing the volume to up to 1.14 and 1.39 ml for formulation 5 and 7 respectively did not lead to loss of stability as evidenced by the size, PDI and zeta potential measurement taken post purification which showed negligible changes when compared with values from before purification (Table 2.10). This high concentration of CDDP, close to the initial CDDP concentration used in the fabrication step, demonstrated the possibility of manipulation of the liposomes within a range of concentration without compromising their physical characteristics.

Table 2.7 Size, PDI and zeta potential of concentrated CDDP-loaded liposome suspensions produced from formulation 5 and 7 using TFR and FRR of 3:1 and 12 ml min^{-1} respectively, measured post purification. Pre-purification data were as denoted in Table 7. Data are means ± SD from three independent samples.

	Size (nm)	PDI	Zeta potential (mV)
Formulation 5	109.63 ± 0.37	0.05 ± 0.012	-25.03 ± 1.14
Formulation 7	74.75 ± 0.50	0.12 ± 0.027	-21.23 ± 0.87

2.4.6 Release study

CDDP-loaded liposomes produced from formulation 5 were subjected to 4°C and 37°C during the release study for 72 hours to simulate storage and human *in vivo* temperature. It was observed that at storage condition, the liposomes managed to retain the entrapped CDDP with very minimal leaking (Fig. 2.8). This further proves the stability of the liposomes, particularly in the storage condition and suggests the possibility of long-term storage with minimal or no degradation of both the liposomes and the entrapped material.

Burst release of CDDP was observed at 37°C for the first 8 h and slow release after 8 h up to 72 h (Fig. 2.8). This rapid and sizeable release of entrapped drug from liposomes within the first 10 h is in line with previous reports (Bruglia et al., 2015; Catanzaro et al., 2018; Hua, 2014). It was suggested that incorporation of cholesterol alters the mechanical strength of the lipid bilayer membrane and the effect is governed by several factors (Redondo-Morata, Giannotti, & Sanz, 2012). The study shows that increasing molar concentration of cholesterol in a liposome composition increases the mechanical strength of the membrane at RT.

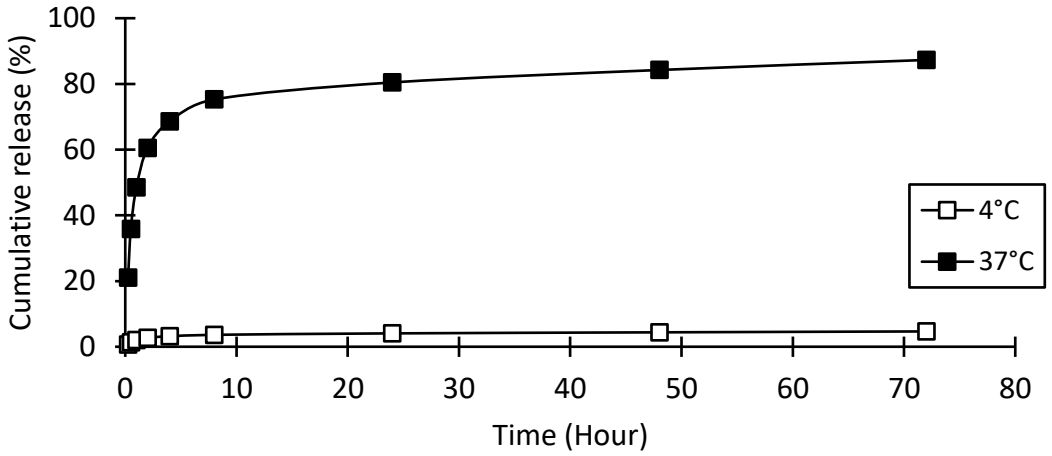

Figure 2.8 Cumulative release profile of CDDP from formulation 5 liposome (n = 1) over 72 h at 4°C and 37°C, expressed in percentage of total entrapped CDDP.

Reduction of the mechanical strength was observed as the temperature increases to the region of physiological temperature. This phenomenon, whilst expected in a liposomal system, hinders the possibility of creating a controlled-release mechanism from said system. Several modifications could be introduced to the liposomal system in order to mitigate this burst release, among those is the incorporation of drug-loaded liposomes in microparticles (Hasan et al., 2007). This modification in particular dramatically reduces the initial burst release effect of the entrapped drug and might be considered as the choice for this project.

2.5 Conclusion

Microfluidics technique with SHM method is deemed suitable for fabrication of highly uniform-sized liposomes. Smaller sized liposomes can be produced by increasing the molar ratio of cholesterol. Modification of aqueous-to-lipid FRR and volumetric TFR are useful in order to achieve the optimal size of the liposomes. Several formulations and combinations of FRR and TFR were found to be suitable candidates for the eventual entrapment of CDDP using the aforementioned microfluidics technique. The chosen formulations, 5 and 7, with FRR and TFR of 3:1 and 12 ml min^{-1} were found to be entrapping CDDP with sufficient efficiency without any discernible changes in terms of physical characteristics post purification. CDDP-loaded liposomes from formulation 5 were found to be maximally retaining the entrapped drug in the storage condition but showed initial burst release commonly associated with the liposomal system at 37°C. Further work should be implemented within the scope in this project in order to determine the suitability and stability of the liposome formulations to be used with irinotecan and a combination of both irinotecan and cisplatin.

Chapter 3

Scale-up Fabrication of Liposomes

3.1 Introduction

The preparation of liposomes takes many shapes and forms and one of the earliest and commonly used method is thin film hydration. This method, as described in literature, involves formation of a thin lipid layer by removing the solvent in a lipid – solvent mixture and subsequently mixing with an aqueous solution to form liposomes (Patel, Rathi, Mongayt, & Torchilin, 2011; Uhumwangho & Okor, 2005). Filter extrusion would then be carried out on the liposomes as a part of the post-production processes in order to produce liposomes with desired size and uniform size distribution (Nayar, Hope, & Cullis, 1989). This poses a challenge in scaling up liposome production using film hydration method due to technical difficulty of increasing liposome yield from the method and making it economically feasible. While thin film hydration is a common method for laboratory-scale production of liposomes, it has been shown that filter extrusion, a method utilised to produce uniformly sized unilamellar liposomes fabricated from thin film hydration method, can be scaled up from a simple laboratory process (Ong et al., 2016) to a continuous and high volume process (Schneider, Sachse, Röβling, & Brandl, 1995) (Schneider et al., 1996).

In this chapter, liposome production on a large scale was explored. Several types of blank and dye-loaded liposomes were produced using NanoAssemblr Blaze, a liposome fabricator for large volume production of up to 1000 ml utilising microfluidics technique with SHM. and its laboratory scale (1 – 15 ml production volume) counterpart, the NanoAssemblr Benchtop. The resultant liposomes from both fabricators were then analysed and compared in terms of physical characteristics, entrapment efficiency and release profile in order to determine the reproducibility of the liposomes when production scale-up is applied.

3.2 Materials

8-hydroxypyrene-1,3,6-trisulfonic acid trisodium salt, also known as pyranine, was obtained from Sigma-Aldrich (Dorset, UK). Triton™ X-100 was purchased from Sigma-Aldrich (Dorset, UK). Dulbecco's PBS used for the aqueous phase buffer were provided by Precision Nanosystems Inc. (Vancouver, Canada). Dulbecco's PBS was diluted with double distilled water from a 10X stock without calcium and magnesium (pH = 7.4) purchased from Corning (NY, USA). All other materials described herein were previously mentioned in Chapter 2 and obtained from Sigma-Aldrich unless stated otherwise.

3.3 Methods

3.3.1 Fabrication of blank and dye-loaded liposomes

Liposomes were fabricated using microfluidics technique with SHM method utilising NanoAssemblr Benchtop (Precision Nanosystems Inc., Vancouver, Canada) for small scale production and NanoAssemblr Blaze (Precision Nanosystems Inc., Vancouver, Canada) for large scale production. Formulation 5 and 7 as stated in Chapter 2 were chosen for the liposome fabrication with a couple of modifications, namely reducing the concentration of DSPG stock solution in ethanol to 1.5 mg ml^{-1} and initial lipid concentration in the lipid phase from 10 mg ml^{-1} to 7.29 mg ml^{-1}. Molar ratio for each of the lipid in the formulations was maintained as in previous study in Chapter 2. Table 3.1 details the volume required from each stock solution and ethanol to make up the lipid phase for both formulations and production scales. Reduction of DSPG stock solution concentration necessitates addition of solid DSPG in the lipid phase for Formulation 5 as the volume of DSPG stock solution needed to be mixed would be greater than the total volume of the lipid phase itself.

Table 3.1 Volume of ethanol, phospholipids and cholesterol stock solutions in µl needed to make 1 and 5 ml lipid phase for small and large-scale production respectively of each of the formulation. * = value in mg.

Formulation	Production scale	Phospholipids			Cholesterol	Ethanol
		DSPC	DPPC	DSPG		
5	Small	109.6	101.8	1.78*	64.4	724.2
	Large	548.0	509.0	8.89*	322.0	3621.0
7	Small	99.6	92.6	673.2	121.8	12.8
	Large	498.0	463.0	3366.0	609.0	64.0

Blank liposomes of both formulations were made using Dulbecco's PBS as the aqueous phase. Two pyranine solutions in Dulbecco's PBS were made with concentration of 1 and 10 mg ml^{-1} as the aqueous phase for the production of dye-loaded liposomes. 3 and 15 ml of aqueous phase is required for small and large production scale respectively. Fabrication parameters were set at TFR of 12 ml min^{-1}, FRR of 3:1 and the production was carried out in RT. Start and end process waste were set at 0.25 and 0.05 ml for small-scale production and 2 and 1 ml for large-scale production respectively.

The freshly prepared liposome suspensions were collected from the instruments. A specific volume was taken from the solutions and diluted 4 times using Dulbecco's PBS prior to analysis and post-processing. The diluted liposome suspensions were kept in 4°C for storage.

3.3.2 Characterisation of liposomes

Particle size analysis of the liposomes was performed using a Zetasizer Nano ZS (Malvern Instrument, Malvern, UK). The procedures and settings were as described

in Chapter 2 in order to determine the average particle size and PDI. All measurements were performed in triplicate.

3.3.3 Liposome purification

Pyranine-loaded liposomes were purified from unentrapped pyranine using filter centrifugation. 4 ml of diluted liposomal solution was added into Amicon® Ultra-4 centrifugal filter (Merck Millipore, UK) with 100 kDa NMWL and centrifuged at 1308 x*g* and 25°C for 30 mins.

Three centrifugation runs were performed, and the filtrate was collected at the end of each centrifugation run and fresh aqueous buffer was added to the concentrated liposome suspension with volume equivalent to the collected filtrate. One final centrifugation run was then carried out for 1 h to concentrate the liposome suspension.

The concentrated liposome suspension was then recovered from the centrifugal filter, diluted with fresh buffer to make up a 700 µl solution for release study. The filtrate from each centrifugation run was then combined to determine the amount of unentrapped pyranine for use of entrapment efficiency determination.

3.3.4 Pyranine content and entrapment efficiency determination

Pyranine content in all samples was analysed using fluorescence spectrophotometry in 96-well polystyrene plates, utilising Synergy H1 Hybrid Multi-Mode Microplate Reader (BioTek Instruments Inc, USA) at excitation wavelength of 454 nm and emission wavelength of 512 nm. Two series of standard solutions were made from diluting the pyranine stock solution (0 - 5 µg ml^{-1}) with Dulbecco's PBS and 0.1% Triton X-100 in Dulbecco's PBS. The standard solutions were measured using the method mentioned above to construct standard calibration curves.

Subsequent determination of pyranine concentration in all samples utilised standard calibration curve from Dulbecco's PBS dilution except for lysed liposomes which utilised 0.1% Triton™ X-100 in Dulbecco's PBS dilution.

Entrapment efficiency was calculated using an indirect method mentioned previously (Tomoko & Fumiyoshi, 2005)

$$Encapsulation\ efficiency\ (\%) = \frac{Pyranine_{total} - Pyranine_{free}}{Pyranine_{total}} \times 100$$

where $Pyranine_{total}$ is amount of pyranine in the initial volume of stock solution in the aqueous phase used during the liposome fabrication step and $Pyranine_{free}$ is the amount of unentrapped pyranine collected after the liposome purification step.

3.3.5 Release study

500 µl of concentrated pyranine-loaded liposome suspensions from both formulations fabricated using 10 mg ml^{-1} pyranine in the initial aqueous phase were filled into dialysis tubes (Sigma-Aldrich) with molecular weight cut-off of 14 kDa and immersed in 40 ml of Dulbecco's PBS acting as release medium at 37.6°C. 5 ml aliquot was taken from the release medium at specific time intervals and immediately replaced with fresh buffer of the same volume.

The release study was carried out over a maximum total period of 70 h. The liposome suspension was recovered from the dialysis tube at the end of the release study and the liposomes lysed with Triton™ X-100 to make up a final concentration of 0.1% in Dulbecco's PBS. Both the lysed liposome suspension and the aliquot were stored in 4°C prior to analysis by fluorescence spectrophotometry.

3.3.6 Statistical analysis

Unless stated otherwise, all measurements and statistical analyses were carried out as described previously in Chapter 2.

3.4 Results and Discussion

3.4.1 Liposome fabrication

Formulation 5 and 7 were chosen for the entrapment of pyranine dye for both small and large-scale production to give some idea on the range of liposome sizes fabricated from both scales of production. These particular formulations were chosen as they produced favourable liposomes as stated in Chapter 2 and are likely to be selected as candidates for further studies. Fabrication parameters such as TFR and FRR were kept constant throughout the production process in order to make sure the variations arise only from the difference in formulation.

Changes were introduced in the formulations in terms of DSPG stock solution concentration and the initial lipid concentration in the lipid phase. The former was reduced from 20 mg ml^{-1} to 1.5 mg ml^{-1} and the latter from 10 mg ml^{-1} to 7.29 mg ml^{-1}. These modifications were implemented to accommodate for the large-scale production method using the NanoAssemblr Blaze as the instrument does not have a heating module attached to it that would allow for a higher temperature fabrication.

These changes, whilst lowering the amount of lipid available for entrapment, allow for preparation of lipid phase in RT. All of the phospholipids and cholesterol stock solutions were able to be made in a temperature of 50°C or lower and stable at RT. Interestingly, the lipid phase mixtures for both formulations were also stable in RT for hours post mixing with no cloudiness nor precipitation observed. This stability

provides improved precision of lipid stock solutions mixing to make lipid phase solution as they no longer have to be in a much higher temperature of 70°C as in the case of DSPG stock solution, thus reducing the possibility of errors mentioned in Chapter 2.

As the lipid phase mixture is stable at RT, it eliminates the need for liposome fabrication at a high temperature of 70°C. While this modification was intended for the use of NanoAssemblr Blaze, it also removes the need for the heating block in NanoAssemblr Benchtop, thus allowing the latter to be used with larger gauge syringes which in turn allows for higher production volume per run.

These modifications introduced another issue to the creation of the lipid phase mixture of formulation 5. As shown in Table 3.1 the DSPG used in the lipid phase is stated in mass (mg) instead of volume needed from the stock solution (ml). This is because the DSPG stock solution volume needed to make such lipid phase solution would exceed the total volume of the lipid phase due to the much lower concentration. Therefore, the amount of DSPG needed was weighed first and mixed with appropriate volume of ethanol before other stock solutions were introduced to the mixture.

Dye entrapment was carried out in lieu of CDDP due to the lack of facility for cytotoxic drug handling and disposal in the laboratory where the experiment was carried out. Pyranine was chosen due to its fluorescence and high degree of solubility in aqueous media. Two pyranine solutions of 1 and 10 mg ml^{-1} were made to study the effect of varying concentration of entrapped material on liposome physical characteristics, entrapment efficiency and release profile.

The NanoAssemblr Blaze utilised for large-scale production in this experiment works on the same principle as the NanoAssemblr Benchtop in terms of liposome fabrication. Both aqueous and lipid phases were introduced to the NanoAssemblr Blaze using a continuous flow pumps instead of syringes. This removes the volume limitation of syringes allows for a much higher production volume. Another feature of the NanoAssemblr Blaze is the built-in dilution port that allows for immediate dilution of freshly prepared liposome suspension post fabrication.

3.4.2 Liposome characterisation

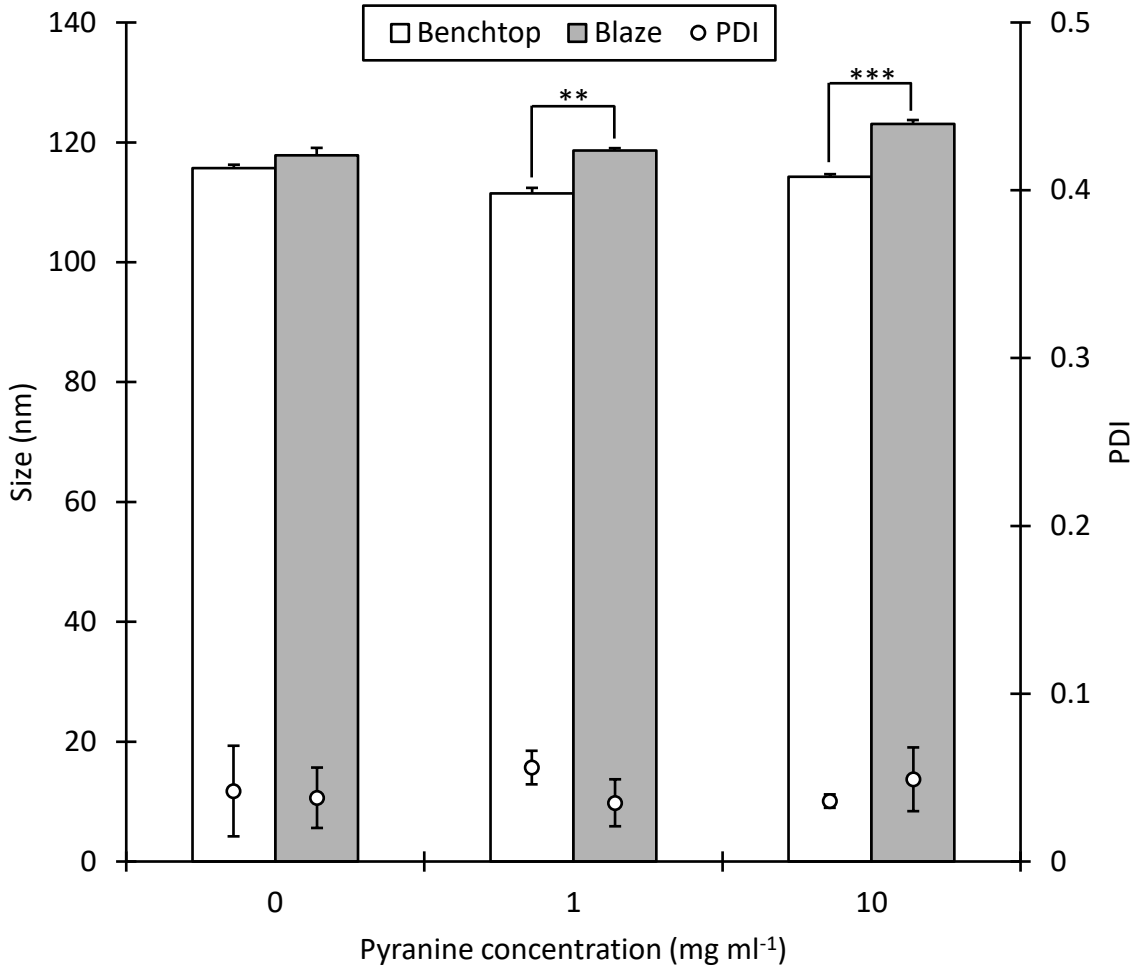

Figure 3.1 Size and PDI of liposomes fabricated from formulation 5, TFR of 12 ml min^{-1}, FRR of 3:1 and a range of pyranine concentration from 0 (blank) to 10 mg ml^{-1} using small (Benchtop) and large-scale (Blaze) production. Results shown are means ± SD from three independent measurements. ** = $p < 0.01$, *** = $p < 0.001$

Fabricated liposomes using both formulations and varying concentrations of pyranine in the aqueous phase were analysed using the DLS to measure size and PDI. It was found that with the liposomes for formulation 7 were smaller than formulation 5, in accordance to previous findings. Significant differences were found between the size of loaded liposomes in formulation 5 (Fig. 3.1) when both scales of production were compared. Dye-loaded liposomes produced from 1 and 10 mg ml^{-1} pyranine in

aqueous phase using NanoAssemblr Blaze were found to be 7.13 nm and 8.8 nm larger respectively in comparison with similar liposomes produced using NanoAssemblr Benchtop. While the size differences are significant, the changes are relatively small (6.4% and 7.7% respectively) and have negligible effect functionally. These changes in size can be attributed to the increasing amount of pyranine in the aqueous phase during the fabrication process.

All blank and pyranine-loaded liposomes fabricated from formulation 5 using both NanoAssemblr Benchtop and Blaze were found to be highly monodispersed with PDI range of 0.035 – 0.056 (Fig. 3.1). The lowest PDI was attained using NanoAssemblr Blaze and 1 mg ml^{-1} pyranine and the highest using the NanoAssemblr Benchtop at the same concentration of pyranine. There were no statistically significant differences among the PDI values.

As mentioned before, liposomes produced using formulation 5 are smaller across the range of pyranine concentration used when compared with formulation 7. There were no significant differences in size between formulation 7 liposomes fabricated using both NanoAssemblr Benchtop and Blaze except when pyranine concentration of 1 mg ml^{-1} was used (Fig. 3.2). The difference of size in that case was 2.84 nm which is an increase of 5.5% from liposomes produced from NanoAssemblr Benchtop. This is a very small change in size and considered as an outlier as there is no apparent trend in size changes in the other sets of liposomes.

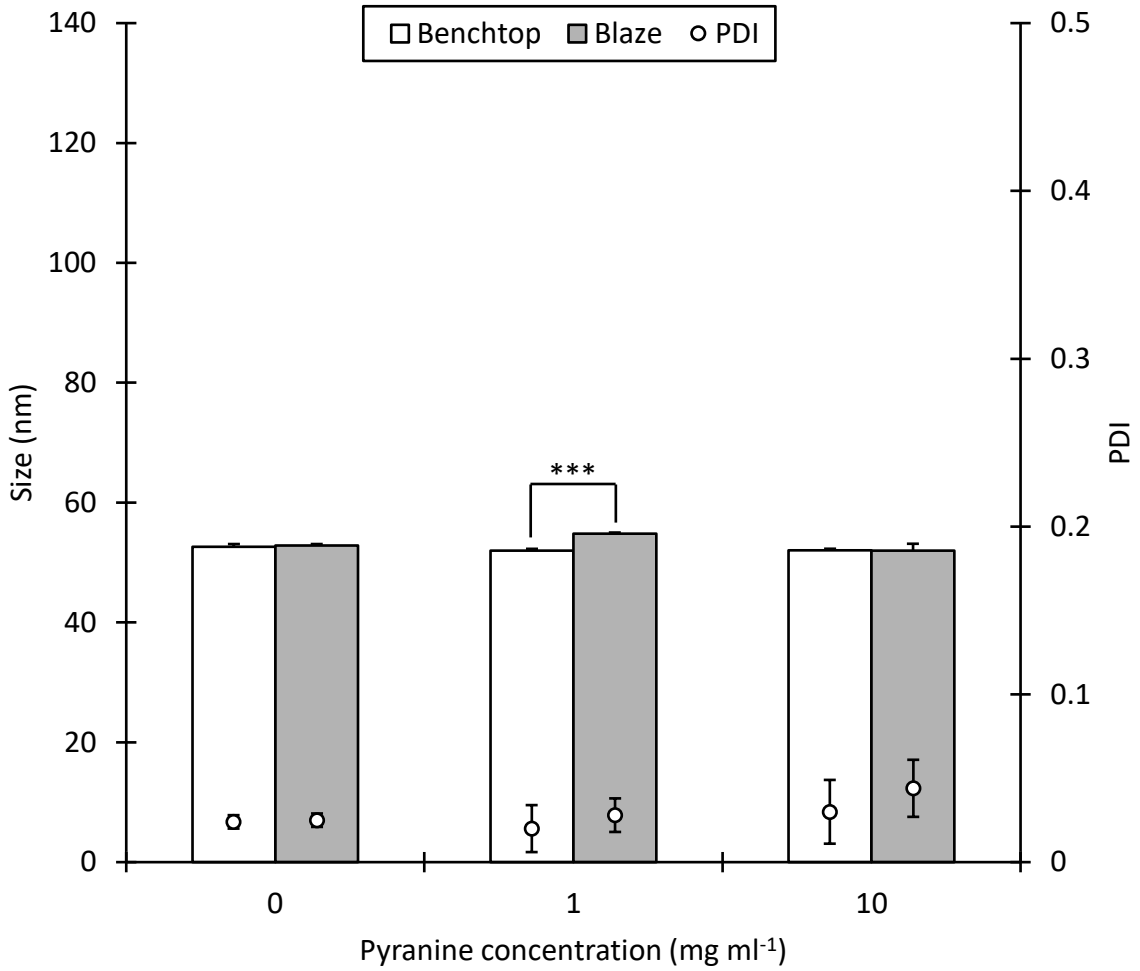

Figure 3.2 Size and PDI of liposomes fabricated from formulation 7, TFR of 12 ml min^{-1}, FRR of 3:1 and a range of pyranine concentration from 0 (blank) to 10 mg ml^{-1} using small (Benchtop) and large-scale (Blaze) production. Results shown are means ± SD from three independent measurements. *** = $p < 0.001$

Liposomes produced from formulation 7 using both production scales and across the range of pyranine concentration are highly monodispersed with PDI range of 0.020 – 0.044 (Fig. 3.2). There were no statistically significant differences between the values of PDI. PDI values of liposomes from formulation 7 are found to be generally lower than PDI values of liposomes from formulation 5, especially in blank and lower concentration of pyranine. This might be due to the higher molar ratio of cholesterol in formulation 7 as suggested by a previous study (Essa, 2010).

3.4.3 Entrapment efficiency

Table 3.2 Entrapment efficiency of pyranine in liposomes fabricated from formulation 5 and 7 using NanoAssemblr Benchtop and Blaze for small and large-scale production respectively, TFR of 12 ml min^{-1}, FRR of 3:1 and initial pyranine concentration range of 1 and 10 mg ml^{-1}. Results shown are mean ± SD from three independent measurements and statistical difference analysis was carried out between liposomes of the same formulation and initial pyranine concentration fabricated on different production scales. ** = $p < 0.01$, *** = $p < 0.001$

Formulation	Initial pyranine concentration (mg ml^{-1})	Entrapment efficiency (%)	
		Benchtop	Blaze
5	1	62.61 ± 0.09 **	65.06 ± 0.28 **
	10	58.78 ± 0.27 ***	61.85 ± 0.31 ***
7	1	24.49 ± 0.17	24.31 ± 0.05
	10	22.61 ± 0.16 **	24.70 ± 0.08 **

Entrapment efficiency of pyranine in formulation 5 liposomes was found to be significantly greater than formulation 7 liposomes (Table 3.2). This difference in entrapment efficiency appears to be related to the size of the resultant liposomes as previously reported elsewhere (Berger, Sachse, Bender, Schubert, & Brandl, 2001). Increasing the concentration of pyranine in the initial aqueous phase from 1 to 10 mg ml^{-1} during the fabrication process had a minuscule but significant effect of lowering the entrapment efficiency (Table 3.2). This virtually negligible difference of entrapment efficiency between low and high content of entrapped material is important in understanding the relationship between the amount of entrapping and entrapped materials to help maximise efficiency in loaded-liposome fabrication.

Interestingly, using different scale of production has a significant but minute differences in entrapment efficiency for all fabrication runs except when formulation 7 was used with 1 mg ml^{-1} in which there was no significant difference observed (Table 3.2). This suggests robustness of both formulations and consistency of resultant products when scaling-up is implemented which in turn, opens up possibilities for a direct scaling-up from laboratory to industrial-size batch production of loaded liposomes.

There was a large and significant difference between the entrapment efficiency of pyranine in this study (Table 3.2) and cisplatin from a previous study (**Error! Reference source not found.**). While the same formulation was used with the same fabrication parameters using similar instrument, some differences should also be noted. Among those are the lower initial lipid concentration, different aqueous buffer was used, and more hydrophilic agent was used for entrapped material. It is unclear at this point which of these parameters contributed to the difference in entrapment efficiency. Further study should be conducted using the same formulation and fabrication parameters with modifications of the aforementioned variables in order to pinpoint the variable or combination of variables that caused the effect and the extent thereof.

3.4.4 Release study

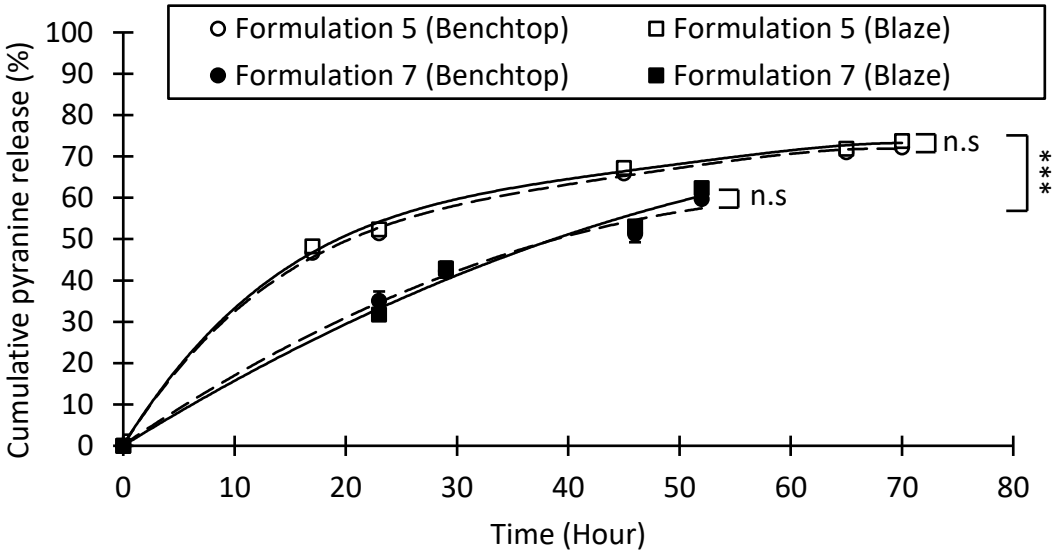

Figure 3.3 Pyranine release characteristics from liposomes fabricated using NanoAssemblr Benchtop and Blaze from formulation 5 and 7, 10 mg ml^{-1} pyranine in the initial aqueous phase, TFR of 12 ml min^{-1} and FRR of 3:1 expressed in percentage of cumulative pyranine release over time. Results are mean ± SD of three independent measurements. Statistical difference analysis was carried out between formulation 5 and 7 at similar time points.

Pyranine release from liposomes of formulation 5 and 7 fabricated using both NanoAssemblr Benchtop and Blaze was quantified by dialysis method in 37.6°C to simulate physiological temperature and Dulbecco's PBS was used as the release medium. Volume of release medium used in this experiment was increased compared to the previous study in Chapter 2 to accommodate for the higher quantity of entrapped material.

Formulation 5 liposomes fabricated using NanoAssemblr Benchtop and Blaze showed no significant difference in the amount of released pyranine over time and the cumulative release tapered out at 73% of the total entrapped pyranine (Fig. 3.3). These liposomes also showed the same release kinetics, indicating the similarity of the

fabricated liposomes using both production scales. Similar observation was also noted for formulation 7 liposomes fabricated using both production scales. There were no significant differences between the percentage of pyranine released from liposomes produced using both NanoAssemblr Benchtop and Blaze and the highest cumulative release was observed at 62% of the total entrapped pyranine.

It was observed that the loaded liposomes exhibited different release kinetics across the formulations. Formulation 7 liposomes were exhibiting significantly lower burst release compared with their formulation 5 counterparts as observed at 22 h time point (Fig. 3.3). Both formulations were releasing the loaded pyranine in a progressive manner over time, but formulation 7 liposomes were releasing significantly lower amount of pyranine compared to their formulation 5 counterparts throughout the release study period. Pyranine release rate was lower for formulation 5 later in the release study period but the same was not observed for formulation 7.

These differences in release characteristics between the two formulations might be caused by the different molar ratio of cholesterol in the formulation. Incorporation of cholesterol in the lipid bilayer affects rigidity and strength of the membrane. Several studies have shown that embedded cholesterol causes an increase in bilayer membrane thickness and lateral order (de Meyer & Smit, 2009), rigidity (Grit, Zuidam, Underberg, & Crommelin, 1993) and thermotropic transition breadth (Eze, 1991) . However, these studies disagreed on the optimal amount of cholesterol incorporation in order to achieve the maximum membrane stability. One study suggested 12.5 mol% of cholesterol is the ideal amount for a dipalmitoylphospatidylcholine – cholesterol system as any addition to this has no significant effect on the membrane fluidity (Sułkowski, Pentak, Nowak, & Sułkowska,

2005). Another study suggested that this bilayer properties modification dramatically increases with addition of up to 30 mol% cholesterol with further addition only increases the effect slightly in a dimyristoylphosphatidylcholine – cholesterol system (de Meyer & Smit, 2009). Another study demonstrated that a liposomal system with a higher cholesterol mol% (40 – 50) exhibited improved mechanical strength and lateral order when compared with systems with lower cholesterol content at high temperature (Redondo-Morata et al., 2012).

Utilisation of a phospholipids mixture in a liposomal system adds another variable in determining the stability, phase transition temperature, release characteristics and more importantly, the role of cholesterol in terms of influence over these parameters. One study explored the effect of cholesterol incorporation in a multi-phospholipids liposomal system and showed that the phospholipids mixture produced liposomes with higher transition peak temperature compared with pure phosphatidylcholine liposomes (Socaciu, Jessel, & Diehl, 2000). The same study also suggested that addition of 16 and 48 mol% cholesterol has no difference in terms of completely removing the temperature transition peak.

When the two formulations were compared, the difference in cholesterol molar ratio between formulation 5 and 7 is quite high as stated in (Table 2.1). This difference suggests that the higher cholesterol molar ratio in formulation 7 liposomes retards the release of pyranine better than formulation 5 liposomes which is as suggested in the literature. While cholesterol plays an important role in determining the release characteristics of the liposomes due to its effect on bilayer membrane stability and fluidity as mentioned previously, the complexity of these liposomal systems might also affect the very same characteristics when the overall systems were considered. Without

further study on the formulations themselves, particularly concerning the effects of varying constituent components variations, it is premature to draw conclusion on either the optimum cholesterol or phospholipids content of the liposome formulation for a specific release characteristic.

3.5 Conclusion

Liposome production scale-up was successfully demonstrated using NanoAssemblr Benchtop and Blaze for small to large-scale using microfluidics technique with SHM method respectively. Similar liposome physical characteristics, entrapment efficiency and release profile were observed across the production scales when the same formulation was used, demonstrating reproducibility of the results when production scaling up is applied. It was discovered that increasing the pyranine concentration in the aqueous phase from 1 mg ml^{-1} to 10 mg ml^{-1} during liposome fabrication effects minor difference in entrapment efficiency. Another discovery is that different release kinetics were observed between formulation 5 and 7 liposomes with slower release observed in formulation 7 liposomes, highlighting the possible correlation between the increased molar ratio of cholesterol and increased delay in pyranine release. These discoveries suggest possibilities of improving the entrapment efficiency and manipulating the formulation to achieve desired release characteristics.

Chapter 4

Fabrication, Purification and Characterisation of Single and Dual-Loaded Cisplatin/Irinotecan Liposomes

4.1 Introduction

CPT-11 is a semisynthetic camptothecin analogue used in treatment of both NSCLC and SCLC (Rothenberg, 2001). Its mechanism of action involves binding with Topoisomerase I – DNA complex and interfering with DNA replication, resulting in cell division arrest and death (Xu & Villalona-Calero, 2002). CDDP is the one of the platinum-based drugs utilised in treatment of various types of cancers (Desoize & Madoulet, 2002), including but not limited to NSCLC (Pignon et al., 2008) and SCLC (Abrams, Lee, Murray, Pryer, & Cherrington, 2003). CDDP acts by binding to cellular DNA, halting cell division and ultimately causing cell apoptosis (Dasari & Tchounwou, 2014). While CDDP alone was used for decades as the first-line treatment for SCLC (Evans et al., 1985), combination treatments such as etoposide and CDDP were favoured as they produced better results (Mascaux et al., 2000). The combination of CPT-11 and CDDP has been shown to be effective against cancer cells *in vivo* (Kano et al., 1992), leading to the combination being tested and applied successfully in a clinical setting (Hanna et al., 2006). More recent evidence shows that the combination of CPT-11 and CDDP produced a better response and survival rate for patients with SCLC compared with etoposide and CDDP combination (Jiang et al., 2010).

Several side-effects have been noted for the prolonged exposure to both chemotherapy agents during treatment course such as nephrotoxicity (Iwasaki et al., 2005) and neutropenia (Kosmas, Tsavaris, Malamos, Vadiaka, & Koufos, 2001) for CDDP with myelosuppression (Innocenti et al., 2014) and diarrhoea (Rougier et al., 1998) for CPT-11. Some countermeasures are deployed in order to improve the quality of life of the patients facing such side-effects such as administration of acetorphan and loperamide to counteract diarrhoea in the case of CPT-11 therapy (Saliba et al., 1998),

but much of these side-effects are unavoidable and can potentially lead to treatment refusal due to unacceptable toxicity (Kim et al., 2017). Another concern of utilising conventional chemotherapy in cancer treatment is the development of drug resistance (Dasari & Tchounwou, 2014; Xu & Villalona-Calero, 2002). One of the strategies proposed to counteract such side-effects and resistance is the use of drug-loaded liposomes (Ramachandran, Quist, Kumar, & Lal, 2006). Utilisation of nanoparticles, for example, allows higher accumulation of the chemotherapy agents at the intended site with much lower dosage requirement, therefore potentially reducing the side-effects and invocation of drug resistance altogether (Fichtner et al., 2003).

Previous studies have shown the therapeutic efficacy of CPT-11/CDDP combination in clinical setting for treatment of lung cancer (Hanna et al., 2006; Jiang et al., 2010). A meta-analysis of 12 randomised controlled trials involving 2030 patients with previously untreated extensive-stage SCLC demonstrated that the CPT-11/CDDP combination significantly improves survival rates in comparison with EC regimen (Liu, Wang, Liu, & Liu, 2018). It should be noted that varying CPT-11 dose and schedule were used in the trials. Combination of liposomal CPT-11 and CDDP has been demonstrated previously with success, showing higher activity *in vitro* against cancer cells when compared with free drugs (Tardi et al., 2009). The study demonstrated the activity of CPT-11/CDDP combination against various cancer cells ranges from antagonism to synergy with variation in molar ratio of the drugs (Tardi et al., 2009). These findings opened a litany of possibilities on the application of such combinations in terms of tailoring the specific dosage of each of the liposomal drugs in order to maximise their effectiveness whilst minimising side effects to the patients. One of these possibilities is the fabrication of liposomes loaded with both drugs with

a specific molar ratio, which was previously demonstrated with dual-entrapment of carfilzomib/doxorubicin (Ashley et al., 2016) and erlotinib/doxorubicin (Morton et al., 2014). It was exhibited in both studies that the dual-entrapment improves tumour cell killing activity by means of synergistic and modified release of the agents respectively. Similar attempt for dual-entrapment will be attempted with CPT-11/CDDP combination in the course of this study.

Liposome purification is one of the highly broached subjects in the field of nanomedicine. In the course of drug entrapment process, production of waste materials in the resultant liposomal solution consisting of unentrapped drug, lipids and solvents is inevitable. Removal of these wastes is highly pertinent in order to obtain a purified end product, which would be indispensable in the accurate quantification of the entrapped material. Several methods have been discussed in the literature such as dialysis (Jin, Engelhart, Adamala, & Szostak, 2018), ultracentrifugation (Bakonyi, Berkó, Budai-Szűcs, Kovács, & Csányi, 2017), filter centrifugation (Cipolla et al., 2014) and TFF (Wagner, Vorauer-Uhl, & Katinger, 2002). More recently, advancement in liposome fabrication particularly in utilisation of microfluidics has been used in conjunction with TFF to create a continuous process from fabrication to purification (Dimov, Kastner, Hussain, Perrie, & Szita, 2017). This study aims to demonstrate fabrication of liposomes loaded with CPT-11, CDDP and CPT-11/CDDP combination in large volume using microfluidics with SHM method followed by purification of the resultant products using filter centrifugation and TFF. The physical characteristics, stability, filtration efficiency and entrapped drugs of the liposomes are quantified at various points throughout the study in order to identify the effects of such parameters on the resultant products.

4.2 Materials

CPT-11 of ≥ 97% purity was one of the drugs used in this study. D-(+)-trehalose dihydrate from starch of ≥ 99% purity was used as the cryoprotectant. Sodium hydroxide (≥ 97% purity) was used with deionised water to create 0.1 M NaOH solution. Triton™ X-100, a nonionic surfactant, was used to lyse liposomes. All other materials described herein were previously mentioned in Chapter 2 and obtained from Sigma-Aldrich unless stated otherwise.

4.3 Methods

4.3.1 Preparation of CPT-11 and CDDP aqueous phase solutions

Three types of aqueous media were utilised in this study, namely NS, PBS and NS with 10 mM trehalose. CDDP was weighed carefully and dissolved with appropriate volume of NS with 10 mM trehalose to make a 3 mM CDDP solution. CPT-11 was weighed and dissolved in NS and PBS aqueous media respectively to make up 1 mg ml^{-1} CPT-11 solutions and in NS with 10 mM trehalose to make up a 1.5 mM CPT-11 solution. Dissolution was carried out according to a method previously described (Ci, Chen, Yu, & Ding, 2014) with slight modifications. Briefly, the solutions were vortexed for 30 s and then heated in water bath at 80°C whilst sonicated for 30 min. They were cooled to RT afterwards. CPT-11/CDDP solution was created by weighing and dissolving CDDP in the CPT-11 solution. CPT-11/CDDP solutions of 1:1 CPT-11 to CDDP mass concentration ratio were made using NS and PBS media and 1:2 CPT-11 to CDDP molar concentration ratio using NS with 10 mM trehalose medium. Incremental heating mechanism was applied to the CPT-11/CDDP solutions in which they were vortexed for 30 s before heated and sonicated in water bath for 10 min at 60°C. The process was then repeated twice with temperature

increment of 10°C for each successive repetition. The solutions were then cooled down to RT and were kept at 4°C and protected from light prior to analysis. The 1.5 mM CPT-11, 3 mM CDDP and CPT-11/CDDP 1.5:3 mM solutions in NS with 10 mM trehalose were used as the aqueous phase for liposome fabrication to produce drug-loaded liposomes.

4.3.2 Liposome fabrication

Liposomes were fabricated with NanoAssemblr Benchtop (Precision Nanosystems, Canada) using microfluidics technique with SHM method. Liposomes of formulation 5, 6 and 7 were chosen to be fabricated as they were proven to be stable as mentioned in Chapter 2. The molar ratios of DSPC, DPPC, DSPG and cholesterol for these formulations were as detailed earlier in Table 2.1. TFR was fixed at 12 ml min^{-1} and aqueous-to-lipid FRR was set at 3:1. Lipid phase of the formulations was prepared in accordance to the method mentioned in Chapter 3. Briefly, the lipid phase mixtures were produced from phospholipids and cholesterol stock solutions in ethanol of 20 mg ml^{-1} to create an initial lipid concentration of 7.29 mg ml^{-1}. Each of the formulations was fabricated at RT using different aqueous phases for a blank formulation and loading different drugs, namely 1.5 mM CPT-11, 3 mM CDDP and a 1.5:3 mM CPT-11/CDDP combination. Blank liposomes were fabricated from formulation 5 using both NS and NS with 10 mM trehalose as the aqueous phases at both RT and 70°C to study the effect of trehalose addition and temperature on physical characteristics of liposomes. Freshly prepared liposome suspensions were diluted 4 times with the corresponding aqueous diluent before proceeding to post-processing steps.

4.3.3 Liposome purification by filter centrifugation

Drug-loaded liposomes were purified from unentrapped drug using filter centrifugation method as mentioned previously in Chapter 3. Briefly, 4 ml of diluted liposomal solution was added into Amicon® Ultra-4 centrifugal filter (Merck Millipore, UK) with 100 kDa NMWL and centrifuged using HERMLE Z 323 K centrifuge (HERMLE Labortechnik GmbH, Germany) with fixed angle rotor at 5000 *xg* and 25°C for 1 h.

6 sets of drug-loaded liposome suspension fabricated from formulation 5 were purified using this method with each set consisting of three independent production batches of the liposome. The sets were treated with different number of rinses, ranging from 0 ml (x0) to 20 ml (x5). These rinses of 4 ml NS with 10 mM trehalose each were administered after each centrifugation run. These liposome suspension sets were then subjected to a final centrifugation run to concentrate the system to approximately 250 µl of remaining volume. Filtrates produced from the centrifugation process from each set were then combined and diluted to 50 ml with blank diluent. Filter centrifugation process was also carried out for formulation 5 and 6 liposomes containing CPT-11 using similar parameters except for number of rinses in which only 3 rinses were applied.

Concentrated liposome suspensions were recovered from the filters after the centrifugation runs were completed. Sufficient amount of blank diluent was used to rinse the filters and were then collected and added to the recovered concentrated liposome to make 1 ml solutions. The filtrates and the concentrated liposome suspensions were then stored at 4°C prior to analysis of drug content and liposome size.

4.3.4 Liposome purification by TFF

TFF of drug-loaded liposomes was carried out using Vivaflow® 50R (Sartorius-Stedim, Germany) utilising Hydrosart® membrane with molecular weight cut-off (MWCO) of 5 kDa. The device was connected to a Masterflex™ economy drive peristaltic pump (Cole-Palmer, USA) with size 16 Masterflex™ easy load pump head (Cole-Palmer, USA) and an air-tight 500 ml sample container (Sartorius, Germany) (Fig. 4.1a). A modification was carried out on the sample container to accommodate for the volume of liposome suspension used for this experiment by means of a holder bracket attached to the lid of the reservoir (Fig. 4.1b). The bracket was designed using SketchUp 2016 (Trimble, USA) software to hold a 15-ml centrifuge tube with a diameter of 17.5 mm and use 3.6 mm external diameter Tygon® LP1200 tubes. The bracket was printed with Replicator 2X Experimental 3D Printer (Makerbot Industries, USA) using acrylonitrile butadiene styrene (ABS) as the construction matrix.

The filtration process was carried out by first draining the device of 10% ethanol in deionised water and rinsing the device by circulating and subsequently draining 50 ml deionised water for three times followed by 50 ml NS with 10 mM trehalose for one time. 80 ml of drug-loaded liposome suspension and 240 ml of NS with 10 mM trehalose solution was loaded in the sample container and the diluent reservoir respectively. The peristaltic pump was turned up gradually until the pressure within the TFF device reached 2.5 bar as displayed by the pressure gauge. The system was left running for 90 minutes and afterwards the remaining liposome suspension was transferred into a 15-ml centrifuge tube and attached to the holder bracket. The process was left running for another 15 mins to further filter and concentrate the liposome

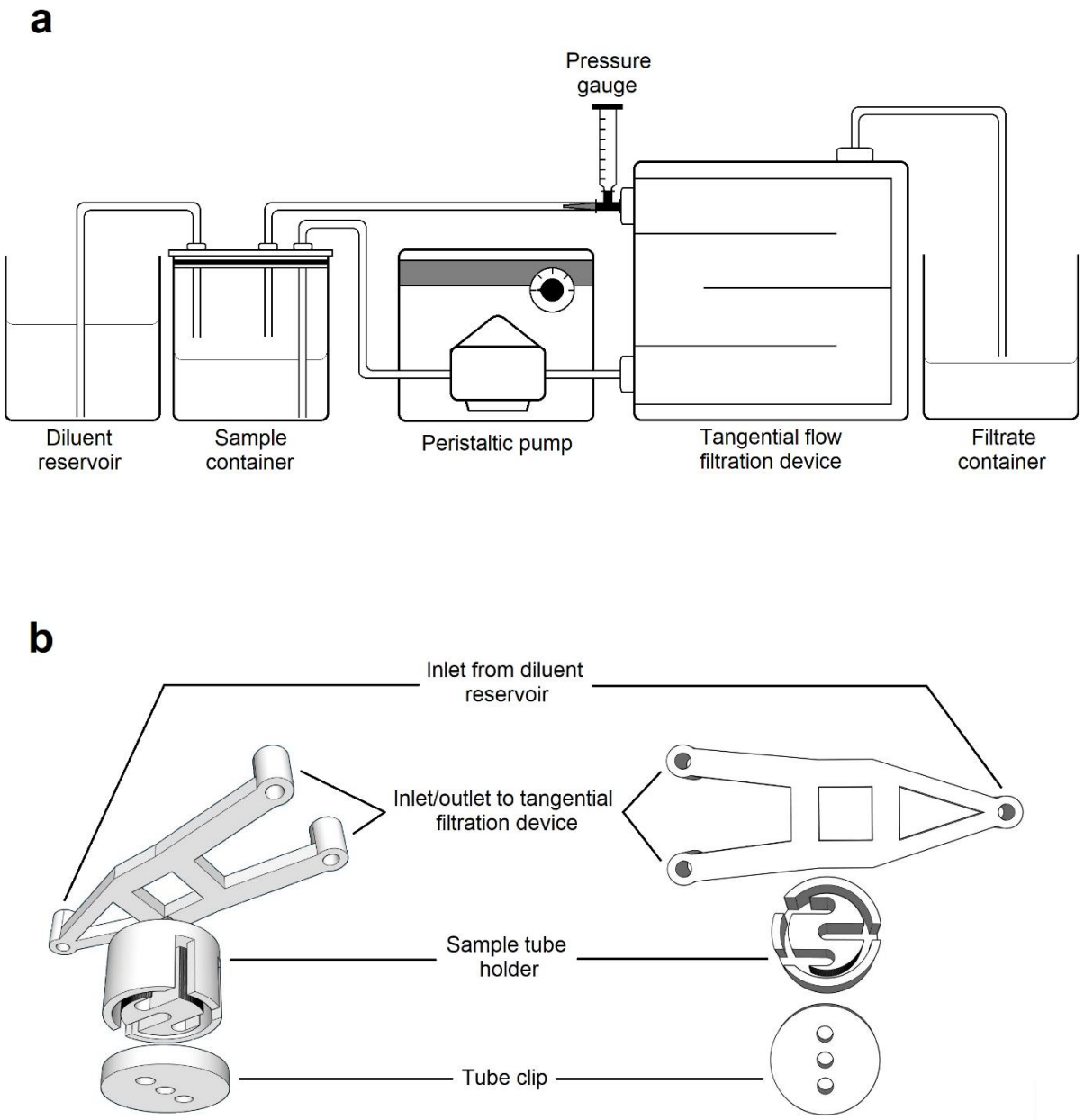

Figure 4.1 (a) Schematic diagram of TFF setup. (b) Exploded view (left) and bottom view (right) of the modification added to the TFF setup. The modification was installed on the lid of the sample container shown in the schematic diagram. Drawings are not to scale.

suspension. 5 ml of diluent was used at the end of the filtration process to rinse the device and recover the remaining liposomes in the system. The concentrated liposome suspension was collected and added with sufficient volume of diluent to make 10 ml of the liposome suspension. The filtrate produced from the TFF device was collected throughout the filtration process and diluted to 250 ml using the diluent. Both concentrated liposome suspension and filtrate were stored at 4°C prior to analysis of liposome size and drug content. The TFF device was cleaned by passing 200 ml of 0.1M NaOH followed by circulating and draining copious amount of deionised water. The device was then filled with 10% ethanol for storage in 4°C.

4.3.5 Physical characterisation and stability study

Liposome size and PDI were measured using dynamic light scattering method as detailed previously in Chapter 2 using a Zetasizer Nano ZS (Malvern Instrument, Malvern, UK). Four samples of blank formulation 5 liposomes obtained from varying fabrication parameters of two different aqueous phases (NS and NS with 10 mM trehalose) and two different fabrication temperatures (RT and 70°C) were subjected to stability study for 28 days. The same study was also carried out for drug-loaded formulation 5 liposomes (CPT-11, CDDP and CPT-11/CDDP combination). Physical characterisation was carried out for blank and drug-loaded liposomes of formulation 6 and 7 prior to filter centrifugation and post-centrifugation for CPT-11-loaded liposomes. Blank and drug-loaded liposomes subjected to TFF method fabricated from all the formulations were characterised pre- and post-filtration.

4.3.6 Drug content analysis

CPT-11 concentration was determined using UV spectrophotometry (Jenway Genova Plus, Cole-Palmer, UK). CPT-11 stock solutions were diluted to a series of standard solutions with a known concentration range. These standard solutions were then measured using the UV spectrophotometry by determining their absorption at detection wavelength (λ_d) of 370 nm. The absorbance readings were then plotted against the CPT-11 concentrations to create standard curve. The CPT-11 containing samples were then measured using the same method and the concentrations were then calculated from the absorbance readings using the corresponding standard curve equation.

The effect of diluent variations and CDDP addition to the UV absorbance of CPT-11/CDDP combination solution was also studied in this experiment. Briefly, CPT-11 stock solutions were diluted to a series of standard solutions with concentrations ranging from 5-25 µg ml^{-1} (NS and PBS) and 5-25 µM (NS with 10 mM trehalose). The standard solutions were then measured using the method mentioned above to create standard curves. The CPT-11/CDDP solutions were then diluted to an expected concentration of CPT-11 of 15 µg ml^{-1} (NS and PBS diluents) and 15 µM (NS with 10 mM trehalose) and measured using the UV spectrophotometry method. The actual concentrations of CPT-11 in those samples were then calculated using the same method as standalone CPT-11 solution mentioned above. The results were expressed in terms of recovery percentage using the following equation.

$$Recovery\ (\%) = \frac{CPT-11_{combination}}{CPT-11_{stock}} \times 100$$

where $CPT\text{-}11_{combination}$ is the CPT-11 concentration measured from the CPT-11/CDDP combination solutions and $CPT\text{-}11_{stock}$ is the CPT-11 concentration measured from the CPT-11 stock solutions.

CPT-11 and CDDP concentration of purified and concentrated liposome suspensions from both purification methods was measured in this study. CDDP concentration of the CDDP-containing samples was determined using the ICP-MS method mentioned previously in Chapter 2. CPT-11 concentration of the liposome samples was determined using the same UV spectrophotometry method. 0.6 ml of the concentrate was diluted with 2.4 ml of 10% Triton X-100 and heated at 50°C for 30 mins in water bath to facilitate lysis of the liposomes. The solution was then cooled down to RT before analysis. The standard curve used for the determination of CPT-11 concentration in the liposome samples was constructed using a series of standard solutions produced from diluting CPT-11 stock solution in 10% Triton X-100 diluted in NS with 10 mM trehalose in 1:4 volume ratio.

4.3.7 Statistical analysis

Unless stated otherwise, all measurements and statistical analyses were carried out as described previously in Chapter 2.

4.4 Results and Discussion

4.4.1 Preparation of CPT-11 and CDDP aqueous phase solutions

CPT-11 was observed to be only slightly soluble in NS, NS with trehalose and PBS at RT even after vortexing and sonication. Heating the solutions to 80°C improves solubility of CPT-11 in all the aqueous media as described previously (Ci, Chen, Yu, & Ding, 2014). The method was slightly modified by significantly reducing the heating

period from 24 h to 30 min and sonicating the solutions throughout the heating period. CPT-11 produced clear, yellowish solution in all the aqueous media after the process and remained stable after cooled down to RT. When CDDP was introduced to the CPT-11 solutions to form the CPT-11/CDDP solutions, formation of precipitates was observed in the solutions, presumably from undissolved CDDP. These precipitates were found to be fully dissolved after the incremental heating process. The resultant clear, yellowish solution remained stable after cooled down to RT.

CPT-11 undergoes reversible, pH-dependent hydrolysis from the active form (lactone) to inactive form (carboxylate). According to a previous study, the lactone form is the most predominant at pH 3 while the carboxylate form is the most predominant at pH 10 (Ci et al., 2014). The carboxylate form retains the side effects associated with administration of CPT-11 due to its acetylcholinesterase inhibition activity while unable to exert its desired pharmacological activity due to the open-ring carboxylate structure (Beretta & Zunino, 2007). Introducing high temperature heating to facilitate CPT-11 dissolution in the aqueous media does not seem to affect the stability of the dissolved CPT-11 in terms of conversion between the two forms (British Pharmacopoeia Commission, 2017; Ci et al., 2014).

NS was chosen over PBS to be mixed with trehalose for the aqueous phase medium due to several reasons. Trehalose, a nonreducing sugar, was chosen over other saccharides to be used in the aqueous phase as cryoprotectant for future freeze-drying process due to its biocompatibility (Rodrigues et al., 2008), lower reactivity and higher glass transition temperature (T_g) (Abdelwahed, Degobert, Stainmesse, & Fessi, 2006). Introduction of trehalose added another spectrum in the complexity of the delivery system in terms of entrapment efficiency as trehalose is a relatively large molecule

with a molecular weight of 342.296 g mol^{-1} which could compete with drug loading inside the liposome, resulting in lower entrapment efficiency (Zaru, Mourtas, Klepetsanis, Fadda, & Antimisiaris, 2007). A trehalose concentration of 10 mM was chosen to emulate a previous study in order to minimise the effect of trehalose on the entrapment efficiency of the drugs whilst obtaining a stable and acceptable freeze-dried liposome end product (Zaru et al., 2007).

The use of PBS as the aqueous medium is associated with high conversion rate of CPT-11 from lactone to carboxylate form. A previous study has shown that in PBS, only 13% of CPT-11 remains in lactone form (Burke, Munshi, Mi, & Jiang, 1995). CDDP diluted in NS produced a low pH solution as demonstrated by a previous research showing that 0.1 and 0.4 mg ml^{-1} CDDP in NS produced solutions of pH 4.2-4.4 and 3.7-3.8 respectively (Sewell, 2010). This low pH CDDP solution in NS could help in retaining a high lactone form fraction of CPT-11 in the CPT-11/CDDP solution, thus improving its cytotoxic effect. The pH stabilising effect of PBS which maintains its pH at 7.4 also has a detrimental effect on CDDP. A study has shown that the degradation rate of CDDP is higher in a solution with high pH (Zieske et al., 1991). In addition, NS was chosen because of its compatibility to be used as vehicle for in vivo drug administration and ability to stabilise CDDP in aqueous solution by preventing substitution of chlorine ions with hydroxide ions (Karbownik et al., 2012) while another study has determined that PBS is not very efficient in preventing the substitution process (Davies et al., 2000).

The CPT-11-to-CDDP molar ratio of 1:2 was chosen for the CPT-11/CDDP solution in NS with trehalose as this combination has been shown to have the maximum synergistic effect of both drugs against A549 cancer cells with the lowest

concentration difference between the constituent drugs (Tardi et al., 2009). All CDDP containing solutions were protected from light to prevent accelerated degradation (Zieske et al., 1991). They were stored at RT instead of 4°C as previous experiences have shown that storing CDDP solution in 4°C caused formation of crystals in the solution. CPT-11 and CPT-11/CDDP solutions in all aqueous media were stable during the observation period of 2 weeks after they were prepared except for CPT-11/CDDP solution in NS with trehalose which produced visible precipitates 3 days after preparation. Heating the solution to 80°C successfully dissolved the precipitates but the effect of this reheating process to the chemical structure and cytotoxic effect of the drugs is still unknown.

4.4.2 Liposome fabrication

Several changes were introduced to the liposome fabrication process for this experiment. The aqueous phase medium was changed from PBS to NS and NS with 10 mM trehalose as described previously. Fabrication process temperature was also changed from 70°C to RT. These alterations necessitate detection and quantification, if any, of changes to the physical characteristics and stability of the liposomes or during the fabrication process itself. Blank liposomes were fabricated from Formulation 5 was chosen to this effect. Fabrication parameters were set at 12 ml min^{-1} and 3:1 for TFR and FRR respectively for this experiment to match with previous experiment described in Chapter 3.

The lipid mixture prepared using the composition described yielded a lipid phase stable at RT as mentioned in Chapter 3, therefore allowing the fabrication process to be carried out at 70°C using the heating block and RT with the heating block removed. This step is necessary to observe and compare between the liposomes

produced at RT and 70°C. The resultant blank liposome products of this experiment from both fabrication temperatures and using both NS and NS with 10 mM trehalose were found to be stable visually without any precipitation immediately after production and subsequent dilution.

Blank and drug-loaded liposomes were fabricated using formulation 5, 6 and 7 using larger volume of both lipid and aqueous phases to mimic large-scale production as was described in Chapter 3. This higher volume of production was achieved due to stabilisation of the lipid phase at RT, removing the need for the heating block on the NanoAssemblr Benchtop subsequently enabling larger syringes to be used. Due to the design of the NanoAssemblr Benchtop, lower production volume was expected when compared with NanoAssemblr Blaze which has been designed for large, continuous production as demonstrated in Chapter 3.

The larger liposome production volume is instrumental in rendering the TFF process feasible. This is due to the relatively larger volume of liposome suspension required to effectively run the aforementioned process in comparison with filter centrifugation process. In order to obtain this volume, 2 fabrication runs producing a total 40 ml of undiluted liposome suspension were carried out in order to yield enough liposome suspension for both filter centrifugation and TFF processes. The same amount of liposome suspension can be obtained using the NanoAssemblr Benchtop with the heating block on, but the lower yield would require the fabrication process to be repeated in a higher number of times. This, in turn, could lead to inconsistencies between batches due to human error.

The blank and drug-loaded liposome suspensions produced from all formulations were found to be stable without any precipitation immediately after fabrication. The solutions were diluted post-fabrication in order to lower the concentration of ethanol and increase the stability of the liposomes, as per previous experiments.

4.4.3 Liposome purification by filter centrifugation

Liposome purification is an important step in the production of drug-loaded liposomes. Unentrapped drugs that remained in the liposome suspension can interfere with subsequent quantitative analyses such as determination of entrapment efficiency and *in vitro* tests as they can greatly influence findings by providing false representative results for both instances.

Filter centrifugation as a method for liposome purification has been explored previously utilising pyranine-loaded liposomes. However, it is pertinent to determine the point in which the unentrapped materials are fully removed from the liposome suspension. This experiment was designed with 6 varying number of rinses to determine the end point of this purification method in which the unentrapped drugs were fully removed from the solution via incremental rinsing technique. This technique was chosen in lieu of bulk treatment due to the limitation of the centrifugal filter device which can only hold 4 ml at a time.

Quantification of the drugs in the concentrated liposome suspensions was utilised to determine the effectiveness of the purification method and number of rinses required in order to achieve complete removal of the unentrapped drugs from the liposome suspensions. It was hypothesised that the drug concentration within the

liposome suspensions will continuously decrease with increasing number of rinses until a certain equilibrium point in which no decrease of drug concentration could be detected. At this point it is assumed that all unentrapped drugs were completely removed from the solution and the only drug concentration detected was from the entrapped drug released from the lysed liposomes.

As shown in Fig. 4.2, this equilibrium point varies slightly between the drugs and combination thereof from 4 ml (CPT in CPT-11/CDDP combination) and 8 ml (others) of rinses. However, 12 ml of rinse was chosen to be implemented in all liposome purification studies in order to improve the certainty of complete removal of the unentrapped drugs whilst maintaining the minimum number of rinses and therefore the amount of time required. The earlier hypothesis was also proved with the pattern of drug concentration over number of rinses. It is also interesting to note that the concentrations of both drugs in the CPT-11/CDDP combination were lower in comparison with standalone CPT-11 and CDDP. This suggests that both drugs competed for entrapment within the liposomes as both of them are soluble in aqueous solution.

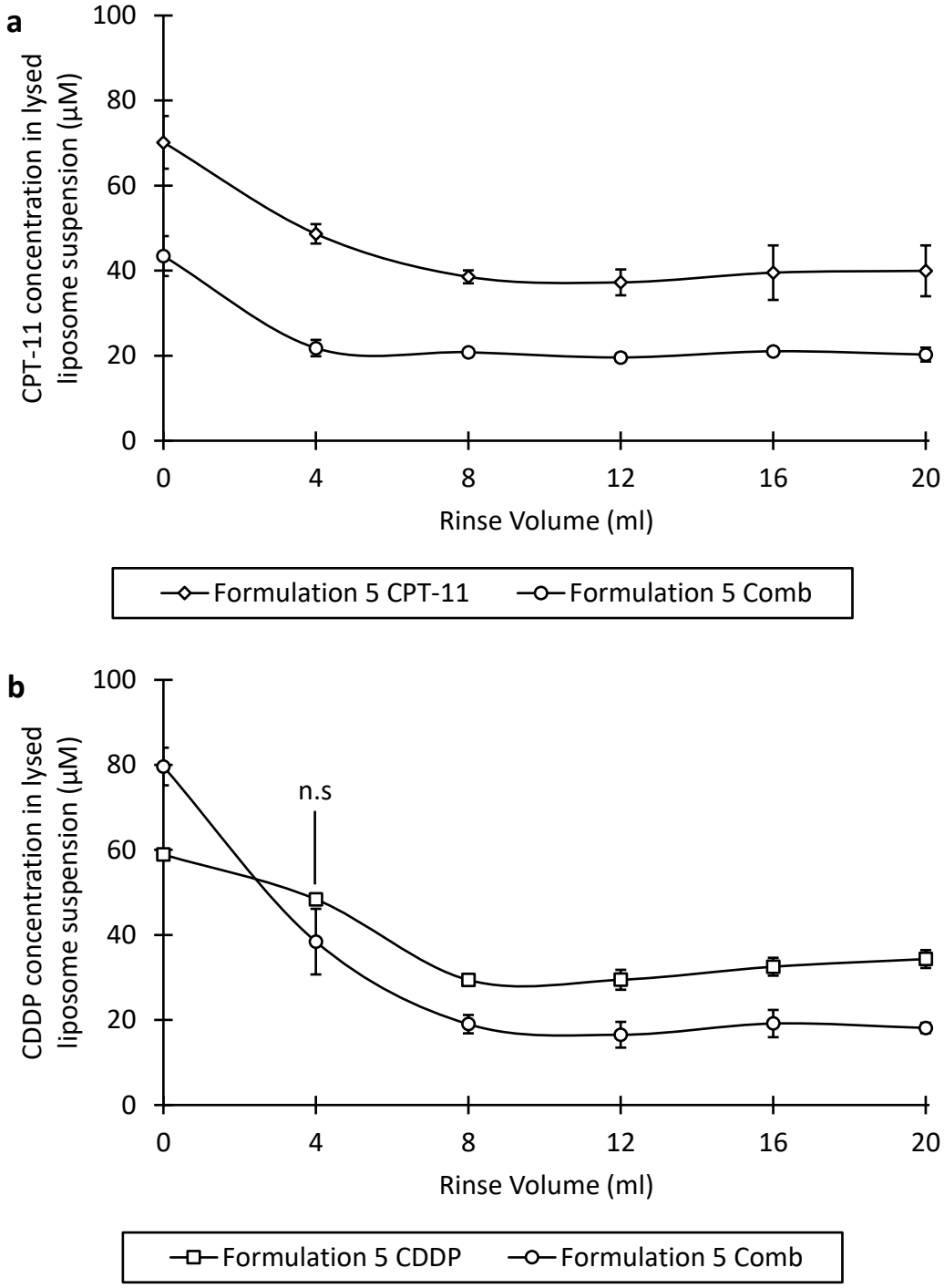

Figure 4.2 Concentration of CPT-11 (a) and CDDP (b) in lysed formulation 5 liposomes containing CPT-11, CDDP and CPT-11/CDDP combination post filter centrifugation with varying volume of rinses in between centrifugation cycle from 0 ml (x0) to 20 ml (x5) in increments of 4 ml. Data points of the same rinse volume for both (a) and (b) were found to be significantly different ($p < 0.05$) except if stated otherwise.

4.4.4 Liposome purification by TFF

In this study, TFF was explored as one of the liposome purification methods. TFF was considered due to its compatibility in purifying large volume of solution in a continuous manner in a shorter period of time. Vivaflow® 50R with Hydrosart® membrane (5 kDa MWCO) was chosen for this specific purpose due to its simple setup, reusability, extremely hydrophilic and virtually non-fouling capacity.

The modification on the sample container was necessitated by the low volume of the liposome suspension at the end of the filtration cycle and the need to maintain adequate pressure inside the TFF device in order to allow further purification and concentration of the remaining sample. As the sample container itself is voluminous (500 ml) in relation to the concentrated liposome suspension (~10 ml), the latter was carefully recovered from the sample container at the end of the filtration cycle, placed in a 15 ml centrifuge tube attached to the holder bracket and the filtration was resumed. ABS was chosen as the material for the holder bracket due to its convenience to be used with the 3D printer and resistance to chemical and solvent cracking (Nugent, 2011).

The use of size 16 peristaltic tubing in the original setup of the sample container was also replaced in favour of the smaller and more flexible Tygon® LP1200 tubing to accommodate for the smaller diameter of the centrifuge tube and placement of the tubing within the holder bracket. These changes had no effect on sample circulation, creation and maintenance of pressure within the system and therefore normal filtration process was not affected.

The TFF device relies on peristaltic pump to create sufficient pressure within the system in order to commence the filtration process. However, due to the mechanism on which peristaltic pumps operate, continuous application of force on the PVC tubing over prolonged period might cause severe structural failure on the tubing due to material fatigue (Kim & Yoon, 1998) which would lead to loss of sample. In order to mitigate this problem, visual inspection on the tubing and test run was conducted prior to the actual filtration run to detect any leakages and remove any weakened parts of the tubing. The part of the tubing subjected to the peristaltic pump was also checked hourly and replaced if structural integrity of that specific part was found to be compromised.

In contrast with the filter centrifugation method, variation in the number of rinses was not implemented in this purification process. Instead, the fresh diluent volume utilised for this method was set at three times of the sample volume, which is based on the number of rinses found to be effective in complete removal of unentrapped drugs with the filter centrifugation method (x3). In this case, diafiltration was achieved with the use of airtight sample container. As the circulating sample volume within the system diminishes with the formation of filtrate, negative pressure was created within the sample container and drew fresh diluent from the diluent reservoir. This draws some similarities with the incremental rinsing technique particularly with the incremental addition of fresh diluent in lieu of bulk dilution.

The nature of TFF and its modularity provide several advantages in terms of liposome purification over filter centrifugation. Larger volume of liposome purification can be achieved using TFF within a shorter period of time when compared with filter centrifugation. Complete removal of unentrapped drugs and concentrating

the liposome suspension utilising filter centrifugation method was achieved with x3 number of rinses which was carried out over 240 mins of centrifugation. Using similar volume of rinse with TFF method, the purification and concentration of the liposome suspension process took 105 mins to complete from the initial 80 ml liposome suspension. The modularity of the TFF device allows for similar devices to be connected with the system. This would increase the surface area on which the filtration process takes place and therefore increasing the rate of filtration, thus further improving the purification time.

Concentration capability of both purification methods was also observed. Filter centrifugation method yielded roughly 500 µl of concentrated liposome suspension after the final centrifugation run from the initial 4 ml of liposome suspension, which is a reduction of volume by a factor of 8. In contrast, the TFF method yielded approximately 4 ml of concentrated liposome suspension after the final 15 mins run from the initial 80 ml of liposome suspension which is a volume reduction by a factor of 20. Further concentration attempts for both filter centrifugation and TFF methods were to no avail as a physical dead stop is present for the former to prevent sample from drying out and lack of systemic pressure for the latter to continue with the process. This suggests that the TFF method is more efficient in diluent removal and sample concentration when these two methods are compared. Findings of a previous study regarding liposome purification demonstrated that TFF produced six times more filtrate volume than dead-end cake filtration when the same filtration pressure was utilised (Hwang & Chang, 2004) which is in line with this study.

Some drawbacks of TFF method were also observed, particularly within the scope of this study. Due to the design of the Vivaflow® 50R, each device requires a

minimum of 10 ml for recirculation volume and <0.5 ml non-recoverable hold-up volume exists within the device. This necessitates a larger volume of final rinse in order to recover most of the liposomes from the system in comparison with filter centrifugation method. While increasing the number of TFF devices within the system decreases purification time, higher volume of rinse would be required for this modification. Preparing the TFF system also took a longer time than filter centrifugation particularly on cleaning and rinsing the device. It is therefore more suited for the TFF method to be utilised in a large continuous production in which the aforementioned drawbacks should be greatly diminished in scale and effect.

4.4.5 Characterisation and stability study

Liposomes fabricated from all formulations in this experiment, both blank and drug-loaded were subject to variations in terms of fabrication temperature, aqueous medium, drug content and purification methods. It is important that these liposome products were subjected to characterisation and stability studies as detailed in Chapter 2 to detect any changes arising from the changes implemented in any of the parameters outlined. A recent study has shown that using different aqueous media has an effect on the size of the fabricated nanoparticles (Obeid, Khadra, et al., 2017). It was suggested in the study that the difference in the size might have been caused by the different ions present in the aqueous media. Since only NS was used within this experiment, any changes to the characteristics of the liposomes arising from the aqueous medium would be attributed to the presence of trehalose. A preliminary study was carried out using blank liposomes fabricated from formulation 5 using both NS and NS with 10 mM trehalose as the aqueous phase and produced in both RT and 70°C. The resultant products were measured over 28 days in terms of size and PDI to determine their

stability. As shown in Fig. 4.3, it was observed that the mean size for all the liposomes fabricated is 119.68 ± 2.33 nm with PDI of 0.066 ± 0.022 and demonstrated no significant difference in terms of size (Fig. 4.3a) and PDI (Fig. 4.3b) immediately after fabrication and over the course of 28 days. This suggests that changes in fabrication temperature and aqueous medium have no effect on the characteristics of the resultant liposomes nor their stability over time.

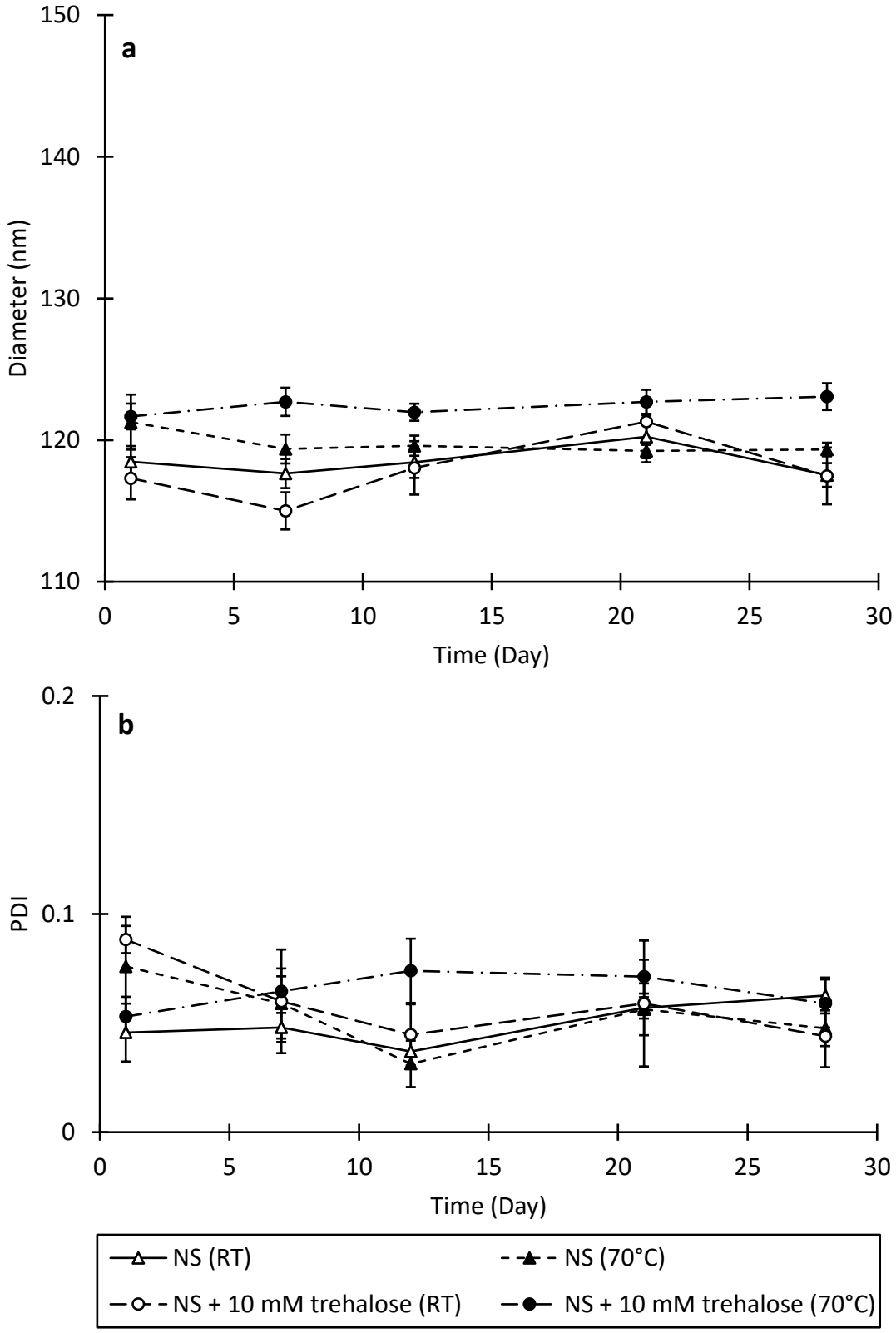

Figure 4.3 Size (a) and PDI (b) of blank liposomes fabricated from formulation 5 using different aqueous phase (NS and NS with 10mM trehalose) and fabrication temperature (RT and 70°C) measured over 28 days.

The effect of purification process on the characteristics and stability of the drug-loaded liposomes was also studied. Liposomes were fabricated from formulation 5 at RT using NS with 10 mM trehalose as aqueous medium and loaded with CPT-11, CDDP and CPT-11/CDDP combination. These liposome suspensions were subjected to filter centrifugation with varying number of rinses as mentioned previously with one uncentrifuged sample as control. Uncentrifuged samples of drug-loaded formulation 5 liposomes were measured post fabrication at 135.27 ± 2.97 nm, 141.42 ± 1.42 nm and 141.09 ± 2.81 nm with PDI of 0.116 ± 0.016, 0.085 ± 0.018 and 0.069 ± 0.027 for CPT-11 (Fig. 4.4), CDDP (Fig. 4.5) and CPT-11/CDDP (Fig. 4.6) respectively. These control samples were found to be not significantly different in terms of both size and PDI with their counterparts subjected to any and all number of rinses for filter centrifugation. It was also found that both uncentrifuged and centrifuged samples are stable over the period of 28 days evidenced by the lack of difference in terms of size and PDI over the study period. It is also interesting to note that concentrating the liposome samples up to a factor of 8 from the original volume demonstrated no effect on their characteristics when compared with uncentrifuged samples. This is in an agreement with a previous study (Domazou & Luigi Luisi, 2002) and suggests robustness of the liposomes against concentration, although the extent of such characteristic was not tested in this study.

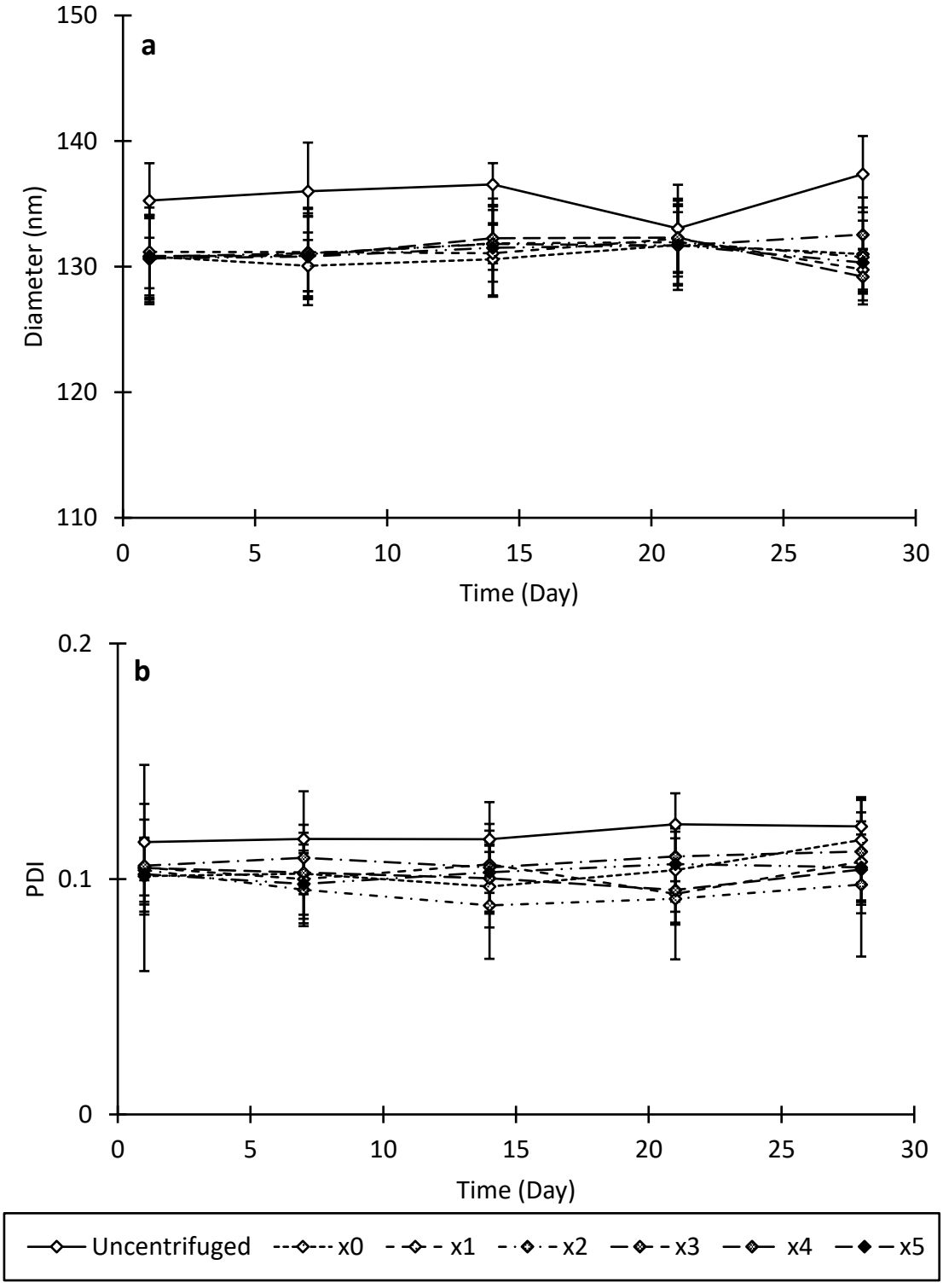

Figure 4.4 Size (a) and PDI (b) of CPT-11-loaded liposomes produced from formulation 5 using 1.5mM CPT-11 in NS with 10mM trehalose as aqueous phase and fabricated at RT temperature measured over 28 days. The liposome samples were uncentrifuged or subjected to filter centrifugation with a range of rinse number from no rinsing (x0) to 5 times (x5).

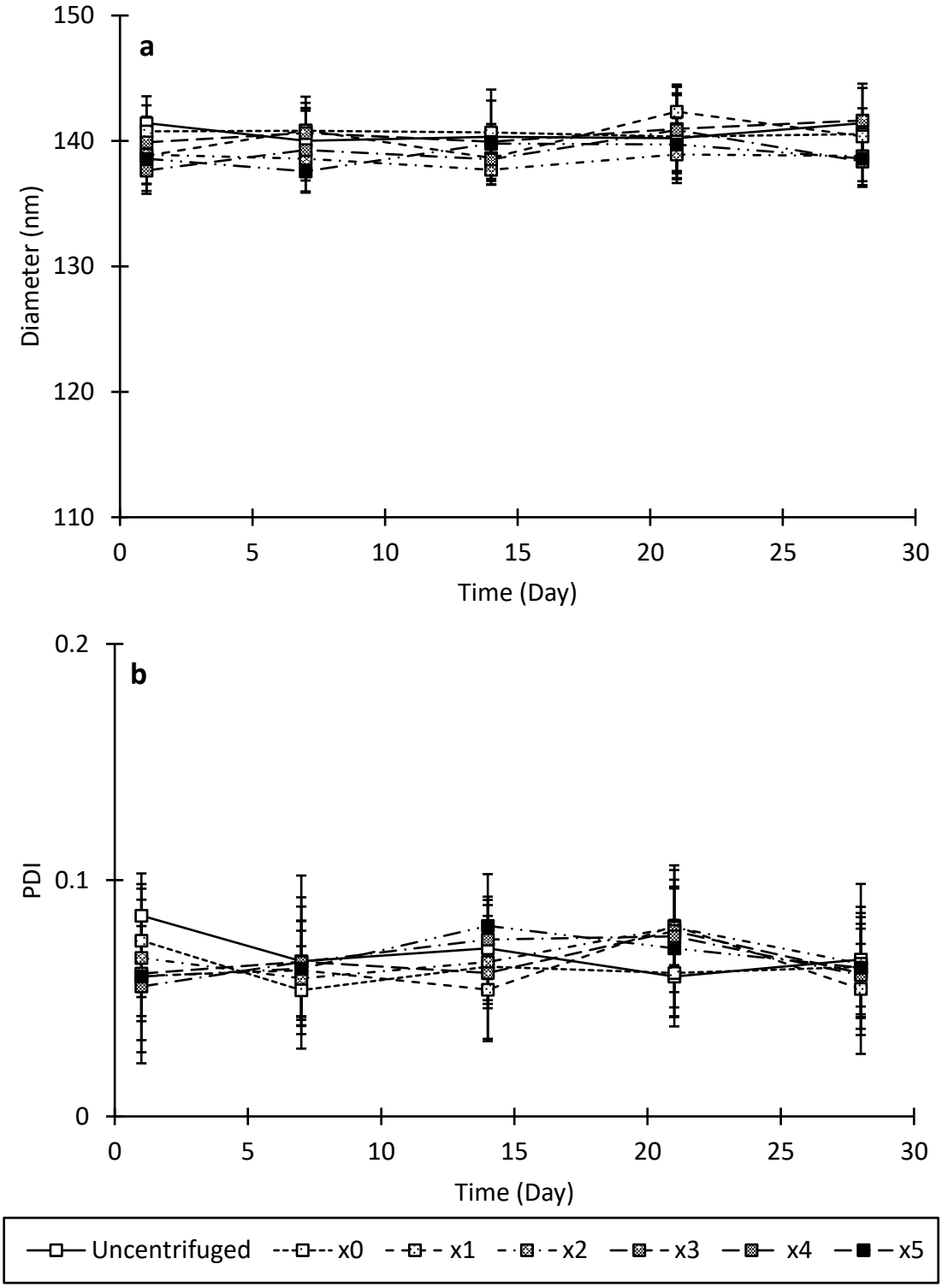

Figure 4.5 Size (a) and PDI (b) of CDDP-loaded liposomes produced from formulation 5 using 3 mM CDDP in NS with 10 mM trehalose as aqueous phase and fabricated at RT temperature measured over 28 days. The liposome samples were uncentrifuged or subjected to filter centrifugation with a range of rinse number from no rinsing (x0) to 5 times (x5).

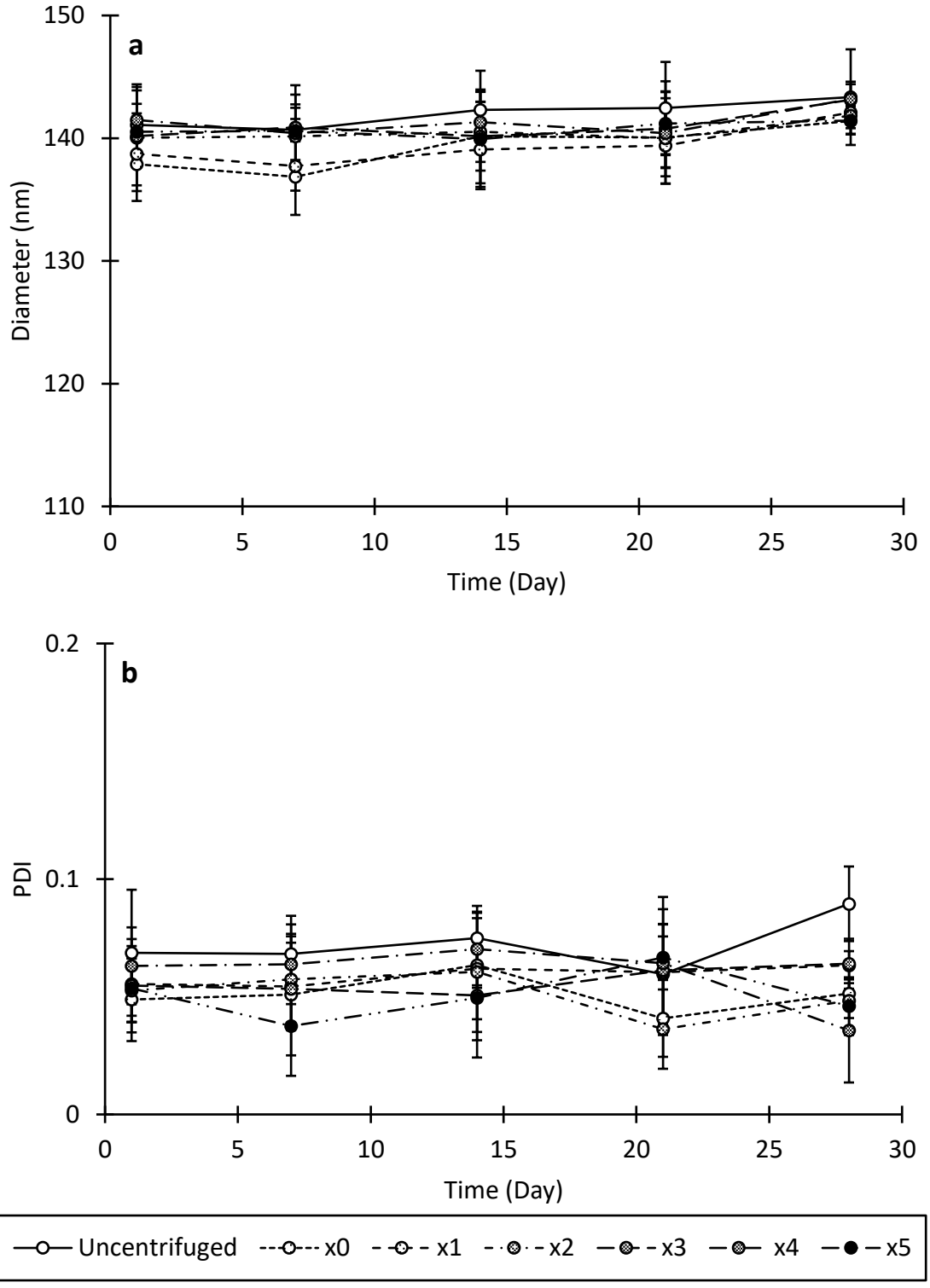

Figure 4.6 Size (a) and PDI (b) of CPT-11/CDDP combination-loaded liposomes produced from formulation 5 using 1.5:3mM CPT-11/CDDP combination in NS with 10mM trehalose as aqueous phase and fabricated at RT temperature measured over 28 days. The liposome samples were uncentrifuged or subjected to filter centrifugation with a range of rinse number from no rinsing (x0) to 5 times (x5).

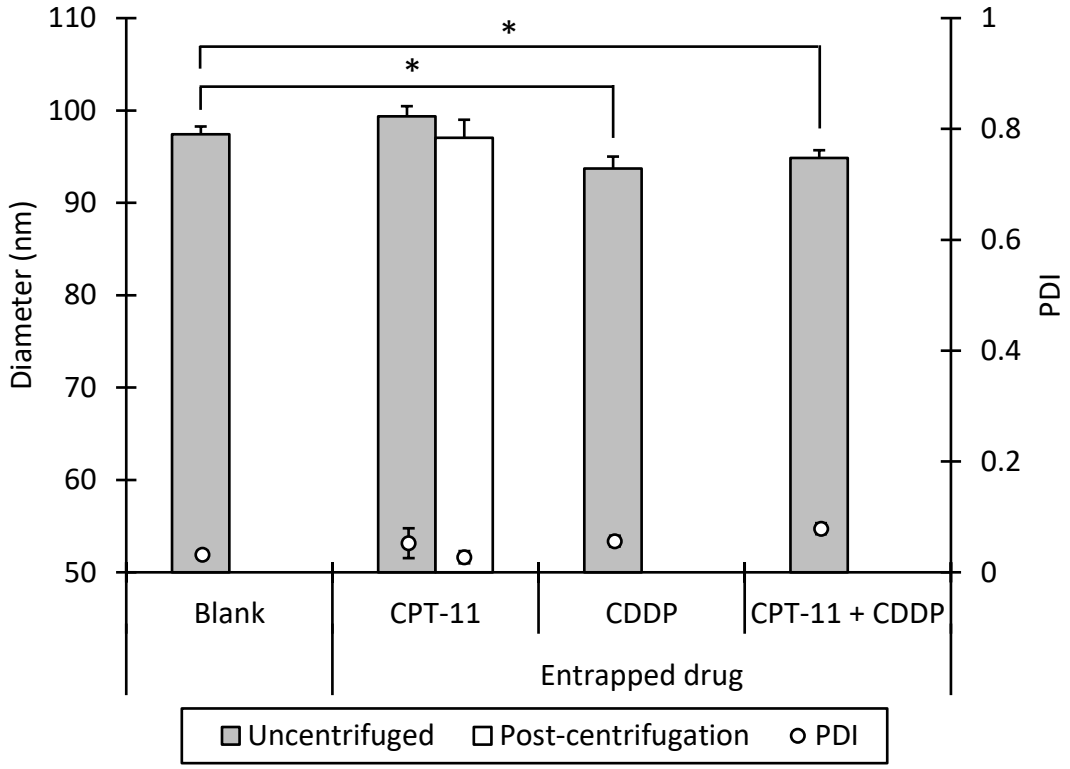

Figure 4.7 Size and PDI measured from uncentrifuged blank and drug-loaded liposomes produced from formulation 6. Post-centrifugation CPT-11-loaded liposomes were measured after filter centrifugation with x3 number of rinses. * = $p < 0.05$

Blank and drug-loaded liposomes fabricated from formulation 6 and 7 were also quantified in terms of size and PDI. Similar fabrication parameters were applied for these formulations including the aqueous medium and drugs loaded into the liposomes. Filter centrifugation was carried out only for CPT-11 loaded liposomes of both formulations at x3 number of rinses to serve as a benchmark against similar level of purification of formulation 5 liposomes and the purified liposomes characterised. Blank liposomes were used as control for size and PDI for both formulations.

In regard to formulation 6, no significant difference in size was observed between the control (99.37 nm ± 0.84) and CPT-11-loaded liposomes (99.37 nm ± 1.10) (Fig. 4.7). Slight differences in size were observed when the control was compared with CDDP (93.70 nm ± 1.31) and CPT-11/CDDP-loaded liposomes (94.88 nm ± 0.82) at 3.73 nm and 2.55 nm respectively (Fig. 4.7). These differences are minuscule in nature and might be caused by the presence of CDDP in the aqueous medium as the similar reduction in size was also observed in CPT-11/CDDP-loaded liposomes. Similar observation of liposome size increase has been noted in previous studies involving dual drug loaded liposomes with oleanolic acid and doxorubicin (Sarfraz et al., 2018) and quercetin and quercetin beta-cyclodextrin complexes (Shaji & Iyer, 2014). In both instances, dual-loaded liposomes were found to be larger than their single-loaded counterparts. However, as this experiment is the only one showing such reduction, it is therefore not possible to conclusively determine the causative effect between these two parameters. No significant difference in size was observed between the control and purified CPT-11-loaded liposomes (97.03 nm ± 1.97) and similarly between the latter and its uncentrifuged counterpart (Fig. 4.7).

Concerning formulation 7, the liposomes were measured at 73.50 nm ± 0.31, 73.38 nm ± 1.61, 72.25 nm ± 0.18 and 73.22 nm ± 0.59 for blank liposome, CPT-11, CDDP and CPT-11/CDDP-loaded liposomes respectively (Fig. 4.8). In contrast with formulation 6, all formulation 7 liposomes showed no significant difference when compared with the control, including the purified CPT-11-loaded liposomes (71.16 nm ± 0.88). No significant difference was also observed between uncentrifuged and purified CPT-11 loaded liposomes.

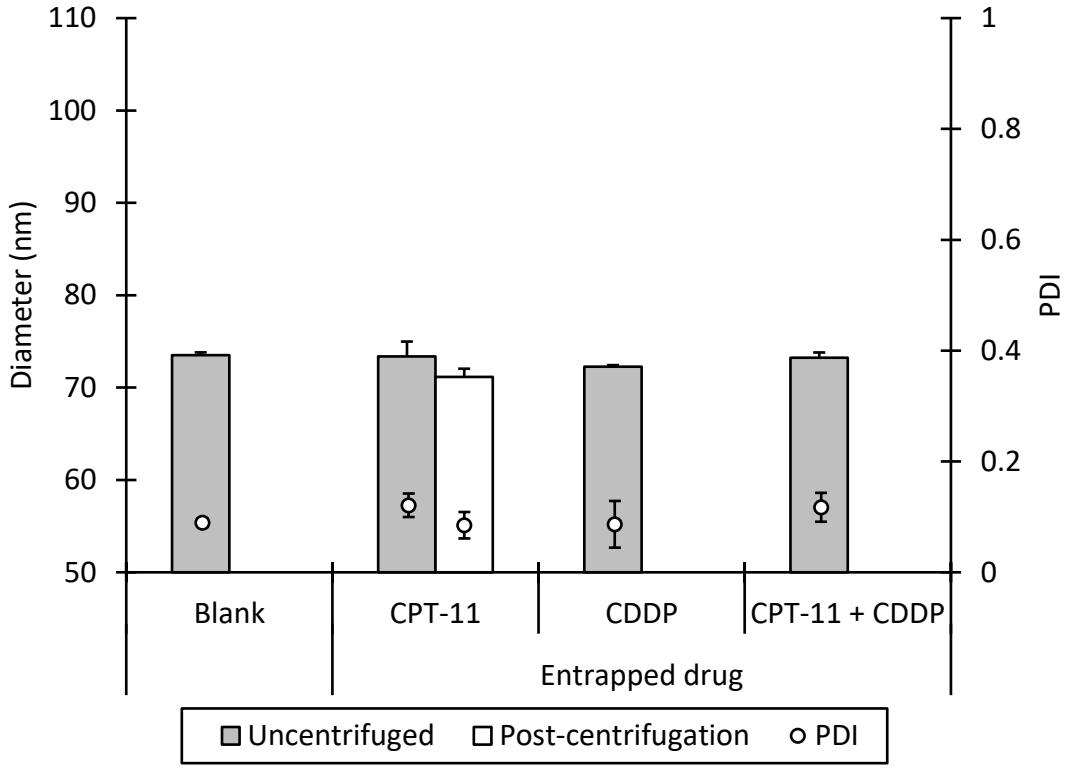

Figure 4.8 Size and PDI measured from uncentrifuged blank and drug-loaded liposomes produced from formulation 7. Post-centrifugation CPT-11-loaded liposomes was measured after filter centrifugation with x3 number of rinses.

PDIs for all liposome suspensions fabricated using formulation 6 were found to be within the range of between 0.027 ± 0.010 for filter centrifuged, CPT-11-loaded liposomes at the lowest and 0.079 ± 0.010 for CPT-11/CDDP-loaded liposomes at the highest. Slightly higher PDI values were observed from formulation 7 liposomes, ranging from 0.085 ± 0.024 for filter-centrifuged, CPT-11-loaded liposomes to 0.117 ± 0.026 for CPT-11/CDDP-loaded liposomes. This demonstrates monodispersity of the liposomes fabricated from both formulations and suggests stability of the fabricated liposomes.

As was observed with previous experiment, filter centrifugation and concentration of both formulation 6 and 7 liposomes did not cause any changes to the size and PDI of the liposomes in comparison with their uncentrifuged counterparts. This further proves the robustness of the liposomes fabricated from these formulations against mechanical stress induced by the centrifugal force applied during the filtration process. However, caution must be applied as this attribute had only been tested within a very narrow range of centrifugal and concentration parameters as mentioned previously. Further tests of these two parameters on the liposomes must be carried out in order to establish the range in which the robustness of the liposomes applies.

Physical characterisation had also been carried out for blank and drug-loaded liposomes fabricated from formulation 5, 6 and 7 pre- and post-filtration utilising the TFF method. It was observed in all formulations that there was no significant difference in size and PDI with respect to pre- and post-filtration of each liposome sample. Regarding formulation 5, the sizes of all the resultant liposomes, both pre- and post-filtration ranged from 114.9 nm to 126.6 nm with a mean size of 120.15 nm ± 2.84 (Fig. 4.9). In comparison with formulation 6 and 7, pre- and post-filtration liposome sizes ranged from 108.1 nm to 120.3 nm with mean size of 114.74 nm ± 3.21 (Fig. 4.10) and 67.4 nm to 78.9 nm with mean size of 72.96 nm ± 2.51 (Fig. 4.11) respectively. This pattern in particle sizes of which formulation 5 > 6 > 7 in this series of formulations fabricated using TFR of 12 ml min^{-1} and FRR of 3:1 has been observed repeatedly from previous experiments in Chapter 2 and 3 and was unaffected by changes in production scale, fabrication temperature, initial lipid phase concentration, aqueous medium, loaded drugs and purification method. This suggests the robustness of these formulations in terms of physical characteristics and stability when subjected

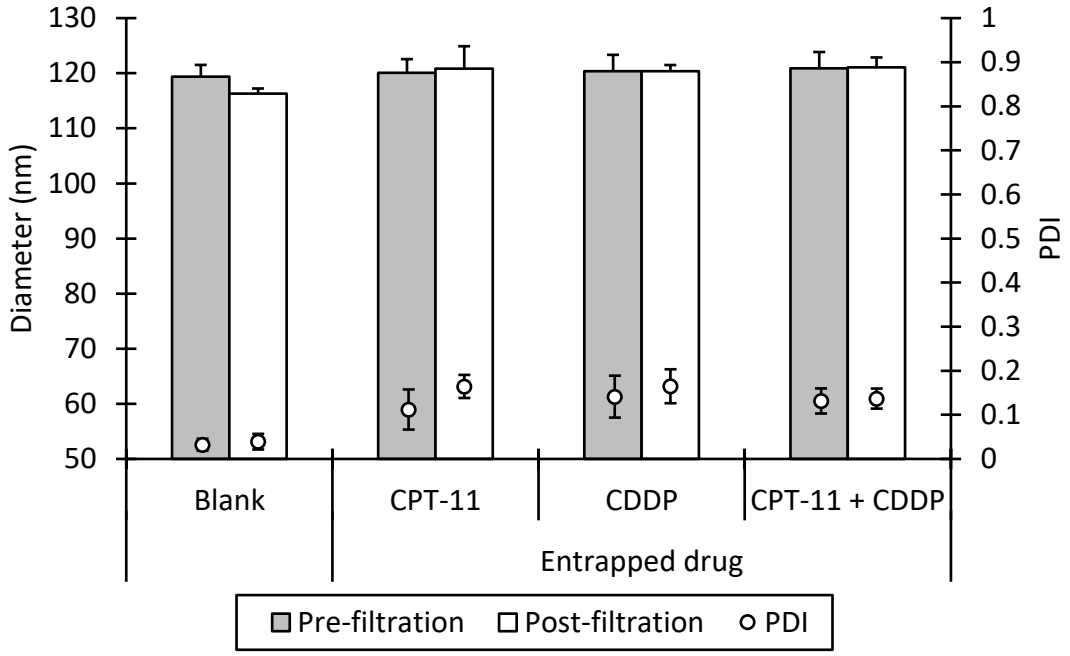

Figure 4.9 Size and PDI of blank and drug-loaded liposomes produced from formulation 5 measured pre- and post-filtration using TFF method. No difference in size and PDI was observed in all corresponding samples pre- and post-filtration process.

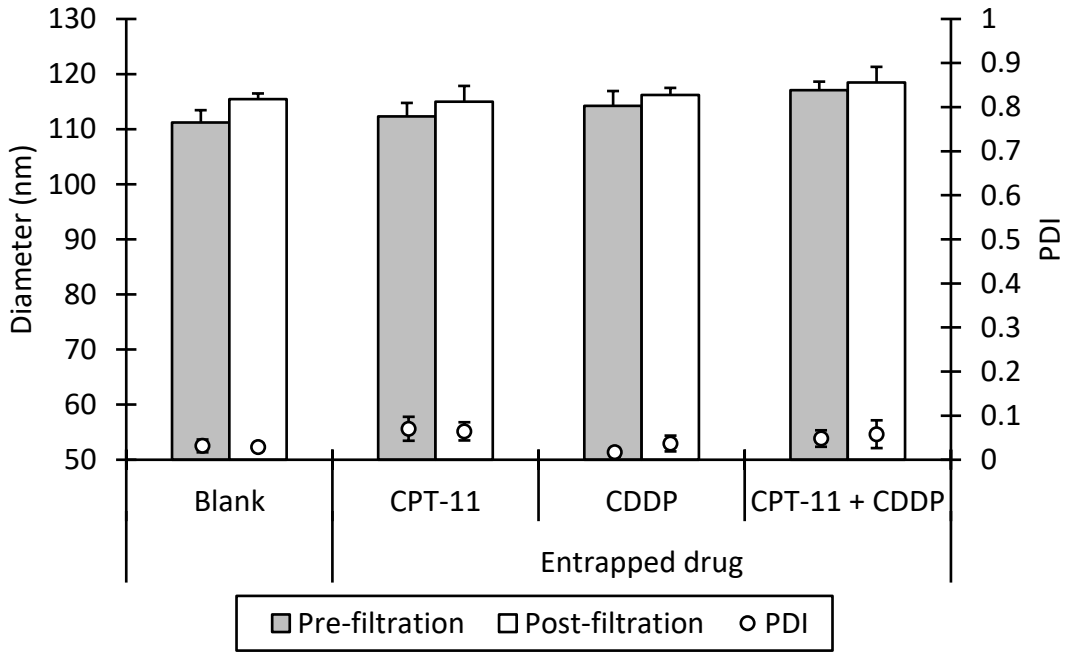

Figure 4.10 Size and PDI of blank and drug-loaded liposomes produced from formulation 6 measured pre- and post-filtration using TFF method. No difference in size and PDI was observed in all corresponding samples pre- and post-filtration process.

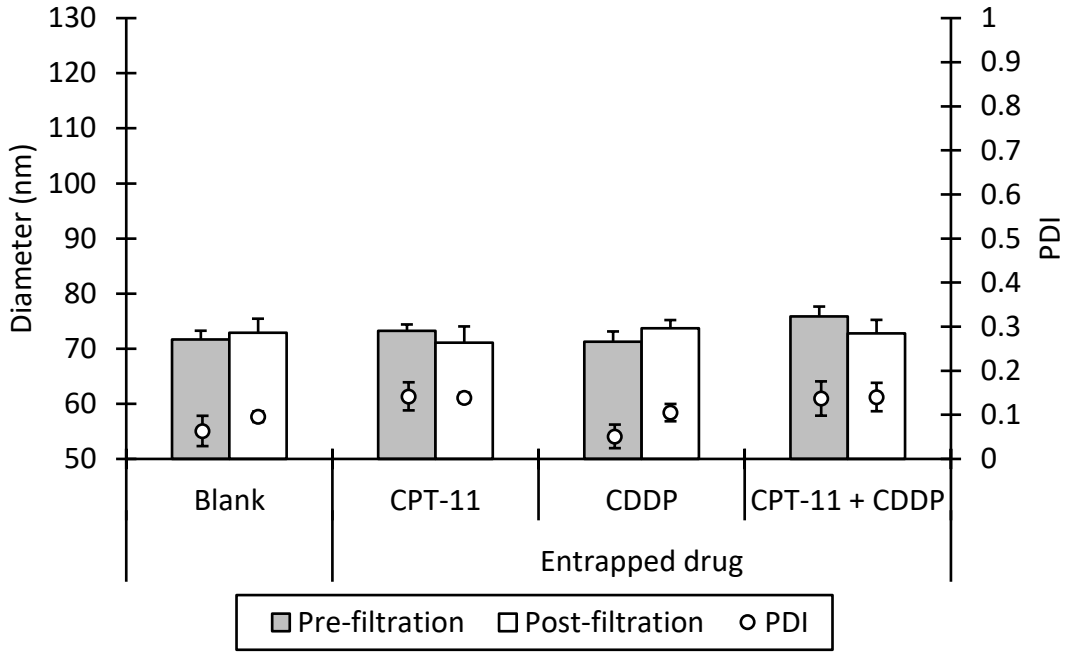

Figure 4.11 Size and PDI of blank and drug-loaded liposomes produced from formulation 7 measured pre- and post-filtration using TFF method. No difference in size and PDI was observed in all corresponding samples pre- and post-filtration process.

to changes in the preparation parameters. This is also the first reported instance of such size pattern of liposomes fabricated using microfluidics technique with SHM for these specific combinations of phospholipids and cholesterol.

As mentioned previously, PDI values of each of the liposome sample pre- and post-filtration did not show any significant difference for all the formulations, both blank and drug-loaded. There is a lack of any discernible pattern across all the formulations with the PDI values of individual liposome samples ranging from 0.002 to 0.235 (Fig. 4.9 – 4.11). However, it is pertinent to note that in the case of formulation 5, blank liposome samples had the lowest PDI in comparison with their drug-loaded counterparts (Fig. 4.9). The equivalent difference was not detected in formulation 6 and 7, instead the blank liposome samples had closely matched PDI values with their

CDDP-loaded counterparts in both formulations whilst CPT-11-containing liposomes had higher PDI values in relation to their blank and CDDP-loaded counterparts (Fig. 4.10 – 4.11). This discrepancy in PDI values might be attributed to the presence of CPT-11 in the system although further study is warranted to conclusively prove the causative link between these two parameters.

4.4.6 Drug content analysis

Table 4.1 CPT-11 recovery results from CPT-11/CDDP solution in various aqueous medium derived from expected and measured concentration of the drug.

	CPT-11 concentration		
Aqueous medium	Expected	Measured	Recovery (%)
NS	15 µg ml^{-1}	16.056 µg ml^{-1}	107.0
PBS	15 µg ml^{-1}	15.742 µg ml^{-1}	104.9
NS with trehalose	15 µM	15.235 µM	101.6

Standard curves plotted from CPT-11 absorbance at 370 nm detection wavelength in all aqueous media as shown in Fig. 4.12 demonstrated linearity evident by the squared correlation coefficient of 1 (CPT-11 in NS with trehalose) or close to 1 (CPT-11 in NS and PBS). Table 4.1 details the CPT-11 measured concentrations based on absorbance for CPT-11/CDDP solutions in all aqueous media and each one was calculated using corresponding standard curve. CPT-11/CDDP solution in NS with trehalose gave the closest measured to theoretical value at 101.6%. UV absorption spectrum of CPT-11 solutions in all buffers from 200 – 450 nm detection wavelength showed two distinct peaks at 260 nm and 370 nm as previously described (Ci et al., 2014). UV absorption at 370 nm wavelength was chosen in line with previous finding (Ci et al., 2014) in order to minimise absorption readings variation caused by

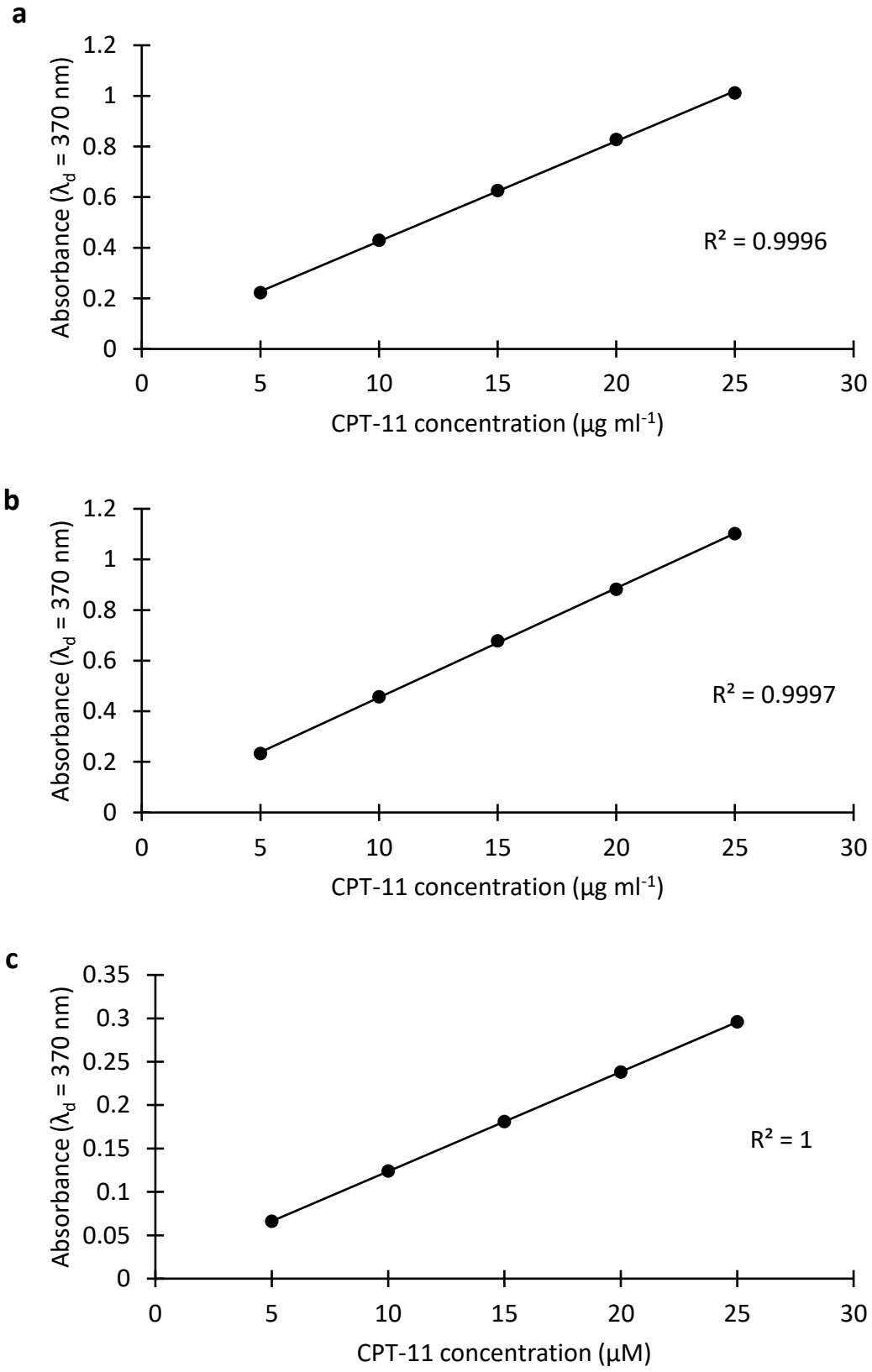

Figure 4.12 Standard curve of absorption at λ_d of 370 nm for CPT-11 in (a) NS, (b) PBS and (c) NS with trehalose.

difference in pH. It was observed during the course of this study that solutions with higher concentration of CPT-11 have higher absorption at 260 nm than 370 nm detection wavelength. This difference decreases with decreasing concentration of CPT-11. Similar observations have been recorded in a previous study (Ci et al., 2014), showing the effect of increasing pH to lowering UV absorption at 260 nm detection wavelength. It is therefore hypothesised that high concentration of CPT-11 is associated with the low pH. As mentioned in a previous study (Ci et al., 2014), this low pH works favourably in the functional sense of the system due to the higher percentage of active form (lactone) of CPT-11 in low pH.

The recovery percentage of CPT-11 in NS with trehalose of 101.6% demonstrates the feasibility of UV spectrophotometry for accurate CPT-11 quantification in CPT-11/CDDP solution with the cryoprotectant buffer. This is due to the low UV absorption of CDDP (Basotra, Singh, & Gulati, 2013) which does not interfere with UV absorption of CPT-11 in the same solution.

In order to accurately measure the CPT-11 content within the purified and concentrated liposome suspension, the liposomes were lysed for the drug content to be released into the surrounding medium. Previous studies had no common agreement on the concentration of Triton X-100, a nonionic surfactant, required for complete liposome lysis with the values varying from 0.1% (Kulma et al., 2017) (Järvå et al., 2018), 0.5% (Arouri et al., 2015), 0.6% (Cao et al., 2017) and 10% (Jimah, Schlesinger, & Tolia, 2017). This variation in the amount of Triton X-100 required for liposome lysis might arise from the different lipid components used in the liposomes

in each study. The studies also did not mention other parameters involved during the liposome lysis process.

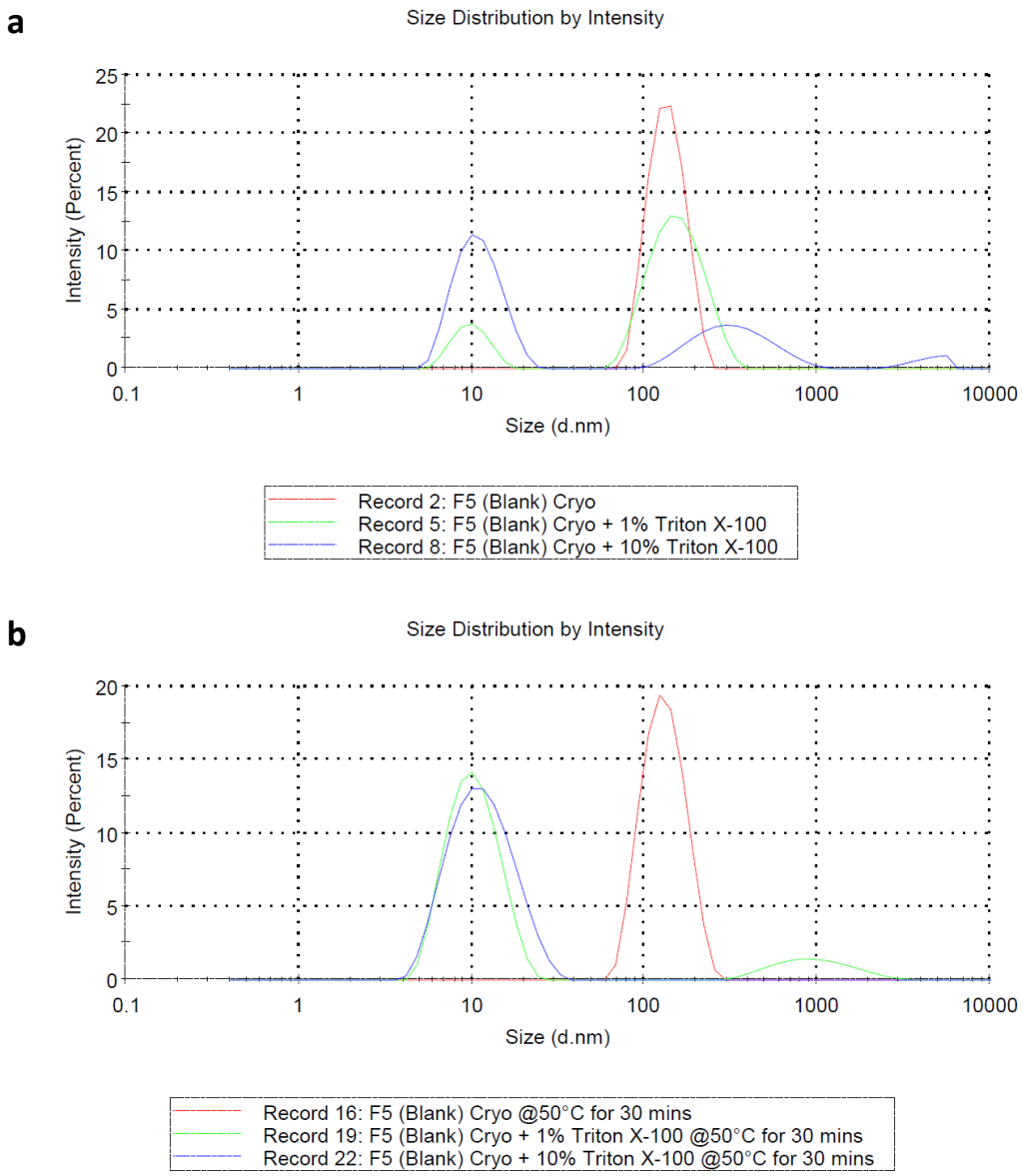

Figure 4.13 Size distribution of blank formulation 5 liposomes subjected to 1% and 10% v/v Triton X-100 at (a) RT and (b) 50°C for 30 mins for lysis. Untreated samples in both temperatures served as controls.

To gain an insight on the amount of Triton X-100 and conditions required for complete lysis of liposome, a brief experiment was carried out on liposome lysis utilising varying amount of Triton X-100 (1% and 10% v/v) in RT and 50°C for 30 mins. The result, as detailed in Fig. 4.13, shows that exposure to Triton X-100 at both concentrations and temperatures produced varying degree of liposome lysis. Partial lysis is characterised by any overlap of the peak with the control sample, suggesting presence of particles unaffected by the lysis and therefore remained at their original size. It was observed that the addition of higher concentration of Triton X-100 at RT increases the proportion of lysed liposomes with the intensity peaks increasingly displaced from the control peak (Fig. 4.13a).

However, exposing similar systems to a higher temperature of 50°C for 30 mins demonstrated distinguishably different outcomes. As shown in Fig. 4.13b, exposure to such conditions using 1% Triton X-100 displaced most of the intensity peak from the control with minimal overlap to the latter. Using 10% Triton X-100 in such conditions completely displaced the peak without any overlap to the control, suggesting complete lysis of the liposomes and the subsequent release of the entrapped drugs. The Triton X-100 concentration used was in line with a previous study (Jimah et al., 2017). However, the study utilised different phospholipids for liposome fabrication and 1:1 volume ratio of liposome to 10% Triton X-100 as opposed to 1:4 volume ratio for both materials in this study. 1:4 liposome to 10% Triton X-100 volume ratio in 50°C for 30 mins were therefore used for the lysis process for all CPT-11-loaded liposomes from all formulations.

Quantification of the entrapped drugs was carried out on the drug-loaded liposome suspensions fabricated from all formulations which were subsequently purified and concentrated using both filter centrifugation and TFF methods. The results, as shown in Fig. 4.14, show a massive difference in concentration of all entrapped drugs between liposomes purified using filter centrifugation (Fig. 4.14a) and TFF (Fig. 4.14b). This is due to the same dilution factor used during the quantification process for all samples from both purification methods and as was mentioned previously, TFF method yielded purified liposome suspension with higher concentration than filter centrifugation method.

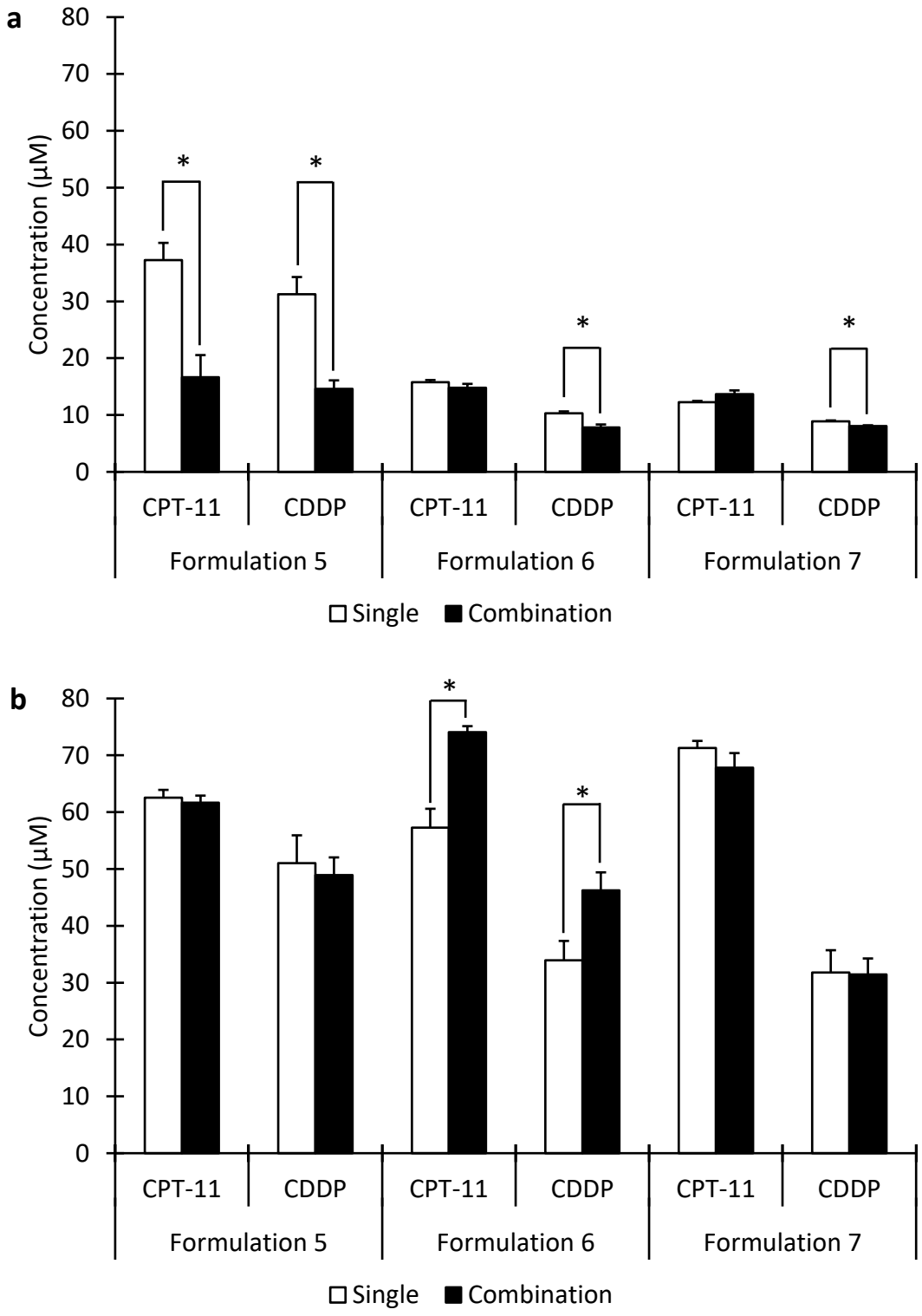

Figure 4.14 Concentration of loaded CPT-11 and CDDP in liposomes fabricated from formulation 5, 6 and 7 purified using (a) filter centrifugation and (b) TFF methods for both single and combination of the drugs. Significance was determined using t-test with * = $p < 0.05$

As shown in Fig. 4.14a, drug concentration in liposomes loaded with each of the drugs demonstrated a decreasing pattern from formulation 5 to 7. The same pattern cannot be observed along the formulations with the drugs combination-loaded liposomes, suggesting interactions between the two drugs limiting the loading of both drugs into the liposomes. Due to the hydrophilic nature of both drugs, it is highly likely that the drugs were loaded into the interior of the liposomes as opposed to the intramembrane space of the lipid bilayer. It is therefore interesting to note that in formulation 5, the sum of concentration of CPT-11 and CDDP is approximately equal to the concentration of each drug when loaded separately (Fig. 4.14a). The same phenomenon, however, was not observed with formulation 6 and 7 with similar concentration of each of the drug when loaded in combination or separately.

A previous study have shown that molecular weight and structure play important role in determining encapsulation efficiency into liposomes with smaller and lipophilic molecules correspond with higher loading efficiency (Huang, Li, Bruni, Messa, & Cellesi, 2017). The previous study, however, used molecules with huge variation of molecular weight, ranging from carboxyfluorescein (376.32 g mol^{-1}) to dextran (40 000 g mol^{-1}) to demonstrate the effect of molecular weight on encapsulation efficiency and albumin to demonstrate the effect of relative lipophilicity on the same parameter. Another study have shown that increasing amount of cholesterol in liposome formulation decreases encapsulation efficiency of hydrophilic material due to decreasing internal aqueous volume of liposome (Glavas-Dodov et al., 2005). This is in line with the findings of current study, in which increasing molar ratio of cholesterol from formulation 5 to 7 resulted in smaller sized liposomes and reduction of the amount of encapsulated CDDP (Fig. 4.14b).

These findings warrant further investigation as to what parameters govern the loading efficiency of the constituent drug when drugs combination of CPT-11 and CDDP is involved. Previous studies involving dual drug entrapment in liposomal systems yielded various results ranging from no difference between single and dual drug entrapment of 5-fluorouracil and apigenin in DSPC liposomes (Sen, Banerjee, & Mandal, 2019) to lower entrapment efficiency of dual drug entrapment of oleanolic acid and doxorubicin in comparison with its single drug counterpart in a HSPC-DSPE liposomal system (Sarfraz et al., 2018). Lower drug loading was also observed for CDDP across the formulation when compared with CPT-11 for both single-loaded and combination-loaded liposomes. Similarly, significantly lower CDDP concentration within the liposomes loaded with the drugs combination was also observed when compared with liposomes loaded with only CDDP. This is despite the CDDP concentration is twice the CPT-11 in the aqueous phase during the liposome fabrication phase and might be caused by the lower hydrophilicity of CDDP (Cayman Chemical, 2018) in comparison with CPT-11 (LC Laboratories, 2018) which hampers its ability to be loaded within the liposomes. Previous studies involving single entrapment of CDDP and CPT-11 in DSPE-PEG have shown that the entrapment efficiency of CPT-11 is relatively higher at 95.3% (Z. Zhang & Yao, 2012) in comparison with CDDP at 25.9% (Catanzaro et al., 2018).

Drug-loaded liposomes subjected to TFF method yielded no similar pattern as observed previously with filter centrifugation method. The only patterns observed for these liposomes are the decreasing concentration of CDDP within the liposomes from formulation 5 to 7 when the drug was loaded separately from CPT-11 and the lack of significant difference between the concentrations of the drugs in the liposomes from

formulation 5 and 7 when loaded in combination or separately (Fig. 4.14b). These results are in stark contrast with the results obtained from filter centrifuged liposomes in Fig. 4.14a, suggesting differences in the extent of purification of both methods. Another factor that might contribute to this difference is the manner in which the liposomes were collected at the end of the purification process. Due to the closed and contained nature of filter centrifugation method, it is arguably more precise and consistent in yielding the resultant purified liposome while with the TFF method, collection of the purified liposomes involves rinsing a larger surface area with areas less affected with main flow of the rinsing solution such as bends and connecting points which would conceivably prevent some of the liposomes from being harvested and therefore would alter the yield significantly. Further studies should be carried out to mitigate these differences or improve the TFF method altogether in order to improve reproducibility of the yield.

Table 4.2 Ratio of CPT-11 to CDDP molar concentration in liposomes fabricated from formulation 5, 6 and 7 loaded with the combination of both drugs purified using filter centrifugation and TFF methods.

Formulation	Filter centrifugation	TFF
5	11:10	13:10
6	17:10	16:10
7	19:10	22:10

With regard to liposomes loaded with CPT-11/CDDP combination, a greater scrutiny was given on the concentration of the drugs within the liposomes post fabrication and purification. It was observed that the ratio of CPT-11 to CDDP increases from formulation 5 to 7 and this phenomenon was observed from all liposomes purified using either method (Table 4.2). This is particularly interesting due to the fact that the initial concentration ratio of CPT-11/CDDP aqueous phase during the fabrication process is 1:2 and it was therefore assumed that the same proportion of both drugs would be loaded into the liposomes. As previously mentioned, the CPT-11/CDDP concentration ratio of 1:2 was selected in order to achieve the highest synergistic activity of these two drugs against A549 cancer cells with the lowest difference of concentration between them (Tardi et al., 2009). However, this figure referred to the concentration ratio of the drugs derived from a mixture of liposomes loaded with the individual drugs as opposed to liposomes containing a mixture of both drugs. This stark difference in the drug concentration ratio, in some cases completely opposite from the initial concentration ratio, signifies a loading condition favouring for CPT-11 and as was mentioned previously, might also be caused by a competition between these two drugs vis-à-vis drug loading into the liposomes. Further studies should be carried out in order to establish the proper fabrication parameters to achieve the desired drugs concentration ratio within the liposomes, possibly by manipulating the initial drug concentration in the aqueous phase, the initial lipid concentration or the constituent lipids.

4.5 Conclusion

Fabrication of liposomes loaded with CPT-11, CDDP and CPT-11/CDDP combination from formulation 5, 6 and 7 was demonstrated successfully using NanoAssemblr Benchtop. These liposomes had been successfully characterised with mean sizes ranging from 73 nm for formulation 7 liposomes to 120 nm for formulation 5 liposomes and PDI range of 0.002 to 0.235 across the formulations for both blank and drug-loaded liposomes and determined to be physically stable over the period of 28 days post fabrication. Purification of liposomes was carried out using both conventional filter centrifugation and novel TFF methods and it was discovered that with filter centrifugation, rinsing with 3 times of the original volume yielded the best purification result whilst TFF method was demonstrably more suited for purification of large volume of liposome suspension with faster (105 mins to filter centrifugation's 240 mins) and superior concentration capability (volume reduction by a factor of 20) in comparison with filter centrifugation (volume reduction by factor of 8). Quantification of CPT-11/CDDP combination in the liposomes demonstrated differences in the concentration of CPT-11 and CDDP entrapped compared with the initial molar concentration of the drugs (1:2) in the aqueous phase during the fabrication process. This discrepancy in CPT-11 to CDPP molar concentration ratio, ranging from 11:10 to 22:10 post purification, demonstrated that entrapment of CPT-11 was seemingly favoured over CDDP in all of the formulations. This provides a crucial insight of the determining factors in the entrapment of such drugs and is invaluable in refining the fabrication process in order to achieve the desired drug entrapment especially when drugs combination is involved.

Chapter 5

Lyophilisation, Morphology and Cytotoxicity Study of Single and Dual-Loaded Cisplatin/Irinotecan Liposomes

5.1 Introduction

Degradation of liposomes is one of the primary concerns during the transportation and storage of the material over a period time. This process can be caused by hydrolysis and oxidation of the phospholipid components due to their prolonged exposure to aqueous medium (Allen Zhang & Pawelchak, 2000). As a result of this degradation, drug content and physical characteristics of the liposomes such as membrane rigidity, size and size distribution might be altered (Zhang et al., 2004). The alteration in drug content as a result of the liposome degradation is particularly concerning due to its effect on the cytotoxicity of the liposomes and might render them unable to exert the cytotoxic activity with any degree of consistency. One of the strategies to improve the stability of the liposomal products over a long period of time is by removal of water via lyophilisation. The process, also known as freeze-drying, involves sublimation of frozen water from a sample through reduction of ambient pressure. The method, whilst efficient in removing water content, exposes the liposomes to the harsh freezing and dehydration conditions which are not conducive to the structural integrity of liposomes, leading to leakage of liposomal content (Harrigan, Madden, & Cullis, 1990).

This necessitates the addition of cryoprotectant in order to prevent damage to the liposomes during the lyophilisation process. Several sugars, including but not limited to glucose (Konan, Gurny, & Allémann, 2002), sucrose (Abdelwahed, Degobert, & Fessi, 2006) and lactose (Cui, Hsu, & Mumper, 2003) were reported to be successfully used as cryoprotectant for various nanoparticles previously. Trehalose is a type of non-reducing disaccharide produced by various organisms and microorganisms such as silk moth (*Telea polyphemus*) (Wyatt & Kalf, 1957),

roundworm (*Ascaris lumbricoides*) (Fairbairn & Passey, 1957), species of *Streptomyces* (Martín, Díaz, Manzanal, & Hardisson, 1986) and mycobacteria (Elbein & Mitchell, 1973). It is also found to be utilised as cryoprotectant in certain plants in order to survive harsh condition such as flower of stone (*Selaginella lepidophylla*) (Zentella et al., 1999). Previous study has shown that trehalose is at least superior to sucrose in terms of cryoprotection of a liposomal system with lower chemical reactivity, hygroscopicity and higher T_g (Crowe, Reid, & Crowe, 1996). While trehalose is a preferred choice of cryoprotectant of biomaterials, the degree of cryoprotection depends on the type of the nanoparticles, concentration of the nanoparticles and the trehalose itself (Abdelwahed, Degobert, Stainmesse, et al., 2006).

One of the important aspects of physical characterisation of liposomes is morphology study. Several imaging methods such as AFM, environmental scanning electron microscopy (ESEM), TEM and confocal microscopy are available for this purpose and have been successfully utilised in a previous study (Ruozi et al., 2011). It is mentioned in the study that the different microscopic studies provided different information on the physical characteristics of liposomes such as shape, morphology, dimensions and surface properties for AFM and dimensions for ESEM. While each of the techniques has its own advantages in procuring the morphological information of the liposomes, the sample preparation required for the method and the technique itself may introduce several limitations which need to be taken into account with regards to the evaluation of the data obtained (Robson et al., 2018).

Evaluation of cytotoxicity of drug-loaded liposomes is crucial in order to establish the efficacy of the drug in its entrapped form against target cells. The most

commonly used method to assess such efficacy is by monitoring the metabolic activity of the cells using the colourimetric tetrazolium salt assay, also known as the 3-(4,5-dimethylthiazol-2-yl)-2,5-diphenyltetrazolium bromide (MTT) assay (Hansen & Bross, 2010). The assay utilises MTT compound, a colourless substance which is introduced to the cells as part of the technique. Living cells undergoing normal metabolic process are able to convert the MTT compound to formazan crystals whose concentration can then be measured in order to determine the viability of the cells. Reduced formazan concentration reflects reduced live cells number, which in turn can be interpreted as reduced overall cell viability (van Meerloo, Kaspers, & Cloos, 2011). While MTT assay may not accurately portray anticancer activity of test compounds when compared between *in vitro* outcomes versus clinical application (Eastman, 2016), the assay is nevertheless an important screening tool to establish potential cytotoxic activity of novel compound and/or combination of drugs (Hubeek et al., 2006).

This study utilises A549 cell line which is a human lung alveolar carcinoma epithelial cell line obtained from European Collection of Authenticated Cell Culture. Isolated and cultured from the explanted tumour of a 58 year-old Caucasian male, A549's potential as a testbed for lung cancer therapy was first discovered in 1973 due to its high population doubling number for lung carcinoma tissue and demonstrated the highest colony formation percentage during the study (Giard et al., 1973). Since then A549 cell line has been highly utilised as the model for testing the efficacy of new therapeutic agents targeting lung cancer (Foldbjerg, Dang, & Autrup, 2011; Geiger, Muller, Dean, & Fabbro, 1998; Yin, Zhou, Jie, Xing, & Zhang, 2004).

In this chapter, attempts and the subsequent findings on the lyophilisation of the liposomes is presented. Microscopy studies were carried out in order to gain an understanding of the morphology and surface characteristics of the liposomes under various conditions. MTT assay was utilised to determine the cytotoxicity of the drug-loaded liposomes against a specific cancer cell line and their efficacy was compared against non-entrapped drugs.

5.2 Materials and Methods

All materials described herein were as mentioned previously in Chapter 4 and obtained from Sigma-Aldrich unless stated otherwise.

5.2.1 Freeze-drying and characterisation of liposomes

A set of blank liposome solutions were produced from formulation 5 lipid phase and aqueous phases of NS with varying concentration of trehalose (10, 50, 100, 200 and 400 mM) using NanoAssemblr (Precision Nanosystems, Canada) set at TFR = 12 ml min^{-1} and FRR = 3:1. The resultant liposome solutions were purified using filter centrifugation as mentioned previously in Chapter 4 with three times rinsing using the corresponding aqueous phase as diluent. 20 ml of blank and drug-loaded liposomes were produced from all formulations and aqueous phase diluent of NS with 10 mM trehalose using similar method mentioned above. The liposome solutions were purified using TFF method (Vivaflow 50R, Sartorius, Germany) as mentioned previously in Chapter 4. The liposome solution was rinsed with 240 ml diluent (NS with 10 mM trehalose) during the purification process and concentrated to approximately 4.5 ml. 4 ml of diluent were used to rinse the whole system and the concentrated liposome solution was topped up to 10 ml with the diluent. A set of 1 ml solutions of these blank and drug-loaded liposomes with trehalose concentration of 10,

30, 80, 105, 155, 205, 405, 605 and 805 mM were made by mixing the concentrated liposome solutions and the corresponding trehalose solution in NS in 1:1 ratio. All liposome solutions were sized using Zetasizer Nano-ZS (Malvern Instrument, UK).

Freeze-drying (FD) process were subsequently carried out using Epsilon 2-4 LSCplus (Martin Christ, Germany). The 1 ml samples were frozen on the shelf from RT to -40°C at a cooling rate of 0.7°C min^{-1} and held at -40°C for 10 mins. Pressure inside the chamber was lowered to 0.340 mBar for the main drying phase. This phase lasted for 22 h before the temperature was gradually increased to 20°C within 13 h. The final drying phase was initiated at this point by lowering the pressure to 0.021 mBar and held for 10 h. The resultant products were rehydrated to 1 ml using deionised water and sized using Zetasizer Nano-ZS (Malvern Instrument, UK).

5.2.2 Morphology study of liposomes

Two methods of morphology study were carried out on the liposome samples, namely AFM and SEM. Liposome samples for AFM analysis was diluted 10 times with deionised water. 5 µl from each of these diluted samples was placed on the surface of cleaved mica and air-dried in RT for up to 1 h. The AFM analysis was then carried out using the same procedure and instrument as outlined in Chapter 2. The formulation 5 liposome sample used for SEM analysis was placed onto a silver foil on a sample stub and subsequently subjected to FD process with modified trehalose concentration post purification of 405 mM. The sample was then gold-coated for a thickness of 5 nm using a sputter coater (Leica EM ACE200, Leica Microsystems, Austria) prior to SEM analysis (Keysight 8500B, Keysight Technologies, US).

5.2.3 Cytotoxicity study of liposomes

A549 cells were obtained from European Collection of Authenticated Cell Culture and cultured in F12K medium (Gibco, Ireland) containing 2mM glutamine, 10% v/v foetal bovine serum and 1% penicillin-streptomycin at 37°C in a 5% CO_2 atmosphere. The cells were then transferred to 96-well plates (Corning, US). Cell density used for this experiment is $1.0x10^4$ cells cm^{-2}. The cells were incubated (37°C, 5% CO_2) for 24 h prior to addition of non-entrapped drugs, blank and drug-loaded liposomes from all formulations and afterwards incubated for 72 h. 20 µl of 5 mg ml^{-1} of MTT were added to each well after the incubation period and afterwards incubated in similar conditions for another 5 hours. Solution in each well was carefully removed after the incubation period and replaced with 100 µl dimethyl sulfoxide (DMSO) and incubated for another 10 mins to solubilise formed formazan crystals. The plates were then read with Multiskan Ascent (Fisher Scientific, Sweden) plate reader at 570 nm wavelength.

5.2.4 Statistical analysis

Data obtained from *in vitro* study were utilised to plot dose-response curves using Origin 2018 (OriginLab Corporation, USA). The half maximal inhibitory concentration (IC_{50}) for each of the drugs or drug-loaded liposomes was derived from the plotted curves. Unless stated otherwise, all measurements were performed in triplicate from independent samples and *t*-test statistical analysis was carried out using Minitab version 17.1.0 (Minitab Inc., USA). Results are expressed in mean ± SD. Significance was defined as $p < 0.05$ (marked with *), $p < 0.01$ (marked with **) and $p < 0.001$ (marked with ***). Non-significance was defined as $p > 0.05$ and denoted as n.s.

5.3 Results and Discussion

5.3.1 Freeze-drying and characterisation of liposomes

FD process was carried out on all blank and drug-loaded liposomes of formulation 5, 6 and 7. Lyophilisation is a harmful process for liposome integrity (Ozer & Talsma, 1989). FD and the subsequent rehydration process can damage the liposomes due to formation of piercing ice crystals during the freezing step (Khan, Elhissi, Shah, Alhnan, & Ahmed, 2013; van Winden, 2003) and fusion of the liposomes which can lead to lipid membrane rupture, drug leakage and alterations of the physical characteristics (Crommelin & Van Bommel, 1984; Ingvarsson, Yang, Nielsen, Rantanen, & Foged, 2011). These changes are detrimental to the stability and drug content consistency of the lyophilised liposomes (van Winden, 2003). The addition of a cryoprotectant stops the formation of ice crystals via the vitrification process in which the T_g of the suspension is lowered, thereby preventing formation of ice crystals but forming highly viscous solution instead in order to protect the liposomes from being adversely affected by the freezing step in the FD process (Christensen et al., 2007; Crowe et al., 1996; Wolfe & Bryant, 1999). The presence of cryoprotectant also prevents liposome aggregation and subsequently fusion by binding directly to the polar head of the lipid membrane at its glassy state (Crowe, Oliver, Hoekstra, & Crowe, 1997; Ohtake, Schebor, & de Pablo, 2006; Ohtake, Schebor, Palecek, & de Pablo, 2005). Trehalose, a nonreducing disaccharide is considered as the choice cryoprotectant for this study due to its biocompatibility and non-toxicity (H. Huang et al., 2017).

Trehalose was chosen as the cryoprotectant for all liposome suspensions due to its superior ability with regard to entrapped drug retention within liposomes in

comparison to other saccharides (Crowe, Crowe, Carpenter, & Wistrom, 1987; El-Nesr, Yahiya, & El-Gazayerly, 2010; Sun, Leopold, Crowe, & Crowe, 1996). Trehalose, however, is a large saccharide molecule with molecular weight of 342.3 g mol^{-1} which prevents it from crossing over the lipid membrane (Pereira, Lins, Chandrasekhar, Freitas, & Hünenberger, 2004). This poses a challenge as increasing the amount of trehalose in the aqueous phase during liposome fabrication will introduce another variable in drug loading into the liposome and might result in lower drug loading (Zaru et al., 2007). This will severely affect the viability of the liposomes for drug carriers as a high amount of trehalose might provide sufficient cryoprotection but hinder sufficient drug loading. An approach to this conundrum is by varying the concentration of trehalose inside and outside the liposomes as carried out by a previous study (Ohtake et al., 2006). Manipulation of trehalose concentration in this study was achieved by increasing the concentration of trehalose in the liposome suspension post fabrication and purification. This approach would allow for higher drug loading without compromising cryoprotection. It is therefore pertinent to study two aspects in this freeze-drying process, the amount of trehalose needed for sufficient cryoprotection and whether increasing the amount of trehalose outside of liposomes alone is sufficient to provide comparable cryoprotection.

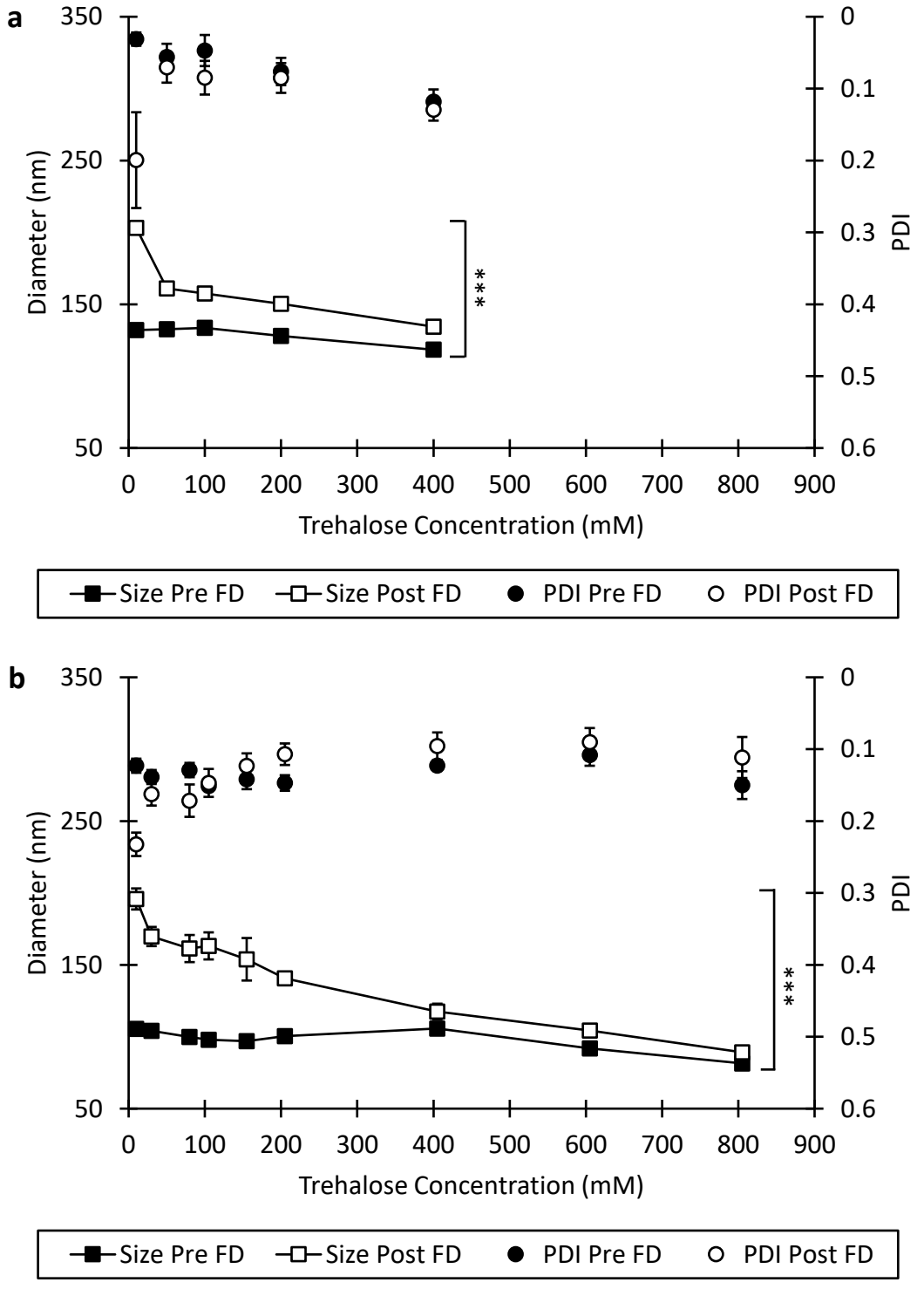

Figure 5.1 Size and PDI of blank liposomes fabricated from formulation 5 pre and post FD using (a) various concentration of trehalose in the initial aqueous phase during fabrication and (b) modified concentration of trehalose in the liposome suspension post purification. Some error bars are hidden within the data points. *** = $p < 0.001$ denotes significance between corresponding data points pre and post FD.

Blank formulation 5 liposomes were used to study the effect of variation in trehalose concentration in the initial aqueous phase during fabrication and modified trehalose concentration post purification on size difference of liposomes pre and post FD. As shown in Fig. 5.1a, increasing the concentration of trehalose from 10 mM to 400 mM in the initial aqueous phase during fabrication progressively lowered the size and PDI difference of the liposomes pre and post FD with the lowest size difference of 16.05 nm and PDI difference of 0.01 at 400 mM. Similar trend of decreasing size and PDI difference was observed with increasing modified trehalose concentration post purification from 10 mM up to 805 mM (Fig. 5.1b). The lowest size difference pre and post FD of 7.71 nm was achieved at 805 mM with PDI difference of -0.03. Similar reduction of liposome size with increasing concentration of trehalose as cryoprotectant was observed in previous studies using ftorafur and vitamin A entrapped in soybean lecithin liposomes (Hua, Li, Liu, & Sun, 2003) and 5-fluouracil entrapped in egg lecithin liposomes (Nounou, El-Khordagui, Khalafallah, Khalil, & Rasheed, 2005). However, another study utilising prednisolone sodium phosphate entrapped in DPPC and DSPE liposomes with trehalose as cryoprotectant demonstrated increased liposome size post FD with such increase unaffected by increasing concentration of trehalose (Sylvester et al., 2018).

Size difference change is quite pronounced when trehalose concentration was increased from 205 mM to 405 mM, from 40.28 nm to 11.79 nm, a 71% decrease in size difference. Increasing the concentration of trehalose greater than 405 mM has shown lower effect in terms of size difference. Doubling trehalose concentration from 405 mM to 805 mM reduced the size difference from 11.79 nm to 7.71 nm, a 35% decrease in size difference, which is a stark contrast in size difference change from

increasing trehalose concentration from 205 mM to 405 mM. As the concentration of trehalose increases, liposome size pre-FD decreases from 105.43 nm to 81.48 nm at trehalose concentration of 805 mM.

This progressive reduction in size is highly likely to be caused by the increasing trehalose concentration outside the liposome which increased the osmotic pressure and causing water to move out from the inside of the liposomes. At 400 mM trehalose concentration for initial aqueous phase during fabrication and 405 mM modified trehalose concentration post purification the size differences pre and post-FD were 16.05 nm and 11.79 nm respectively, which translates into a non-significant difference of 4.26 nm.

This proves that at a certain trehalose concentration point, modifying trehalose concentration outside the liposomes post purification is sufficient in providing comparable cryoprotection with having the same concentration of trehalose for both inside and outside of the liposomes. Increasing trehalose concentration in the initial aqueous phase during fabrication past 400 mM increases the viscosity of the aqueous phase itself. This might introduce another variable in the liposome fabrication process and affecting the characteristics of the produced liposomes.

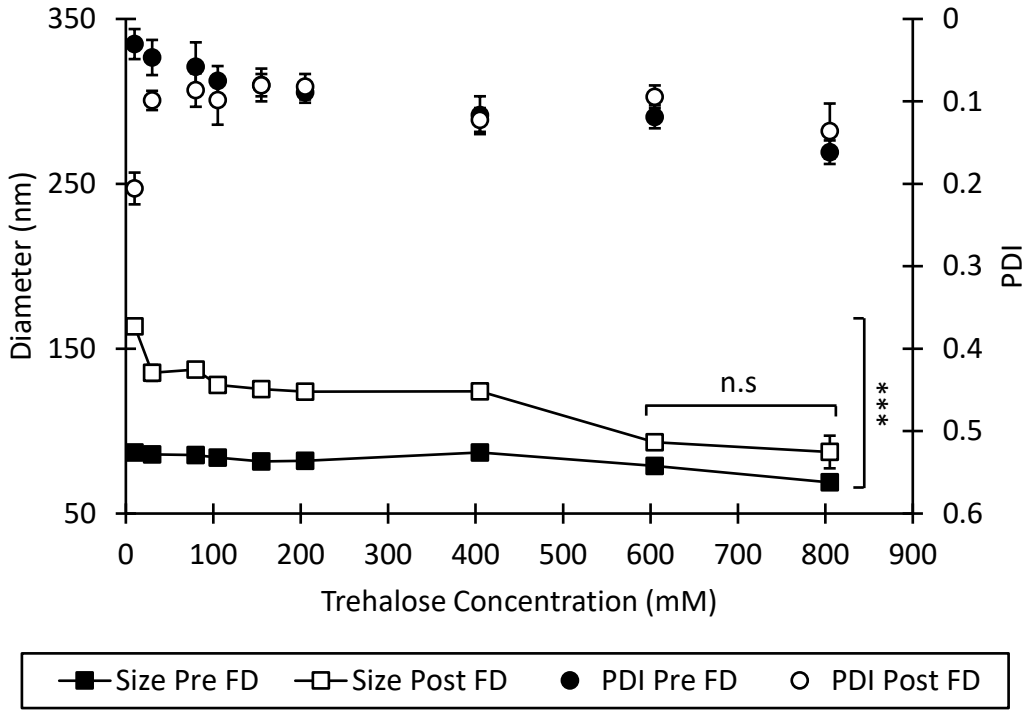

Figure 5.2 Size and PDI of blank liposomes fabricated from formulation 6 pre and post FD using modified concentration of trehalose in the liposome suspension post purification. Some error bars are hidden within the data points. *** = $p < 0.001$ denotes significance between corresponding data points pre and post FD. Non-significance is denoted by n.s.

Modified trehalose concentration post purification was then chosen as the cryoprotection method during FD for blank liposomes of formulation 6 and 7. As shown in Fig. 5.2, the size and PDI differences of the blank formulation 6 liposomes pre and post FD continually decreases with increasing concentration of trehalose. The lowest size difference was 14.49 nm with PDI difference of -0.02 at trehalose concentration of 605 mM. Increasing the trehalose concentration to 805 mM caused a slight increase the size difference but it is not significant in comparison with 605 mM trehalose concentration. Fig. 5.3 shows similar decrease in size and PDI differences pre and post FD for blank formulation 7 liposomes with increasing concentration of trehalose. As with the case of blank formulation 6 liposomes, the lowest size and PDI

differences were at trehalose concentration of 605 mM, which are 7.59 nm and 0.03 respectively. It was also observed that the size and PDI differences from 10 mM to 805 mM trehalose concentration vary from one formulation to another, with formulation 6 and 7 liposomes showing the lowest and highest size and PDI differences change across the trehalose concentration respectively.

One of the major variations between the formulations is the increasing cholesterol content from formulation 5 to 7. Physical aspects of liposomes with high cholesterol content such as formulation 7 liposomes are not expected to be highly affected by the FD process due to the reduction of phase transition temperature and prevention of lipid components phase separation (Ohtake et al., 2005; Popova & Hincha, 2007). Our study however, contradicted this finding as evidenced in Fig. 5.3, in which the liposomes of Formulation 7 with high cholesterol content are greatly affected at low trehalose concentration. Formulation 5 liposomes with the lowest cholesterol content, on the other hand, did not appear to be the least affected by the FD process, suggesting that the complex composition of phospholipids and cholesterol in each of the formulations interacted uniquely with the varying concentration of trehalose which gave rise to varying degree of cryoprotection (Franzé, Selmin, Samaritani, Minghetti, & Cilurzo, 2018).

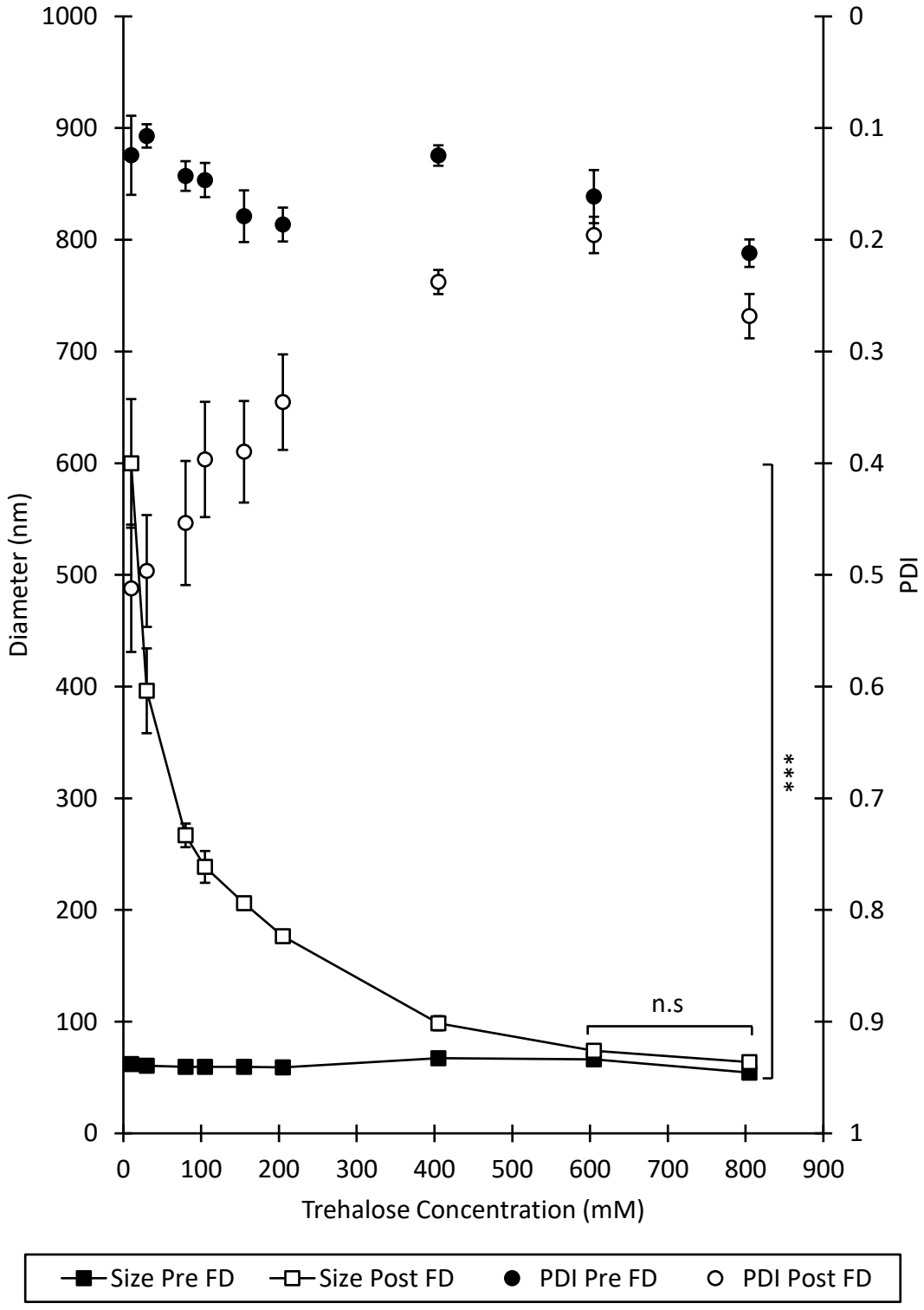

Figure 5.3 Size and PDI of blank liposomes fabricated from formulation 7 pre and post FD using modified concentration of trehalose in the liposome suspension post purification. Some error bars are hidden within the data points. *** = $p < 0.001$ denotes significance between corresponding data points pre and post FD. Non-significance is denoted by n.s.

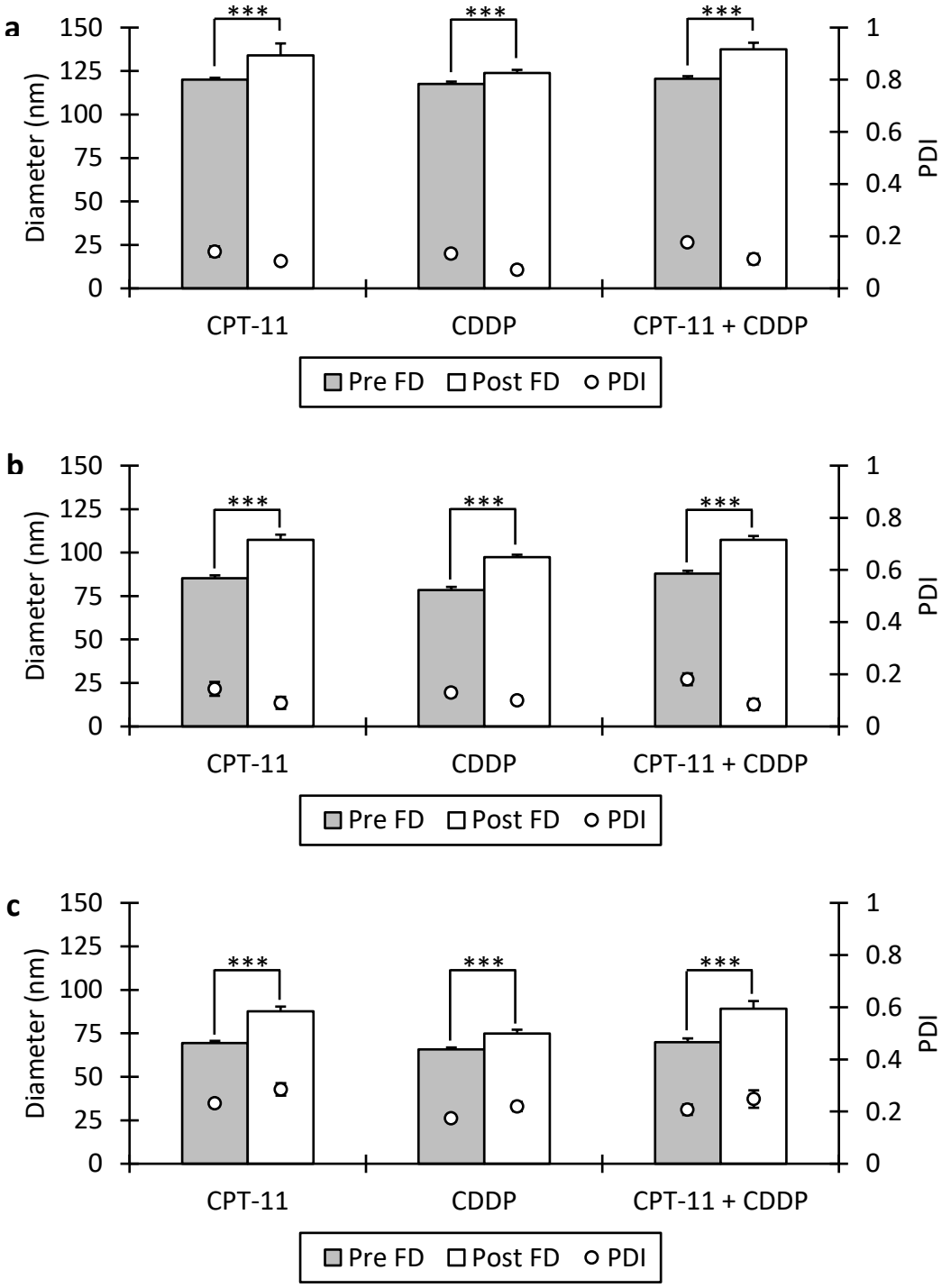

Figure 5.4 Size and PDI of drug-loaded liposomes fabricated from (a) formulation 5, (b) formulation 6 and (c) formulation 7 pre and post FD using modified concentration of trehalose of 405 mM for formulation 5 and 605 mM for both formulation 6 and 7 in the liposome suspensions post purification. Some error bars are hidden within the data points. *** = $p < 0.001$ denotes significance between corresponding data points pre and post FD.

Using the method of modifying trehalose concentration post purification and the trehalose concentration of 405 mM for formulation 5 and 605 mM for formulation 6 and 7, drug-loaded liposomes of each formulation were treated with respective concentration of trehalose prior to FD. As shown in Fig. 5.4, size differences pre and post FD for all drug-loaded liposomes of all formulations are highly significant with post FD liposome sizes are larger in all cases. The size differences vary from one formulation to another with formulation 5 liposomes yielding the lowest size differences (Fig. 29a) and formulation 6 producing the highest size difference (Fig. 5.4b) for CPT-11, CDDP and CPT-11 + CDDP combination. This is in contrast with the previous findings with blank liposomes and might be caused by the incorporation of drugs within the liposomes which altered the composition of system, therefore affecting the degree of cryoprotection afforded by trehalose at various concentration.

Several previous studies demonstrated various findings on the optimal trehalose concentration for liposome cryoprotection. 175 mM – 234 mM of trehalose were found to be sufficient for cryoprotection of phosphatidylcholine liposomes entrapping fluconazole (El-Nesr et al., 2010), 292 mM trehalose was found to be the optimal concentration for cryoprotection of soybean lecithin liposomes (Hua et al., 2003) and 211 mM – 396 mM trehalose were found to be providing sufficient cryoprotection for dimethyldioctadecylammonium/α,α′-trehalose 6,6′-dibehenate liposomes (Christensen et al., 2007). The common denominator in all of these studies is the increasing cryoprotection afforded with increasing concentration of trehalose regardless of the type and composition of liposomes involved. These findings demonstrated the high variability of the amount of trehalose required for sufficient cryoprotection for various liposomal systems, therefore necessitating tailored trehalose

concentration for the liposomal systems in this study. The size differences of liposomes pre and post FD, whilst statistically significant, are functionally insignificant as the post FD sizes still fall within the size range preferable for cell uptake.

The lowest size difference pre and post FD is CDDP-loaded liposomes in all formulations when compared with their CPT-11 and CPT-11 + CDDP combination-loaded counterparts (Fig. 5.4). It is postulated that the presence of CPT-11 within the liposomes reduced the cryoprotection of trehalose due to the higher liposome size difference pre and post FD for both CPT-11 and CPT-11 + CDDP combination-loaded liposome. There is limited research regarding the effect of entrapped material on the physical characteristics of liposomes. A previous study has shown that ATP-loaded liposomes have no impact on the size increase of the liposomes post FD when compared with their blank counterparts (Vincourt, Nguyen, Chaumeil, & Dumortier, 2010). However, the entrapped and entrapping materials in the study are not the same in this study, therefore a direct parallel cannot be drawn. Further tests are required in order to confirm the correlation between the presence of CPT-11 and reduction of trehalose cryoprotection.

Figure 5.5 Freeze-dried products of blank (a) formulation 5 liposomes and (b) formulation 7 liposomes both in modified trehalose concentration post purification (10 mM – 405 mM), (c) formulation 5, 6 and 7 liposomes in modified trehalose concentration post purification of 605 mM and (d) formulation 5, 6 and 7 liposomes in modified trehalose concentration post purification of 805 mM. Check mark (✔) denotes FD products demonstrating pharmaceutical elegance while cross mark (✘) denotes FD products demonstrating collapsed cakes and meltback appearance.

Physical appearance of FD products is also important in assessing the suitability and stability of the products. Fig. 5.5a and 5.5b show FD products of blank formulation 5 and 7 respectively with increasing amount of trehalose from 10 mM to 405 mM. At the lowest trehalose concentration of 10 mM, blank liposomes of both formulations formed distinct cakes with minimal shrinkage post FD. As the concentration of trehalose increased the FD products became progressively worse with further shrinkage of the cake at 30 mM trehalose concentration for formulation 5 and subsequent increase in trehalose concentration produced collapsed cakes with meltback appearance up to trehalose concentration of 205 mM in both formulation 5 and 7. These collapsed cakes and the subsequent meltback appearance might be resulted from product temperature above the collapse temperature (T_c) during primary drying, which is usually a few degrees higher than T_g (Depaz, Pansare, & Patel, 2016). As product temperature was increased above T_c, reduction in viscosity resulted in free flow of the product and the subsequent loss of the product's microstructure attained during the freezing process, usually during the start of the secondary drying process (Pikal & Shah, 1990).

While it was suggested that the appearance of the FD products may or may not have a bearing on its safety and efficacy (Franzé et al., 2018), meltback is a particular concern when it comes to FD products due to its impact on reconstitution time, residual moisture, stability and potency as mentioned from a previous study (Patel et al., 2017) and general lack of pharmaceutical elegance. In this study, meltback FD products were found to have an increased reconstitution time. It was also found in this study that the appearance of the FD product does not necessarily correlate to sufficient cryoprotection as formulation 5 and 7 blank liposome with trehalose concentration of

10 mM formed acceptable cake but as shown in Fig. 5.1b and Fig. 5.3 the size differences pre and post FD are the largest. While it is possible to obtain FD products with acceptable characteristics for liposome products with trehalose concentration from 30 mM to 405 mM by optimising the lyophilisation process to tailor for the requirement of each system, including but not limited to further reducing the temperature during primary drying process to T_c or T_g level, this would consume higher energy, does not necessarily guarantee sufficient cryoprotection and beyond the limitation of this study.

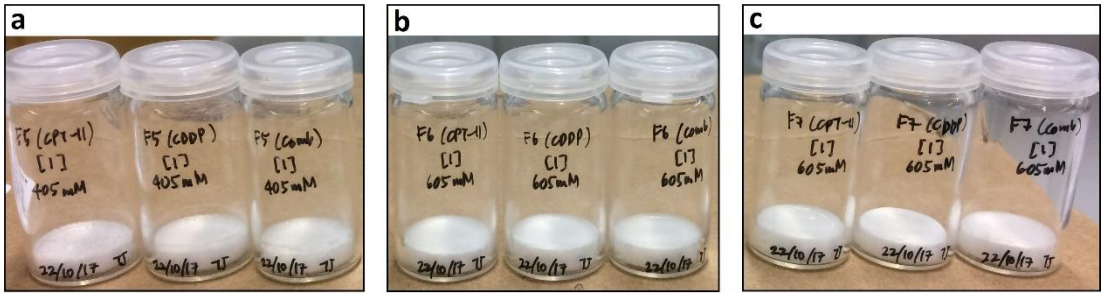

Figure 5.6 Freeze-dried products of CPT-11, CDDP and CPT-11/CDDP combination-loaded (a) formulation 5 liposomes in modified trehalose concentration post purification of 405 mM, (b) formulation 6 liposomes and (c) formulation 7 liposomes, both in modified trehalose concentration post purification of 605 mM.

FD products for blank liposome from formulation 5 and 7 with 405 mM trehalose were found to be acceptable with properly formed cakes as shown in Fig. 5.5 (a) and (b). Further increase of trehalose concentration to 605 mM and 805 mM introduced no changes in the quality of FD products for all formulations as shown as Fig. 5.5 (c) and (d). Similar visual quality of FD product was also observed with drug-loaded liposomes of all formulations as shown in Fig. 5.6. Drug-loaded liposomes of formulation 5 (Fig. 5.6a) was freeze-dried using trehalose concentration of 405 mM while formulation 6 (Fig. 5.6b) and 7 (Fig. 5.6c) used trehalose concentration of 605 mM to achieve the smallest size difference pre and post FD in accordance to the

previous findings in this study. These findings proved that at the trehalose concentration levels which provide sufficient cryoprotection for the drug-loaded liposomes, the FD products formed decent cakes and are acceptable as final pharmaceutical products. These findings, combined with findings of a previous study demonstrating that using 10 mM trehalose optimised loading of rifampicin into phosphatidylcholine, DPPC and DSPC liposomes (Zaru et al., 2007) provides the best parameters in which the final products in this study are optimised both in cryoprotection and drug entrapment in the liposomes.

5.3.2 Morphology study of liposomes

Morphology study of liposomes was previously explored in Chapter 2 on blank liposomes, providing an insight into the use of AFM in order to obtain an understanding on the shape of the liposomes. However, as mentioned previously in the same chapter, liposome size obtained from the AFM might not correlate with the DLS due to the different methods of detection, conditions in which the samples are measured and the quantification procedure for each of the methods. Several modifications have been introduced to the preparation, fabrication and purification of the liposomes and therefore it is imperative to study whether these alterations affect any changes on the morphology.

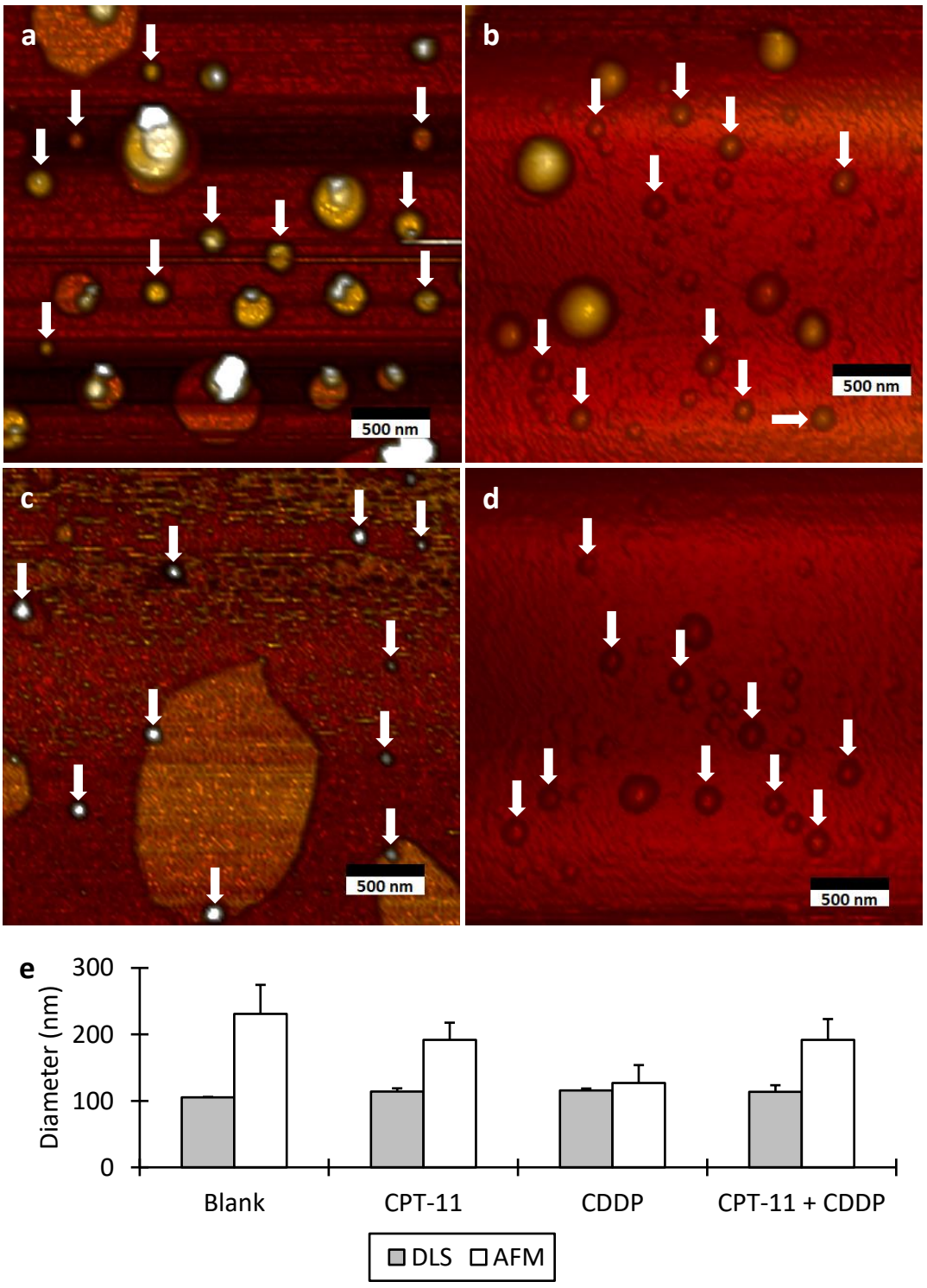

Figure 5.7 AFM images of (a) blank, (b) CPT-11-loaded, (c) CDDP-loaded and (d) CPT-11/CDDP combination-loaded liposomes fabricated from formulation 5. The white arrows indicate the position of individual liposomes within the image. Diameter of blank and drug-loaded liposomes of formulation 5 (e) were obtained from DLS and AFM methods. Some error bars are hidden within the data points.

In this study, AFM and SEM were utilised to analyse blank and drug-loaded liposomes from formulation 5, 6 and 7. As shown in Fig. 5.7 (a) to (d), blank and drug-loaded liposomes of formulation 5 were found to be circular and flat when observed using the AFM. These circular disks were measured using NanoScope Analysis software in order to determine their diameter and give rough estimation in relation to data obtained from DLS analysis. Fig. 5.7 (e) details these findings and it was observed that the size obtained from AFM measurement is larger than DLS measurement for both blank and drug-loaded liposomes. This is in accordance to the observation detailed in Chapter 2, in which the dehydrated and flattened appearance of the liposomes on the mica surface gave rise to the increased diameter when measured using AFM.

Several limitations impede direct liposome size comparison measured using AFM and DLS as both methods have different manner of measurements, sample preparation and condition during measurement and number of liposomes measured for each method. It is because of these reasons statistical analysis of liposome diameter measured using AFM and DLS to check for significant difference was not carried out. However, obtaining liposome diameter using AFM gave an insight into the morphology of the liposomes under certain conditions. Liposome samples prepared for measurement using the AFM were diluted using deionised water instead of 10 mM trehalose in NS due to a high presence of salt crystals on the mica surface when the sample was dried which interferes with procurement of the images of the liposomes.

The increase in diameter, while expected with AFM measurements, varied between blank and drug-loaded liposomes when such variations are minuscule to non-existent with DLS measurement of the same samples. It is possible that the dilution affected the liposomes by reducing osmotic pressure in the solution surrounding the liposomes, causing water to enter the liposomes following osmotic gradient. Similar findings have been observed in previous studies in which linearly proportional liposome swelling to osmotic pressure across the membrane was observed (Haines, Li, Green, & Cummins, 1987), accurate sizing of liposomes demonstrating osmotic response to the dilution of external medium (Hantz, Cao, Escaig, & Taillandier, 1986) and the reduction of osmotic pressure causes an increase in liposome deformation (Foo, Chan, & Liu, 2003). The variations in the size difference might be precipitated by the content of the liposome. It was observed in this study that the blank liposome has the largest diameter followed by drug-loaded liposomes, therefore postulating that the blank liposome has the highest osmotic pressure.

The size difference between drug-loaded liposomes is another interesting observation in this study. It was discovered that CDDP-loaded liposome exhibited the lowest diameter among drug-loaded liposomes while CPT-11 and CPT-11 + CDDP combination-loaded both have similar diameter and larger than their CDDP-loaded counterpart. This difference might be induced by the presence of CPT-11 within the liposomes which alters the osmotic pressure, causing higher influx of water into the liposomes. Similar observation was noted in a previous research of which the degree of liposome swelling is proportional to the degree of osmotic gradient, which is attributed to entrapped material (Lehtonen & Kinnunen, 1994). However, no direct correlation between the presence of CPT-11 and the increase in diameter of liposomes

when measured using AFM can be made within the scope of this study due to the limitations of the method and the number and selection of the samples.

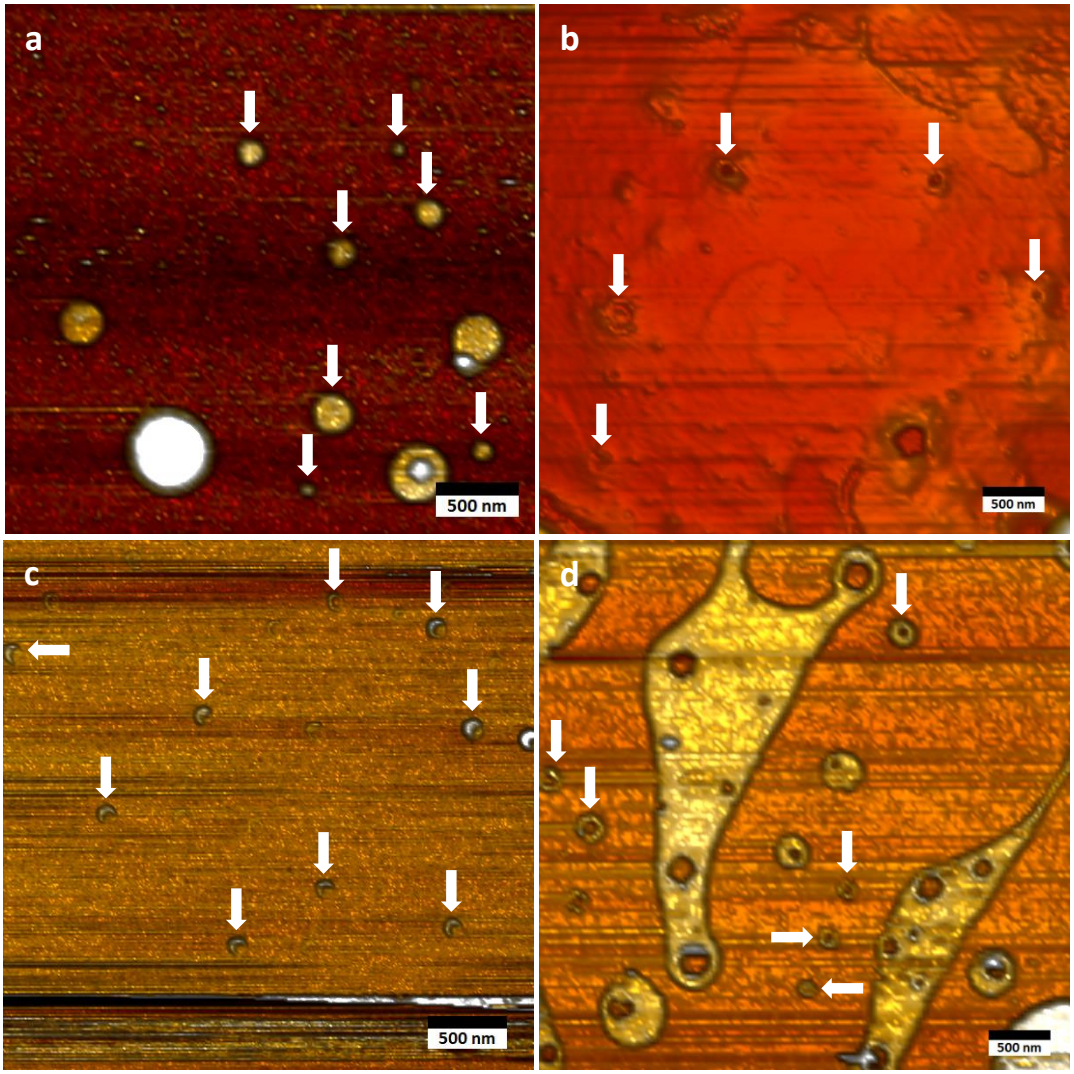

Figure 5.8 AFM images of (a) blank, (b) CPT-11-loaded, (c) CDDP-loaded and (d) CPT-11/CDDP combination-loaded liposomes fabricated from formulation 6. The white arrows indicate the position of individual liposomes within the image.

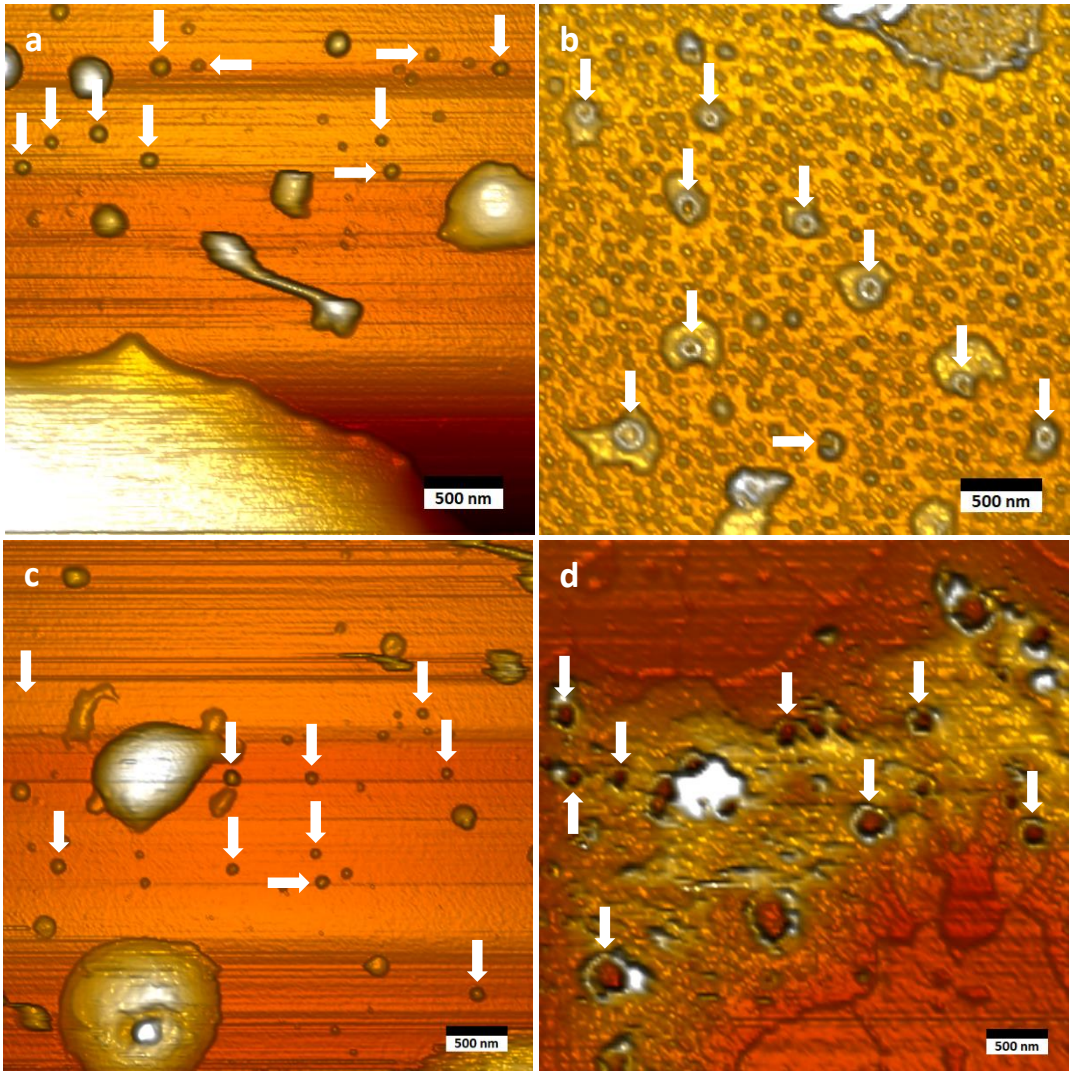

Figure 5.9 AFM images of (a) blank, (b) CPT-11-loaded, (c) CDDP-loaded and (d) CPT-11/CDDP combination-loaded liposomes fabricated from formulation 7. The white arrows indicate the position of individual liposomes within the image.

Blank and drug-loaded liposomes of formulation 6 and 7 were also observed using the AFM in this study. Several interesting observations were made in regard with the liposomes of these two formulations. As exhibited in Fig. 5.8 (a) and Fig. 5.9 (a), blank liposomes of both formulations were found to be flat and circular. However, drug-loaded liposomes of formulation 6 (Fig. 5.8b – 5.8d) and formulation 7 (Fig. 5.9b and 5.9d) were observed to be concave discs except for CDDP-loaded liposome of formulation 7 (Fig. 5.9c). This concave disk-appearance of the drug-loaded liposomes

suggests a physical change effecting the liposomes during the drying process of the samples, which is possibly precipitated by the presence of the drug content within the liposomes. However, it was not determined whether this concave shape was caused by a simple depression at the middle of the flat liposome disc or due to the rupture of the liposome induced by the drying process. Due to the altered shape of the drug-loaded liposomes of both formulations, a direct size comparison between blank and drug-loaded liposome was not possible due to poorly defined border of the concave-shaped appearance of the liposomes.

SEM analysis of the liposome samples was carried out in order to determine the morphology of the liposomes after the freeze-drying process. It was discovered that the presence of trehalose, while providing cryoprotection, complicates image acquisition of the liposomes using the SEM. As shown in Fig. 5.10, trehalose forms an interconnecting matrix of substance covering the liposomes. Similar finding was observed in a previous research in which trehalose was used as the cryoprotectant and a cover continuous matrix was found to be interfering with proper visualisation of the particles (Fonte et al., 2012). In that study, larger particles in the range of 5 – 20 µm were used, therefore better visualisation of the shape and surface of the particles was possible in comparison with the nanoparticles used in this study. Therefore, better visualisation might be achieved with removal of trehalose post FD.

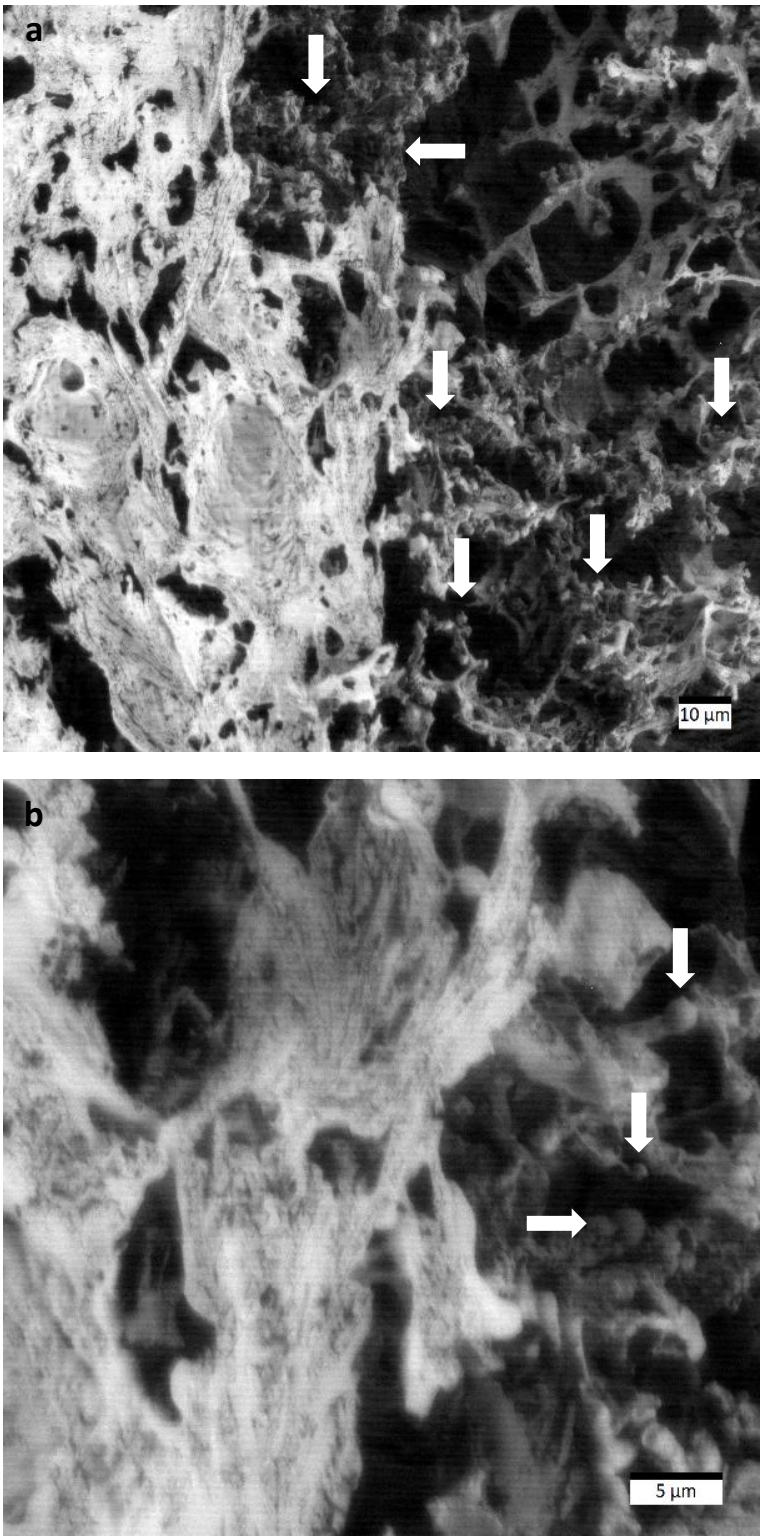

Figure 5.10 SEM images of blank formulation 5 liposomes at (a) low magnification (1416x) and (b) high magnification (5000x). The white arrows indicate globular formations of interconnecting trehalose matrix, possibly containing cluster of liposomes.

Removing trehalose altogether from the liposome suspension should mitigate the issue but the liposomes might not be able to withstand the harsh conditions involved in freeze-drying process. This study, while providing an insight into the morphology of the liposomes obtained from SEM, did not produce quantitative data on the physical characteristics of the liposomes. Further study and modifications to the sample preparation may be able to provide clearer images and possibly shed some light on the surface characteristics of the nanoparticles.

5.3.3 Cytotoxicity study of liposomes

To understand the efficacy of the drug-loaded liposomes and compare their efficacy against non-entrapped drugs, an *in vitro* experiment was carried out as a part of this study. A549 cancer cell was chosen for this experiment to reflect the intended lung cancer target for the drug-loaded liposomes in this study. MTT assay was selected for this experiment to assess the cytotoxicity of non-entrapped and liposome-entrapped CPT-11, CDDP and CPT-11 + CDDP combination on the A549 cancer cells viability post exposure to the samples by measuring the concentration of formazan formed within the wells. The cytotoxicity of blank liposome samples was also tested in this experiment in order to determine the effect of the liposome itself on the cancer cell-killing efficacy of the entrapped drugs.

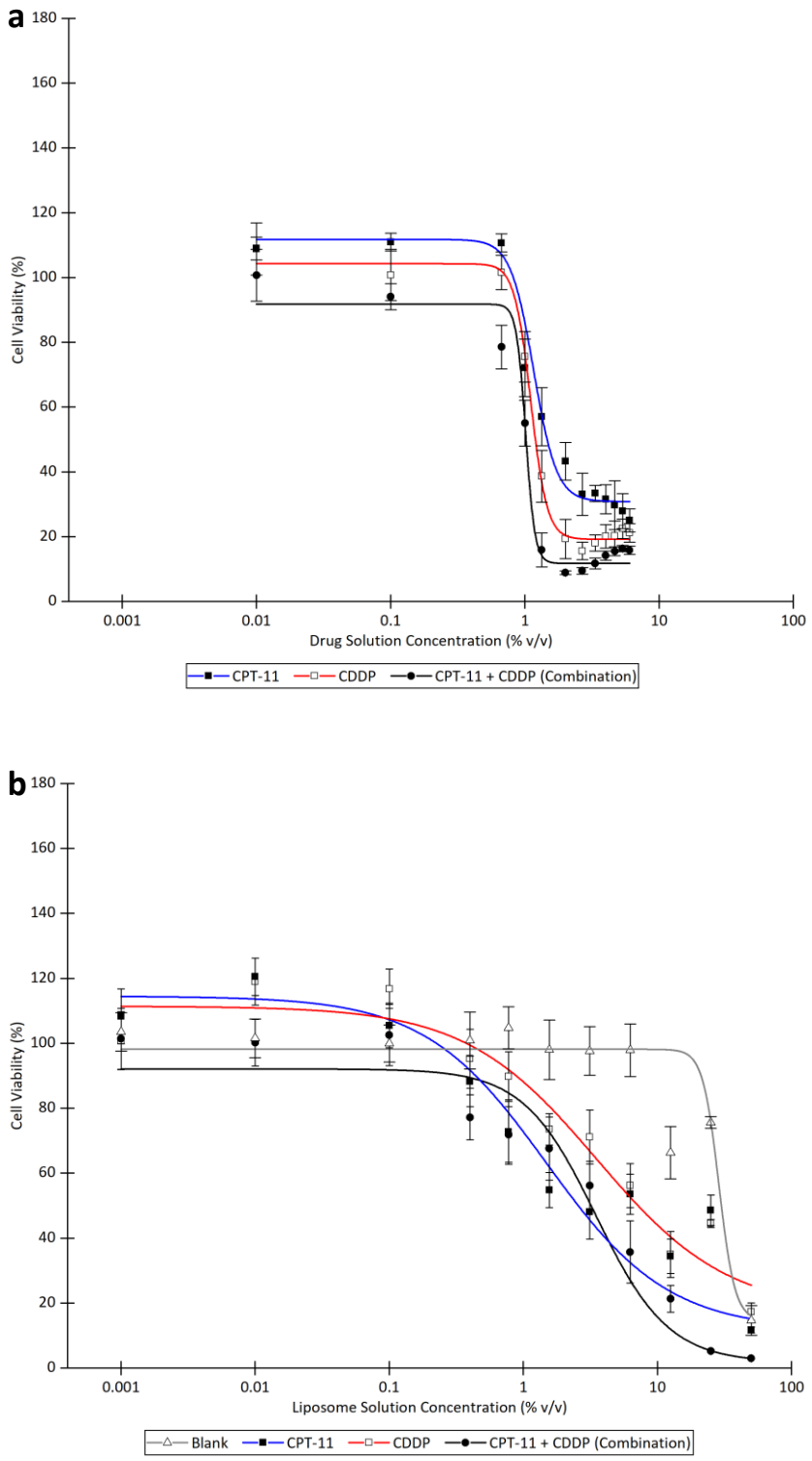

Figure 5.11 Dose-response curve of (a) non-entrapped drugs and (b) blank and drug-loaded liposomes of formulation 5, plotted from percentage of cell viability versus control against concentration of sample solution in wells. Some error bars are hidden within the data points.

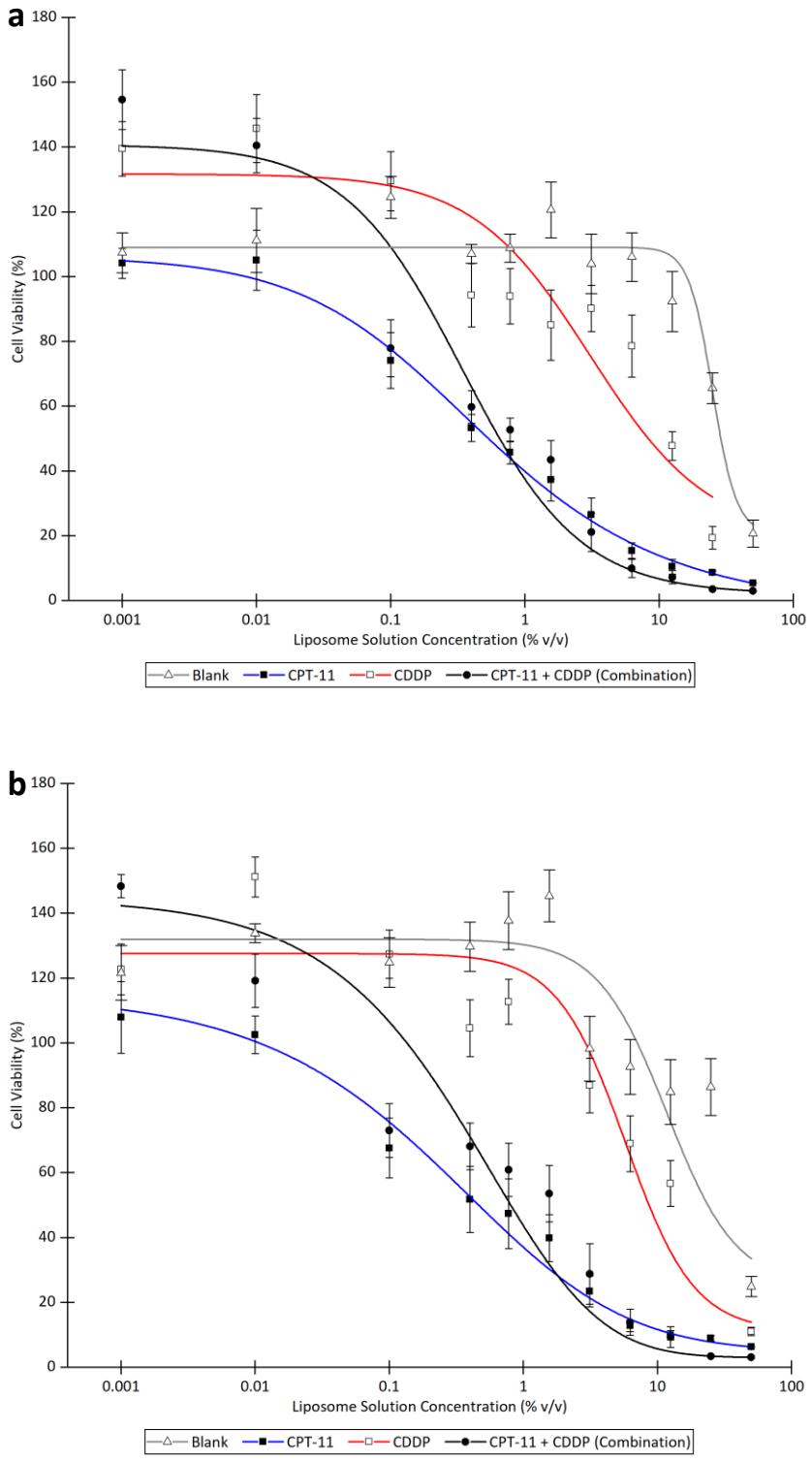

Figure 5.12 Dose-response curve of drug-loaded liposomes of (a) formulation 6 and (b) formulation 7, plotted from percentage of cell viability versus control against concentration of sample solutions in wells. Some error bars are hidden within the data points.

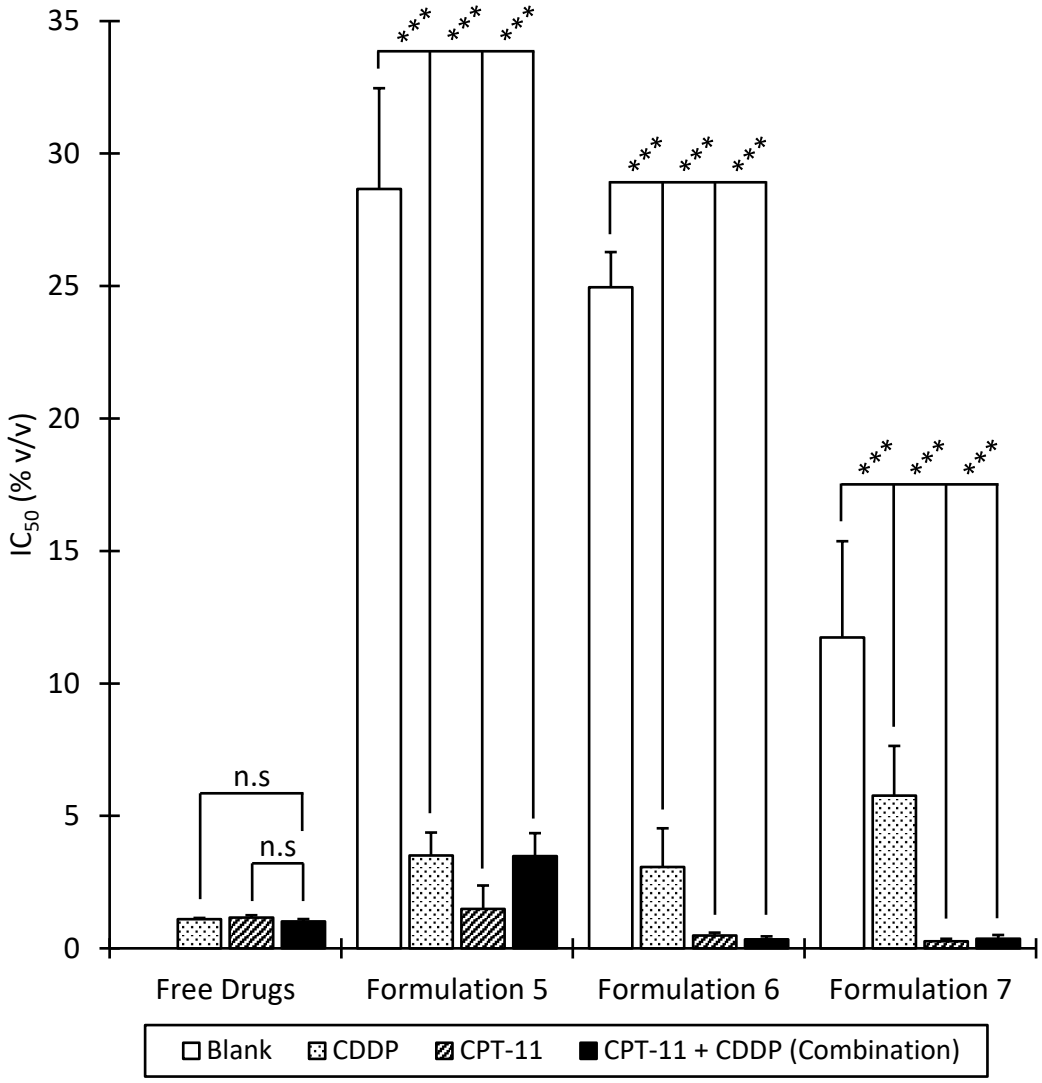

Figure 5.13 IC_{50} values of free drugs, blank and drug-loaded liposomes of all formulations. The IC_{50} values and SD were derived from drug-response curves as detailed in Fig. 5.11 and 5.12. Highly significant differences (***) were found between the blank liposome and each of the drug-loaded liposomes within individual formulations. No significant differences were found between non-entrapped CPT-11 + CDDP combination and each of the constituent drugs. Some error bars are hidden within the data points.

Table 5.1 Concentration of CPT-11 and CDDP in non-entrapped drug samples and drug-loaded liposomes of all formulations at IC_{50} points outlined in Fig.38. Drug concentration values at IC_{50} points were derived from plotting dose-response curves similar to Fig. 36 and 37 by using percentage of cell viability versus control against drug concentration in μM. Data are expressed as mean ± SD.

	Non-entrapped drugs		Formulation 5		Formulation 6		Formulation 7	
	Standalone	Combination	Standalone	Combination	Standalone	Combination	Standalone	Combination
CPT-11 (μM)	16.77 ± 4.46	4.89 ± 1.75	0.76 ± 0.33	2.09 ± 0.52	0.26 ± 0.06	0.26 ± 0.08	0.20 ± 0.07	0.25 ± 0.09
CDDP (μM)	12.40 ± 1.21	9.78 ± 3.50	1.56 ± 0.39	1.55 ± 0.39	1.04 ± 0.46	0.15 ± 0.05	1.88 ± 0.61	0.13 ± 0.05

The non-entrapped drug samples used in this experiment were diluted directly from the stock solutions of the initial aqueous phase used in the fabrication of the drug-loaded liposomes. As demonstrated in Fig. 5.11a, the drug-response curves for non-entrapped drugs of CPT-11, CDDP and CPT-11 + CDDP combination showed similar profile. The derived IC_{50} value of the CPT-11 + CDDP combination exhibited no significant difference to standalone CPT-11 and CDDP as shown in Fig. 5.13. The actual concentration of the non-entrapped drugs at IC_{50} points were outlined in Table 5.1. It was discovered that albeit lower concentrations of both CPT-11 and CDDP in combination solution compared to standalone solutions required to achieve IC_{50} point, no significant difference was exhibited between them. This finding is particularly interesting due to the absence of antitumor synergistic effect against A549 cancer line arising from the combination of CPT-11 and CDDP as reported previously (Kano et al., 1992; Masumoto et al., 1995) and specifically at the CPT-11/CDDP molar ratio of 1:2 as per finding of another study (Tardi et al., 2009). The variation is probably caused by the difference in concentration of both drugs used in this study. A previous study has shown high variability in CPT-11/CDDP combination concentration that exhibited synergism against colon cancer lines, from 0.17 – 1.7 nM of CPT-11 and 33.3 – 333.3 nM of CDDP (Tsunoda et al., 2000). *In vivo* study of CPT-11/CDDP combination activity against LX-1 human squamous cell lung tumour xenograft in nude mice demonstrated that the dose of 23.5 mg/kg/day and 3 mg/kg/day for CPT-11 and CDDP respectively exerted significant tumour volume reduction in contrast with standalone CPT-11 or CDDP (Kudoh et al., 1993). Ultimately, this finding established the baseline for the subsequent *in vitro* test of the drug-loaded liposomes on which cytotoxicity of the drugs can be compared.

The dose-response profiles for blank and drug-loaded liposomes of formulation 5, 6 and 7 were shown in Fig. 5.11b, Fig. 5.12a and Fig. 5.12b respectively. Cursory analysis of the plots revealed similar dose-response profiles between drug-loaded liposomes of formulation 6 and 7. Similar pattern cannot be discerned with drug-loaded liposomes of formulation 5, although in all three formulations the same drug-loaded liposomes reduced cell viability significantly in comparison with blank liposomes as shown in the IC_{50} values of blank and drug-loaded liposomes for all formulation in Fig. 5.13. This demonstrates that the cytotoxicity of the drug-loaded liposomes can be attributed to the drug content rather than the liposomes itself. Interestingly, the cytotoxicity of the blank liposomes progressively increases from formulation 5 to 7. Several aspects of the formulations can be attributed to this observation such as the lipid composition of the formulations and physical characteristics of the liposomes. However, further study is required to fully establish the correlation of these factors with the increased cytotoxicity or lack thereof.

Another notable observation of drug-loaded liposomes of formulation 6 and 7 is the higher cytotoxicity of CPT-11 and CPT-11 + CDDP combination-loaded liposomes in relation to CDDP-loaded liposomes (Fig. 5.13). This finding is particularly interesting due to the virtually non-existent difference in IC_{50} values of CPT-11 and CPT-11 + CDDP combination-loaded liposomes. As shown in Table 5.1, the IC_{50} point of drug-loaded liposomes of both formulation 6 and 7 indicate that there is no significant difference between standalone and combination concentration of CPT-11 for both formulation 6 and 7. On the other hand, CDDP concentrations in both formulation 6 and 7 liposomes show significant reductions from standalone to combination at IC_{50} point as much as 1.75 μM in the case of formulation 7. In

comparison with drug-loaded liposomes of formulation 5, no significant difference was observed with the CDDP concentration between standalone and combination-loaded liposomes while significant increase in CPT-11 concentration was observed from standalone to combination-loaded liposome at IC_{50} point. These conflicting findings exhibited the complexities of drug combination-loaded liposome systems. No direct comparison of this data is available with currently published findings, however, a comparable observation with dual entrapment of doxorubicin and vincristine in various types of liposome exhibited varying cytotoxicity at different levels of drug concentration (Zhang et al., 2017). Similarly in dual entrapment of carfilzomib and doxorubicin, it was found that while there is a significant difference of cell viability at lower carfilzomib concentration when compared with a mix of standalone liposomal carfilzomib and doxorubicin, no such difference exists at higher concentration of carfilzomib (Ashley et al., 2016).

Observation of drug-loaded liposomes of formulation 6 and 7 gives rise to the postulation that the cytotoxicity of the drugs combination may be caused solely by the CPT-11 component of the combination. However, in the case of drug-loaded liposomes of formulation 5, significantly higher concentration of CPT-11 was used in the combination-loaded liposome in comparison with its standalone counterpart with the same concentration of CDDP in both cases. It therefore can be argued that in the case of drug-loaded liposomes of formulation 5, CDDP concentration played a major role in determining the IC_{50} point. Several factors may be causing the differences in cytotoxicity of these drug-loaded liposomes such as the composition of the liposomes, physical characteristics of the liposomes and in case of the combination-loaded liposomes, the ratio of the loaded drugs. It is also possible, in the case of formulation

6 and 7, that the increased cytotoxicity was caused by synergistic effect of the drug combination. This study however, used a set of formulations and a fixed ratio of drugs in each of the formulation and therefore afforded an opportunity for a further study on these formulations with variable drug ratio in order to improve the cytotoxicity of the drug-loaded liposomes by tailoring the drug ratio in accordance to the formulation used and the target cells, especially with combination-loaded liposomes.

The most remarkable observation in this study is the concentration of each of the drugs at IC_{50} point for drug-loaded liposomes of all formulations in relation with non-entrapped drugs. As detailed in Table 5.1, it was discovered that liposomes loaded with both CDDP and CPT-11, either standalone or in combination, achieved IC_{50} point at a significantly lower concentration of the respective drugs when compared with their non-entrapped counterparts. CPT-11 + CDDP combination-loaded liposomes of formulation 6 and 7 demonstrated the lowest concentration for each of the drugs in comparison with non-entrapped drugs. Combination-loaded formulation 7 liposomes for example, attained IC_{50} point at CPT-11 and CDDP concentration of 0.25 µM and 0.13 µM respectively. This is a stark difference to its non-entrapped drugs counterparts which achieved IC_{50} point at CPT-11 and CDDP concentration of 4.89 µM and 9.78 µM respectively. Similarly, standalone-loaded formulation 6 liposomes attained IC_{50} point at 0.26 µM and 1.04 µM concentration of CPT-11 and CDDP respectively which is significantly lower than its non-entrapped counterparts at 16.77 µM and 12.40 µM of CPT-11 and CDDP respectively.

Comparable findings have been reported previously with entrapped carboplatin obtaining IC_{50} at a significantly lower concentration in comparison with its unentrapped counterpart, suggesting that entrapment of a platinum-based drug within a nanoparticle improves its cytotoxicity due to the increased availability of the drug at the target site and direct cell uptake of the nanoparticle itself (Sadhukha & Prabha, 2014). A previous study has shown that the combination of CPT-11 and CDDP at a ratio of 1.5:1 within a nanoparticle demonstrated high synergism in its cell-killing activity (Valencia et al., 2013). Targeted polymeric nanoparticles were used in the study as the entrapping material which is likely to improve nanoparticle uptake and drug accumulation within the target cells. It was observed that CPT-11 and CDDP combination-loaded nanoparticles exhibited significantly higher cytotoxicity against human prostate adenocarcinoma cells in comparison with its standalone counterparts (Valencia et al., 2013). This suggests that further improvement is feasible for implementation on the current formulations such as manipulating physical characteristics of the liposomes, modifying drug ratio within the liposomes and adding targeting ligands to optimise target cell uptake of the liposomes and improve their cancer-cell killing activity whilst minimising the side effects of the drug by carrying the lowest concentration of drugs possible.

5.4 Conclusion

Lyophilisation of blank and drug-loaded liposomes of all formulations was achieved successfully via modification of trehalose concentration post purification. Modifying the concentration of trehalose in the liposome suspension post purification was shown to be sufficient and comparable to increasing trehalose concentration in the initial aqueous phase of the liposome fabrication in providing adequate cryoprotection for the liposomes during the freeze-drying process. The resultant products were also found to be physically acceptable as final pharmaceutical products.

Morphology study of the liposomes using the AFM method revealed that the dried liposome samples formed flat discs with a high degree of variations in diameter. SEM study revealed the appearance of spherical objects which are believed to be the suspended, freeze-dried liposomes within an interconnected matrix of trehalose. While these methods are invaluable in providing insights on the appearance of the liposomes in various conditions, no quantitative data in regards to physical characteristics of the liposomes were able to be gleaned from these methods.

In vitro study of the blank and drug-loaded liposomes of all formulations demonstrated that the blank liposomes had significantly higher IC_{50} values in comparison to their drug-loaded counterparts, lending credence that the significantly higher cytotoxic effect of the drug-loaded liposomes was due to their drug payloads. It was also proved in this study that the drug-loaded liposomes, especially combination-loaded liposomes of formulation 6 and 7 were exerting a significantly higher cytotoxicity against A549 cells than their non-entrapped drugs counterparts, paving the possibility of these drug-loaded liposomes to be utilised as a more efficient drug delivery carrier for lung cancer therapy.

Chapter 6

General Conclusions and Future Works

6.1 General conclusions

This chapter aims are to review and summarise the key findings of each chapter and provide future work recommendations. Conclusion for each chapter will be based on the project's objectives and aims. Future work recommendations will then be made based upon the possible refinement of the product in order to enhance its feasibility as a lung cancer therapy.

6.1.1 Formulation of stable liposome formulations with desired physical characteristics and creation of CDDP-loaded liposomes

The results demonstrated in Chapter 2 showed that microfluidics technique with SHM is a suitable for liposome fabrication method producing uniform physical characteristics with the added advantage of aqueous-to-lipid FRR and volumetric TFR modification in order to achieve the optimal size of the liposomes. Several liposomal formulations were found to be suitable candidates for the eventual entrapment of CDDP. The chosen formulations, 5 and 7 were found to entrap CDDP with sufficient efficiency without any discernible changes in terms of physical characteristics post purification. CDDP-loaded liposomes from formulation 5 were found to be able to retain the entrapped drug in the storage conditions tested and exhibited initial burst release at 37°C. The results obtained from this chapter were used as a basis for subsequent studies such as the selected formulations to be used for entrapment of CPT-11 and CDDP.

6.1.2 Fabrication scale-up of loaded liposomes and characteristics analyses and comparisons of such liposomes with their scaled-down counterparts.

In Chapter 3, liposome production scale-up was successfully demonstrated with similar liposome physical characteristics, entrapment efficiency and release profile were observed across the production scales when the same formulation was used, demonstrating reproducibility of the results when production scaling up is applied. It was discovered that variations in concentration of entrapped material during liposome fabrication effects small difference in entrapment efficiency. Another discovery is that different release kinetics were observed between formulation 5 and 7 liposomes whilst no such difference was observed between liposomes produced using small and large scale production using the same formulation. These discoveries suggest scalability of the chosen formulations without any changes arising from increasing production scale.

6.1.3 Formulation and analyses of standalone and combination-loaded CPT-11 and CDDP liposomes and comparison between purification processes of filter centrifugation and TFF.

In Chapter 4, fabrication of liposomes loaded with CPT-11, CDDP and CPT-11/CDDP combination from formulation 5, 6 and 7 was carried out successfully. These liposomes had been characterised, purified and determined to be physically stable over the period of 28 days post fabrication. Purification of liposomes was carried out using both filter centrifugation and TFF methods and it was discovered that TFF method was more suited for purification of large volume of liposome suspension with superior concentration capability in comparison with filter centrifugation. Differences were

detected in the concentration of actual drug entrapped within CPT-11/CDDP combination liposomes compared with the initial concentration of the drugs in the aqueous phase during the fabrication process. This discrepancy provides a crucial insight of the determining factors in the entrapment of such drugs and is invaluable in refining the fabrication process in achieving the desired drug entrapment of dual loaded liposomes.

6.1.4 Lyophilisation, morphology and cytotoxicity studies of the blank, free drugs, standalone and combination CPT-11 and CDDP loaded liposomes.

In Chapter 5, lyophilisation of blank and drug-loaded liposomes of all formulations was achieved with modification of trehalose concentration post purification. Such modification was found to be comparable with increasing trehalose concentration in the initial aqueous phase of the liposome fabrication in providing adequate cryoprotection during FD process with the resultant products physically acceptable as final pharmaceutical products. AFM observation revealed that the dried liposome samples formed flat discs with a high degree of variations in diameter. SEM study revealed the appearance of spherical objects which are believed to be the suspended, freeze-dried liposomes within an interconnected matrix of trehalose. These methods are invaluable in providing insights on the appearance of the liposomes but provides no quantitative data in regards to physical characteristics of the liposomes. *In vitro* study of the blank and drug-loaded liposomes of all formulations demonstrated that the blank liposomes had significantly higher IC_{50} values in comparison to their drug-loaded counterparts, proving that the cytotoxicity of the drug-loaded liposome arose from their payloads. Significantly higher cytotoxicity against A549 cells was

observed of drug-loaded liposomes, especially the dual loaded liposomes of formulation 6 and 7 compared to their non-entrapped drugs counterparts, paving the possibility of these drug-loaded liposomes to be utilised as a more efficient drug delivery carrier for lung cancer therapy.

6.2 Future works

6.2.1 Enhancing delivery by entrapment in biodegradable polymer

One of the major hurdles facing pulmonary delivery of drug is rate of deposition at the intended target site. Unlike the blood vessel which is a continuous closed loop system, closed ended system of the lung presents a challenge in targeting a specific site within the system, especially deep within lung periphery. The delivery process is further complicated by variations of breathing parameters and physical alterations to the airway itself due to the disease or other factors (Labiris & Dolovich, 2003a). When a drug particle is breathed in, several factors determine its eventual deposition site such as particle shape, size, density and aerodynamic diameter (Labiris & Dolovich, 2003b). While the main driving force for the particle movement within the few initial moments of inhalation is the movement of the air into the lung itself, it is quickly reduced to being significantly influenced by Brownian motion and gravitational sedimentation deeper in the periphery. At this stage, particle density and size are more prominent in determining the rate and site of deposition. Smaller particles, specifically in nanometre scale will not have enough time to settle deep in lung periphery due to the fact that their lower density and size will keep the particles afloat for longer time. This will cause the particles to be exhaled, hence preventing them from reaching the intended target site and thus negating their therapeutic effect (Wittgen et al., 2007).

As mentioned in Chapter 1, it is important for the liposomes to have a size within the range of 90-200 nm to improve cell uptake (Win & Feng, 2005). Other reasons for selection of this size range are because opsonisation of liposomes smaller than 100 nm occurs less rapidly, slower drug release rate achieved with liposomes smaller than 200 nm and avoidance of phagocytosis by macrophages while maintaining useful amount of entrapped drug (Labiris & Dolovich, 2003b). While all of these characteristics are favourable for liposomes uptake by the cell and drug release, the actual delivery of such particles to the target site in peripheral lung is difficult to achieve optimally. This is mainly due to the fact that particles within that size range would quickly be exhaled out, therefore reducing the amount of drug delivered to the intended target site and can possibly cause environmental contamination by the entrapped anti-cancer drugs which are both cytotoxic and teratogenic in nature.

Previous studies have been conducted using Sustained Release Lipid Inhalation Targeting (SLIT) cisplatin and liposomal 9NC in which the liposomal drugs were nebulized to achieve the optimal mass median aerodynamic diameter (MMAD) of 1-5 μm which is suitable for peripheral lung deposition (Verschraegen et al., 2004; Wittgen et al., 2007). However, in case of SLIT cisplatin, deposition in intended target site remains low at 10-15%. This could be explained by the fact that the nebulisation vehicle used in this study is the dispersion media of the SLIT cisplatin itself (0.9% NaCl solution) which is supposed to form nebulized microdroplets within the desired size. However, the microdroplet size itself could change when transiting through the air during the inhalation process and becomes smaller due to evaporation. It has been demonstrated that microdroplets with high surface area to volume ratio are especially

affected by this phenomenon (Desai, Esho, & Kaware, 2010). This led to reduced deposition at target site and increased amount of exhaled SLIT cisplatin, which is demonstrated by significant detection of cisplatin up to 1 h after administration of nebulized SLIT cisplatin (Wittgen et al., 2007). Both studies required elaborate experimental setup; full protection clothing for both healthcare workers and patients and HEPA-filtered negative pressure room. Even the self-administered liposomal 9NC required a prior side effects assessment, portable air compressor, HEPA-filtering system and weekly supervision (Verschraegen et al., 2004; Wittgen et al., 2007). Both of these problems need to be addressed in order to ensure that significantly higher percentage of liposomal anti-cancer drug can reach its intended target site and reduce or avoid the exhaled drug altogether in a cost-effective manner.

In order to maximize the deposition of the particles at the intended site, modifications to the size and density of the particles are needed, particularly to achieve the required MMAD. Several studies have been conducted previously to load the nanoparticles in carriers to aid in achieving the favoured characteristics for delivery of the particles to the intended action site, mostly deep within the peripheral lung (Ely, Roa, Finlay, & Löbenberg, 2007; Grenha, Seijo, & Remuñán-López, 2005; Kawashima, Serigano, Hino, Yamamoto, & Takeuchi, 1998; Sham, Zhang, Finlay, Roa, & Loebenberg, 2004; Tsapis, Bennett, Jackson, Weitz, & Edwards, 2002) using various materials, entrapping nanoparticles of varying size ranges with various nanoparticle fabrication methods and ultimately varying degree of success. All of the abovementioned studies used spray drying method for incorporating the nanoparticles inside the carrier particle, which usually consists of inert and biodegradable materials such as lactose. While spray drying method is relatively cheaper and less complicated,

the yield of microparticles with size of less than 5.6 μm is low at 38 – 42% (Sham et al., 2004) and in this study, with very high variation as well at 46.47 ± 15% (Ely et al., 2007). Furthermore, there is no mention in the studies about any method to physically separate the microparticles according to their sizes and recovering them afterwards to be used. This is crucial in order to minimise size variation of the microparticles to ensure maximum delivery to the intended deposition site in the lung. In one of the studies, the use of effervescent carrier particle is especially interesting due to the fact that it provides a mean to release the nanoparticles in the presence of a specific trigger and in a controlled and quantifiable manner (Ely et al., 2007).

The use of carrier particle with modified surface is of special interest in this research. A previous study on the effect of corrugated particle for pulmonary delivery yielded several interesting results, particularly pertaining MMAD and contact surfaces of the particles. Two types of particles were fabricated in this study: corrugated and spherical. While the corrugated particles have larger mass median diameter (MMD), they have lower MMAD compared with the spherical particles. Aerosolisation of both types of particles was tested by a four-stage liquid impinger and the results showed that the corrugated particles were superior to the spherical ones in term of generation of particles less than 5 μm in size and impaction and retention loss. According to the authors, these advantages over the conventional spherical particles can be attributed to the surface morphology of the corrugated particles. While they have significantly larger surface area compared with their spherical counterparts, these surfaces do not necessarily come into contact with each other, but rather limit the surfaces that actually comes in contact with each other, thus increasing the average distance between particles which in turn, reducing the effect of van der Waals forces of cohesion. This

helps in redispersion of the particles and reducing the impaction and retention loss (Chew & Chan, 2001).

Improvement on the surface of the carrier particle itself can also enhance its aerodynamic characteristics during transit through the airways by reducing its aerodynamic drag. It is widely known that spherical particles with smooth surface encounter higher aerodynamic drag during flight compared with spherical particles with dimpled surface (Fig. 6.1). This is excellently demonstrated by golf balls which have multitude of dimples on their surface to improve their flight characteristics. A study (Mohamed & van der Walle, 2006) explored the use of poly(lactic-co-glycolic acid) (PLGA) microcapsules for pulmonary delivery. The authors successfully fabricated the hollow, biodegradable PLGA in the study. More importantly, they have managed to create the PLGA microcapsules with dimpled surface using modification of surfactant used in the research. The subsequent characterisation of the particles yielded some very interesting results. The median diameter of the dimpled PLGA microcapsules is measured around 7.85 μm while the calculated aerodynamic diameter is measured around 3.81 μm. This demonstrated the possibility to create a larger particle which is useful in entrapping a significant number of nanoparticles per microcapsule while having a smaller aerodynamic diameter to be suitable for delivery to peripheral lung. The whole study underpinned the importance of the particles having dimpled surface as the main influence in improving their flow characteristics, citing several previous works (Chew & Chan, 2001; Chew, Tang, Chan, & Raper, 2005).

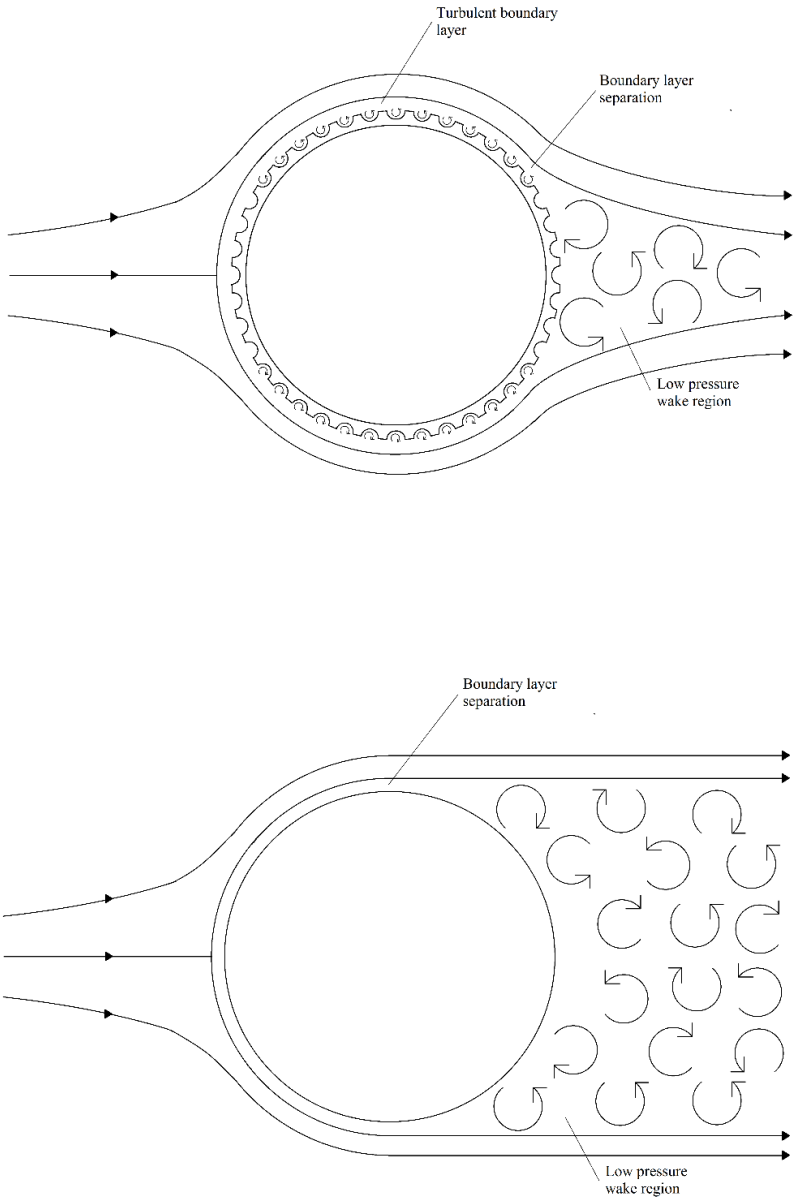

Figure 6.1 Schematic diagram of airflow for dimpled and smooth spherical particles in flight. Low pressure wake region created by disturbance of airflow by a spherical particle causes high drag. The dimpled surface of the particle acts as a generator of mini turbulence on the surface, creating low pressure area on the surface which prevents early boundary layer separation from the surface, thus minimizing the wake region and aerodynamic drag.

6.2.2 Attachment of ligands as active targeting moieties

The use of targeting modality is recognised as one of the methods that can be employed in order to enhance delivery and accumulation of anti-cancer drug at its intended site. This is pertinent to ensure high concentration of the drug is present at the target site to effectively exert its pharmacological effect and also reducing side effects associated with the systemic exposure of the drug (Deshpande, Biswas, & Torchilin, 2013). The most common type of liposomal targeting is by passive targeting. The growing cancerous mass requires a steady supply of nutrient within the mass itself. This gives rise to angiogenesis, a proliferation of blood vessel in the site of tumour. However, due to the nature of unregulated growth of the cancerous mass, the blood vessels are poorly formed and without any lymphatic drainage. The malformed blood vessels are 'leaky' in nature, characterized by having gaps within its wall, ranging from 100 to 780 nm. In contrast to healthy blood vessels which have much smaller gaps of 5 to 10 nm to allow for interstitial fluid containing larger molecules to pass through, these larger gaps allow the liposomes to pass through and retained within it. Unlike healthy systemic circulation which also incorporates lymphatic system drainage for collection of interstitial fluid created by hydrostatic pressure forcing out fluid from blood vessel, these malformed blood vessels lack lymphatic drainage which allow the trapped drug-loaded liposome retained even longer (Haley & Frenkel, 2008). The systemic circulation itself also serves the purpose of carrying more liposomes to be retained within the leaky vasculature. Taking into account that the proposed project is delivery of liposomal anti-cancer drug directly to the tumour site in the lung, passive targeting is less effective due to the fact that little to none of the liposomes are intended for systemic circulation. Hence it is more

effective for the liposomes to be equipped for active targeting modalities, which will help in ensuring the liposomes be taken up by the cancer cells.

6.2.3 Targeting folate receptor

Folate receptor is recognized as one of the targets for active liposomal uptake by cell. The discovery began with identification of monoclonal antibody binding with folate receptors present in various animal tissues. Subsequently, the study also discovered that malignant cell lines express significantly more folate receptors than normal cell lines (Weitman et al., 1992). This marked an important milestone in the use of folate-conjugated macromolecules for the purpose of targeted delivery of anti-cancer agents to the cancer cells (Leamon & Low, 1992). One of the earliest studies on the use of folate-conjugated liposomes for active targeting on cancer cells demonstrated the feasibility of conjugating folate groups with the lipid head groups of the liposomes, resulting in increase of uptake by the cancer cells compared with liposomes without the conjugation. Interestingly, by adding a spacer polyethylene glycol (PEG) group between the folate and lipid head group significantly increasing the liposomal uptake by the cancer cells (Lee & Low, 1994). The use of PEG spacer groups with different molecular masses also affects the binding affinity of the folate conjugate with the folate receptors. PEG_{2000}-conjugated phospholipids when used for the formulation of liposomes gives rise to stealth liposomes, which is suitable to evade the reticuloendothelial system (RES), therefore prolonging its systemic circulation time. However, a high number of PEG_{2000} groups on the liposomes surface can potentially interfere with the binding affinity of PEG_{2000}-folate conjugate. Therefore, the use of PEG_{3350} as the spacer group in this case can enhance the folate conjugate binding ability as the spacer group extend the folate group above the rest of the PEG_{2000}

groups on the liposome's surface (Gabizon et al., 1999). Another study (Yamada et al., 2008) further elaborated the effect of PEG spacer length on folate-conjugated liposomal doxorubicin. The research utilised three different base types of liposomal doxorubicin; non-targeted liposome (NL), non-targeted PEGylated liposome (SL) and folate-PEG_{2000}-PEG_{5000} liposome (ML). NL is not a PEGylated liposome while SL and ML use $mPEG_{2000}$ and $mPEG_{5000}$ as their coating respectively (Yamada et al., 2008). Stability study conducted on these liposomes concluded that they were able to effectively contain the doxorubicin folate conjugation does not cause instability of the membrane; hence folate conjugation does not cause instability of the membrane. In an *in vitro* study, highest cell uptake by A549 cell line was observed with folate-conjugated NL with PEG_{5000} spacer. It is important to note that the A549 cell line used for the *in vitro* study was cultured in folate-deficient medium to prevent folate binding competition between free folate and folate-conjugated liposomes. However, in an *in vivo* study utilising murine model inoculated with M109 cell line, it was discovered that folate-conjugated SL and ML achieved greater cytotoxicity compared with their NL counterpart (Yamada et al., 2008). This is attributed to the presence of PEG coating on both SL and ML, which helps masking them from rapid clearance by RES. Interestingly, folate-conjugated liposomes showed higher serum clearance, therefore their higher anti-cancer activity can be attributed to their specificity to cancer cells (Yamada et al., 2008). Previous study has found that folate conjugation to PEGylated liposome did indeed cause higher rate of serum clearance than non-targeted PEGylated liposome (Gabizon et al., 2003).

6.2.4 Targeting transferrin receptor

Another active targeting modality considered for the liposomes is by using conjugation of transferrin (Tf) molecule to target transferrin receptor (TfR). Tf molecules are glycoproteins bound with iron abundantly found in blood plasma (Daniels, Delgado, Rodriguez, Helguera, & Penichet, 2006). Cell uptake of plasma iron requires binding of Tf with TfR found on cell surface followed by endocytosis of the Tf-TfR complex. Lowering of pH within the vesicles causes the Tf to release its iron load, producing apotransferrin (iron-free transferrin) and both apotransferrin and TfR are returned to the cell surface, completing the endocytic cycle (MacGillivray et al., 1998). As part of normal cell growth, TfR is expressed on cell surface to facilitate the uptake of iron, a significant component of cell growth itself (Ponka & Lok, 1999). It stands to reason that cells with higher proliferation rate such as intestinal epithelium have greater expression of TfR (Omary, Trowbridge, & Minowada, 1980). However, cancerous tissues express prominently more TfRs on its surface in order to gain more iron for the uncontrolled cell growth. More importantly, A549 lung adenocarcinoma cell line which would be specifically used for in vitro test for this project exhibits significant overexpression of TfR (Anabousi et al., 2006). Several previous studies had utilised conjugation of Tf moiety to increase delivery specificity of drug carrier systems such as liposome (Derycke et al., 2004; Kobayashi, Ishida, Okada, & Ise, 2007; Li, Ding, Xu, Wang, & Ping, 2009; Xu et al., 2011). One study was dedicated in comparing the uptake of Tf-conjugated liposomes between several immortalised cancerous lung cell lines (A549, Calu-3 and 16HBE14o). It was discovered that while A549 cell line showed the highest uptake of Tf-conjugated liposomes (Anabousi et al., 2006). An in vivo study involving rats irradiated and inoculated with human large cell lung cancer

H460 carcinoma cells compared the anti-cancer activity of two differently administered (intravenous and intrapulmonary) Tf-conjugated liposomes. It was found that the highest survival rate was achieved with nebulized Tf-conjugated liposomes which uses much lower dose compared to its intravenous counterpart (0.2 mg kg^{-1} versus 2 mg kg^{-1}) (Gaspar et al., 2012). These studies further reinforce the relevancy of targeting TfR within the scope of this project. It is also important to note that there are several concerns regarding the effectiveness of Tf targeting system. Recent evidence showed that Tf conjugation with liposomal 5,10,15,20-tetra(*m*-hydroxyphenyl)chlorin (Foscan), a photosensitizer used in photodynamic therapy of oesophageal cancer, did not significantly improve the cell uptake of the aforementioned liposomes. The authors suggested some possible explanations for this phenomenon, notably leakage of Foscan from the liposomes due to membrane destabilising effect of Tf (Paszko, Vaz, Ehrhardt, & Senge, 2013). Another study showed that Tf-conjugated nanoparticles lose their specificity in biological fluid. It is suggested that due to complex mixture of proteins within the fluid led to formation of protein corona which shields the Tf moiety, causing the loss of specificity. While the nanoparticles continued to enter the cells, the loss of specificity may lead to unintended toxicity to healthy cells (Salvati et al., 2013).

References

Abdelwahed, W., Degobert, G., & Fessi, H. (2006). Investigation of nanocapsules stabilization by amorphous excipients during freeze-drying and storage. *European Journal of Pharmaceutics and Biopharmaceutics, 63*(2), 87-94.

Abdelwahed, W., Degobert, G., Stainmesse, S., & Fessi, H. (2006). Freeze-drying of nanoparticles: Formulation, process and storage considerations. *Advanced Drug Delivery Reviews, 58*(15), 1688-1713.

Abrams, T. J., Lee, L. B., Murray, L. J., Pryer, N. K., & Cherrington, J. M. (2003). SU11248 Inhibits KIT and Platelet-derived Growth Factor Receptor β in Preclinical Models of Human Small Cell Lung Cancer. *Molecular Cancer Therapeutics, 2*(5), 471-478.

Allen Zhang, J.-a., & Pawelchak, J. (2000). Effect of pH, ionic strength and oxygen burden on the chemical stability of EPC/cholesterol liposomes under accelerated conditions: Part 1: Lipid hydrolysis. *European Journal of Pharmaceutics and Biopharmaceutics, 50*(3), 357-364.

American Society for Testing Materials. (1958). *Symposium on Spectrocemical Analysis for Trace Elements*: ASTM International.

Anabousi, S., Bakowsky, U., Schneider, M., Huwer, H., Lehr, C., & Ehrhardt, C. (2006). In vitro assessment of transferrin-conjugated liposomes as drug delivery systems for inhalation therapy of lung cancer. *European Journal of Pharmaceutical Sciences, 29*(5), 367-374.

Arouri, A., Trojnar, J., Schmidt, S., Hansen, A. H., Mollenhauer, J., & Mouritsen, O. G. (2015). Development of a Cell-Based Bioassay for Phospholipase A2-Triggered Liposomal Drug Release. *PLoS ONE, 10*(5), e0125508.

Ashley, J. D., Quinlan, C. J., Schroeder, V. A., Suckow, M. A., Pizzuti, V. J., Kiziltepe, T., & Bilgicer, B. (2016). Dual Carfilzomib and Doxorubicin–Loaded Liposomal Nanoparticles for Synergistic Efficacy in Multiple Myeloma. *Molecular Cancer Therapeutics*, *15*(7), 1452.

Bakonyi, M., Berkó, S., Budai-Szűcs, M., Kovács, A., & Csányi, E. (2017). DSC for evaluating the encapsulation efficiency of lidocaine-loaded liposomes compared to the ultracentrifugation method. *Journal of Thermal Analysis and Calorimetry, 130*(3), 1619-1625.

Balazs, D. A., & Godbey, W. (2011). Liposomes for Use in Gene Delivery. *Journal of Drug Delivery, 2011*.

Basotra, M., Singh, S. K., & Gulati, M. (2013). Development and Validation of a Simple and Sensitive Spectrometric Method for Estimation of Cisplatin Hydrochloride in Tablet Dosage Forms: Application to Dissolution Studies. *ISRN Analytical Chemistry, 2013*, 8.

Ben Amar, N., Saidani, H., Deratani, A., & Palmeri, J. (2007). Effect of Temperature on the Transport of Water and Neutral Solutes across Nanofiltration Membranes. *Langmuir, 23*(6), 2937-2952.

Beretta, G. L., & Zunino, F. (2007). Relevance of extracellular and intracellular interactions of camptothecins as determinants of antitumor activity. *Biochemical Pharmacology, 74*(10), 1437-1444.

Berger, N., Sachse, A., Bender, J., Schubert, R., & Brandl, M. (2001). Filter extrusion of liposomes using different devices: comparison of liposome size, encapsulation efficiency, and process characteristics. *International Journal of Pharmaceutics, 223*(1), 55-68.

Bishop, J. A., Teruya-Feldstein, J., Westra, W. H., Pelosi, G., Travis, W. D., & Rekhtman, N. (2012). p40 (DeltaNp63) is superior to p63 for the diagnosis of pulmonary squamous cell carcinoma. *Mod Pathol, 25*(3), 405-415.

Brenner, D., McLaughlin, J., & Hung, R. (2011). Previous Lung Diseases and Lung Cancer Risk: A Systematic Review and Meta-Analysis. *PLoS ONE, 6*(3).

British Pharmacopoeia Commission. (2017). Irinotecan Hydrochloride Trihydrate. In *British Pharmacopoeia* (Vol. 1). London: TSO.

Brown, K. L., & Conboy, J. C. (2015). Phosphatidylglycerol Flip-Flop Suppression due to Headgroup Charge Repulsion. *The Journal of Physical Chemistry B, 119*(32), 10252-10260.

Bruglia, M., Rotella, C., McFarlane, A., & Lamprou, D. (2015). Influence of cholesterol on liposome stability and on in vitro drug release. *Drug Delivery and Translational Research, 5*(3), 231-242.

Bulbake, U., Doppalapudi, S., Kommineni, N., & Khan, W. (2017). Liposomal Formulations in Clinical Use: An Updated Review. *Pharmaceutics, 9*(2), 12.

Burke, T. G., Munshi, C. B., Mi, Z., & Jiang, Y. (1995). The Important Role of Albumin in Determining the Relative Human Blood Stabilities of the Camptothecin Anticancer Drugs. *Journal of Pharmaceutical Sciences, 84*(4), 518-519.

Cao, H., Fang, X., Liu, P., Li, H., Chen, W., Liu, B., & Kong, J. (2017). Magnetic-Immuno-Loop-Mediated Isothermal Amplification Based on DNA Encapsulating Liposome for the Ultrasensitive Detection of P-glycoprotein. *Scientific reports, 7*(1), 9312.

Carugo, D., Bottaro, E., Owen, J., Stride, E., & Nastruzzi, C. (2016a). Liposome production by microfluidics: potential and limiting factors. *Scientific reports, 6*, 25876-25876.

Carugo, D., Bottaro, E., Owen, J., Stride, E., & Nastruzzi, C. (2016b). Liposome production by microfluidics: potential and limiting factors. *Scientific reports, 6*, 25876.

Catanzaro, D., Nicolosi, S., Cocetta, V., Salvalaio, M., Pagetta, A., Ragazzi, E., . . . Pasut, G. (2018). Cisplatin liposome and 6-amino nicotinamide combination to overcome drug resistance in ovarian cancer cells. *Oncotarget, 9*(24), 16847-16860.

Cayman Chemical. (2013a, November 5). Product Information 1,2-Dipalmitoyl-*sn*-glycero-3-PC.

Cayman Chemical. (2013b, November 7). Product Information 1,2-Distearoyl-*sn*-glycero-3-PC.

Cayman Chemical. (2013c, December 5). Product Information 1,2-Distearoyl-*sn*-glycero-3-PC (sodium salt).

Cayman Chemical. (2018, May 29). Product Information Cisplatin.

Chew, N., & Chan, H. (2001). Use of Solid Corrugated Particles. *Pharmaceutical research, 18*(11), 1570-1577.

Chew, N., Tang, P., Chan, H., & Raper, J. (2005). How much particle surface corrugation is sufficient to improve aerosol performance of powders? *Pharmaceutical research, 22*(1), 148-152.

Chin, J. H., & Goldstein, D. B. (1977). Effects of Low Concentrations of Ethanol on the Fluidity of Spin-Labeled Erythrocyte and Brain Membranes. *Molecular Pharmacology, 13*(3), 435-441.

Christensen, D., Foged, C., Rosenkrands, I., Nielsen, H. M., Andersen, P., & Agger, E. M. (2007). Trehalose preserves DDA/TDB liposomes and their adjuvant effect during freeze-drying. *Biochimica et Biophysica Acta (BBA) - Biomembranes, 1768*(9), 2120-2129.

Ci, T., Chen, L., Yu, L., & Ding, J. (2014). Tumor regression achieved by encapsulating a moderately soluble drug into a polymeric thermogel. *Scientific reports, 4*, 5473.

Cipolla, D., Wu, H., Eastman, S., Redelmeier, T., Gonda, I., & Chan, H. K. (2014). Development and Characterization of an In Vitro Release Assay for Liposomal Ciprofloxacin for Inhalation. *Journal of Pharmaceutical Sciences, 103*(1), 314-327.

Ciuleanu, T., Brodowicz, T., Zielinski, C., Kim, J., Krzakowski, M., Laack, E., . . . Belani, C. (2009). Maintenance pemetrexed plus best supportive care versus placebo plus best supportive care for non-small-cell lung cancer: a randomised, double-blind, phase 3 study. *Lancet, 374*(9699), 1432-1440.

Cogliano, V., Baan, R., Straif, K., Grosse, Y., Lauby-Secretan, B., Ghissassi, F., . . . Wild, C. (2011). Preventable Exposures Associated With Human Cancers. *JNCI Journal of The National Cancer Institute, 103*(24), 1827-1839.

Collisson, E. A., Campbell, J. D., Brooks, A. N., Berger, A. H., Lee, W., Chmielecki, J., . . . John Flynn, H. (2014). Comprehensive molecular profiling of lung adenocarcinoma. *Nature, 511*(7511), 543-550.

Comiskey, S. J., & Heath, T. D. (1990). Serum-induced leakage of negatively-charged liposomes at nanomolar lipid concentrations. *Biochemistry, 29*(15), 3626-3631.

Crommelin, D., & Van Bommel, E. (1984). Stability of liposomes on storage: freeze dried, frozen or as an aqueous dispersion. *Pharmaceutical research, 1*(4), 159-163.

Crowe, Crowe, L. M., Carpenter, J. F., & Wistrom, C. A. (1987). Stabilization of dry phospholipid bilayers and proteins by sugars. *Biochem J, 242*(1), 1-10.

Crowe, Oliver, A. E., Hoekstra, F. A., & Crowe, L. M. (1997). Stabilization of Dry Membranes by Mixtures of Hydroxyethyl Starch and Glucose: The Role of Vitrification. *Cryobiology, 35*(1), 20-30.

Crowe, Reid, D. S., & Crowe, J. H. (1996). Is trehalose special for preserving dry biomaterials? *Biophysical Journal, 71*(4), 2087-2093.

Cui, Z., Hsu, C.-H., & Mumper, R. J. (2003). Physical Characterization and Macrophage Cell Uptake of Mannan-Coated Nanoparticles. *Drug Development and Industrial Pharmacy, 29*(6), 689-700.

Damiati, S., Kompella, U. B., Damiati, S. A., & Kodzius, R. (2018). Microfluidic Devices for Drug Delivery Systems and Drug Screening. *Genes, 9*(2), 103.

Daniels, T., Delgado, T., Rodriguez, J., Helguera, G., & Penichet, M. (2006). The transferrin receptor part I: Biology and targeting with cytotoxic antibodies for the treatment of cancer. *Clinical Immunology, 121*(2), 144-158.

Dasari, S., & Tchounwou, P. B. (2014). Cisplatin in cancer therapy: molecular mechanisms of action. *European journal of pharmacology, 0*, 364-378.

Davies, M. S., Berners-Price, S. J., & Hambley, T. W. (2000). Slowing of cisplatin aquation in the presence of DNA but not in the presence of phosphate: improved understanding of sequence selectivity and the roles of monoaquated and diaquated species in the binding of cisplatin to DNA. *Inorg Chem, 39*(25), 5603-5613.

de Meyer, F., & Smit, B. (2009). Effect of cholesterol on the structure of a phospholipid bilayer. *Proceedings of the National Academy of Sciences, 106*(10), 3654.

Dela Cruz, C., Tanoue, L., & Matthay, R. (2011). Lung Cancer: Epidemiology, Etiology, and Prevention. *Clinics in Chest Medicine, 32*(4), 605-644.

Depaz, R. A., Pansare, S., & Patel, S. M. (2016). Freeze-Drying Above the Glass Transition Temperature in Amorphous Protein Formulations While Maintaining Product Quality and Improving Process Efficiency. *Journal of Pharmaceutical Sciences, 105*(1), 40-49.

Derycke, A., Kamuhabwa, A., Gijsens, A., Roskams, T., De Vos, D., Kasran, A., . . . de Witte, P. (2004). Transferrin-Conjugated Liposome Targeting of Photosensitizer AlPcS4 to Rat Bladder Carcinoma Cells. *Journal of the National Cancer Institute, 96*(21), 1620-1630.

Desai, S., Esho, T., & Kaware, R. (2010). Understanding microdroplet evaporation towards scalable Micro/Nano fabrication. *IIE Annual Conference Proceedings*, 1-6.

Deshpande, P., Biswas, S., & Torchilin, V. (2013). Current trends in the use of liposomes for tumor targeting. *Nanomedicine, 8*(9), 1509-1528.

Desoize, B., & Madoulet, C. (2002). Particular aspects of platinum compounds used at present in cancer treatment. *Critical Reviews in Oncology/Hematology, 42*(3), 317-325.

Dicko, A., Tardi, P., Xie, X., & Mayer, L. (2007). Role of copper gluconate/triethanolamine in irinotecan encapsulation inside the liposomes. *International Journal of Pharmaceutics, 337*(1-2), 219-228.

Dimov, N., Kastner, E., Hussain, M., Perrie, Y., & Szita, N. (2017). Formation and purification of tailored liposomes for drug delivery using a module-based micro continuous-flow system. *Scientific reports, 7*(1), 12045.

Domazou, A. S., & Luigi Luisi, P. (2002). SIZE DISTRIBUTION OF SPONTANEOUSLY FORMED LIPOSOMES BY THE ALCOHOL INJECTION METHOD. *Journal of Liposome Research, 12*(3), 205-220.

Du Plessis, J., Ramachandran, C., Weiner, N., & Müller, D. (1996). The influence of lipid composition and lamellarity of liposomes on the physical stability of liposomes upon storage. *International Journal of Pharmaceutics, 127*(2), 273-278.

Eastman, A. (2016). Improving anticancer drug development begins with cell culture: misinformation perpetrated by the misuse of cytotoxicity assays. *Oncotarget, 8*(5), 8854-8866.

Edwards, K., & Baeumner, A. (2006). Analysis of liposomes. *Talanta, 68*(5), 1432-1441.

El-Nesr, O. H., Yahiya, S. A., & El-Gazayerly, O. N. (2010). Effect of formulation design and freeze-drying on properties of fluconazole multilamellar liposomes. *Saudi pharmaceutical journal : SPJ : the official publication of the Saudi Pharmaceutical Society, 18*(4), 217-224.

Elbein, A. D., & Mitchell, M. (1973). Levels of glycogen and trehalose in Mycobacterium smegmatis and the purification and properties of the glycogen synthetase. *Journal of bacteriology, 113*(2), 863-873.

Ely, L., Roa, W., Finlay, W., & Löbenberg, R. (2007). Effervescent dry powder for respiratory drug delivery. *European Journal of Pharmaceutics and Biopharmaceutics, 65*(3), 346-353.

Engblom, J., Miezis, Y., Nylander, T., Razumas, V., & Larsson, K. (2001). *On the swelling of monoolein liquid-crystalline aqueous phases in the presence of distearoylphosphatidylglycerol*, Berlin, Heidelberg.

Engels, E. (2008). Inflammation in the development of lung cancer: epidemiological evidence. *Expert Review of Anticancer Therapy, 8*(4), 605-615.

Eriksen, M., Mackay, J., & Ross, H. (2012). *The Tobacco Atlas*. Atlanta: American Cancer Society.

Essa, E. (2010). Effect of formulation and processing variables on the particle size of sorbitan monopalmitate niosomes. *Asian Journal of Pharmaceutics, 4*(4), 227.

Evans, W. K., Shepherd, F. A., Feld, R., Osoba, D., Dang, P., & Deboer, G. (1985). VP-16 and cisplatin as first-line therapy for small-cell lung cancer. *Journal of Clinical Oncology, 3*(11), 1471-1477.

Eze, M. O. (1991). Phase transitions in phospholipid bilayers: Lateral phase separations play vital roles in biomembranes. *Biochemical Education, 19*(4), 204-208.

Fairbairn, D., & Passey, R. F. (1957). Occurrence and distribution of trehalose and glycogen in the eggs and tissues of Ascaris lumbricoides. *Experimental Parasitology, 6*(6), 566-574.

Ferlay, J., Soerjomataram, I., Ervik, M., Dikshit, R., Eser, S., Mathers, C., . . . Bray, F. (2013). Cancer Incidence and Mortality Worldwide: IARC CancerBase No. 11 [Internet]. *GLOBOCAN 2012 v1.0*. Retrieved from http://globocan.iarc.fr

Fichtner, I., Reszka, R., Arndt, D., Zeisig, R., Gabizon, A., Glück, R., . . . Zarif, L. (2003). Speaker Abstracts. *Journal of Liposome Research, 13*(1), 97-110.

Fischer, K., & Schmidt, M. (2016). Pitfalls and novel applications of particle sizing by dynamic light scattering. *Biomaterials, 98*, 79-91.

Flynn, G., Shah, Y., Prakongpan, S., Kwan, K., Higuchi, W., & Hofmann, A. (1979). Cholesterol Solubility in Organic Solvents. *Journal of Pharmaceutical Sciences, 68*(9), 1090-1097.

Foldbjerg, R., Dang, D. A., & Autrup, H. (2011). Cytotoxicity and genotoxicity of silver nanoparticles in the human lung cancer cell line, A549. *Arch Toxicol, 85*(7), 743-750.

Fonte, P., Soares, S., Costa, A., Andrade, J. C., Seabra, V., Reis, S., & Sarmento, B. (2012). Effect of cryoprotectants on the porosity and stability of insulin-loaded PLGA nanoparticles after freeze-drying. *Biomatter, 2*(4), 329-339.

Foo, J. J., Chan, V., & Liu, K. K. (2003). Contact deformation of liposome in the presence of osmosis. *Ann Biomed Eng, 31*(10), 1279-1286.

Franzé, S., Selmin, F., Samaritani, E., Minghetti, P., & Cilurzo, F. (2018). Lyophilization of Liposomal Formulations: Still Necessary, Still Challenging. *Pharmaceutics, 10*(3), 139.

Frischknecht, A. L., & Frink, L. J. D. (2006). Alcohols Reduce Lateral Membrane Pressures: Predictions from Molecular Theory. *Biophysical Journal, 91*(11), 4081-4090.

Fröhlich, E. (2012). The role of surface charge in cellular uptake and cytotoxicity of medical nanoparticles. *International Journal of Nanomedicine, 7*, 5577-5591.

Gabizon, A., Horowitz, A., Goren, D., Tzemach, D., Mandelbaum-Shavit, F., Qazen, M., & Zalipsky, S. (1999). Targeting folate receptor with folate linked to extremities of poly(ethylene glycol)-grafted liposomes: In vitro studies. *Bioconjugate Chemistry, 10*(2), 289-298.

Gabizon, A., Horowitz, A., Goren, D., Tzemach, D., Shmeeda, H., & Zalipsky, S. (2003). In Vivo Fate of Folate-Targeted Polyethylene-Glycol Liposomes in Tumor-Bearing Mice. *Clinical Cancer Research, 9*, 6551-6559.

Gaspar, M., Radomska, A., Gobbo, O., Bakowsky, U., Radomski, M., & Ehrhardt, C. (2012). Targeted Delivery of Transferrin-Conjugated Liposomes to an Orthotopic Model of Lung Cancer in Nude Rats. *Journal of Aerosol Medicine and Pulmonary Drug Delivery, 25*, 1-9.

Geiger, T., Muller, M., Dean, N. M., & Fabbro, D. (1998). Antitumor activity of a PKC-alpha antisense oligonucleotide in combination with standard chemotherapeutic agents against various human tumors transplanted into nude mice. *Anticancer Drug Des, 13*(1), 35-45.

Giard, D. J., Aaronson, S. A., Todaro, G. J., Arnstein, P., Kersey, J. H., Dosik, H., & Parks, W. P. (1973). In Vitro Cultivation of Human Tumors: Establishment of Cell Lines Derived From a Series of Solid Tumors2. *JNCI: Journal of the National Cancer Institute, 51*(5), 1417-1423.

Glavas-Dodov, M., Fredro-Kumbaradzi, E., Goracinova, K., Simonoska, M., Calis, S., Trajkovic-Jolevska, S., & Hincal, A. A. (2005). The effects of lyophilization on the stability of liposomes containing 5-FU. *International Journal of Pharmaceutics, 291*(1), 79-86.

Goldstraw, P., Ball, D., Jett, J., Le Chevalier, T., Lim, E., Nicholson, A., & Shepherd, F. (2011). Non-small-cell lung cancer. *The Lancet, 378*(9804), 1727-1740.

Grenha, A., Seijo, B., & Remuñán-López, C. (2005). Microencapsulated chitosan nanoparticles for lung protein delivery. *European Journal of Pharmaceutical Sciences, 25*(4-5), 427-437.

Grit, M., Zuidam, N. J., Underberg, W. J. M., & Crommelin, D. J. A. (1993). Hydrolysis of Partially Saturated Egg Phosphatidylcholine in Aqueous Liposome Dispersions and the Effect of Cholesterol Incorporation on Hydrolysis Kinetics. *Journal of Pharmacy and Pharmacology, 45*(6), 490-495.

Haines, T. H., Li, W., Green, M., & Cummins, H. Z. (1987). The elasticity of uniform, unilamellar vesicles of acidic phospholipids during osmotic swelling is dominated by the ionic strength of the media. *Biochemistry, 26*(17), 5439-5447.

Haley, B., & Frenkel, E. (2008). Nanoparticles for drug delivery in cancer treatment. *The Potential of Nanotechnology in Urologic Oncology, 26*(1), 57-64.

Hammerman, P. S., Lawrence, M. S., Voet, D., Jing, R., Cibulskis, K., Sivachenko, A., . . . Disease working, g. (2012). Comprehensive genomic characterization of squamous cell lung cancers. *Nature, 489*(7417), 519-525.

Hanna, N., Bunn Jr, P. A., Langer, C., Einhorn, L., Guthrie Jr, T., Beck, T., . . . Morrison, M. (2006). Randomized phase III trial comparing irinotecan/cisplatin with etoposide/cisplatin in patients with previously untreated extensive-stage disease small-cell lung cancer. *Journal of Clinical Oncology, 24*(13), 2038-2043.

Hansen, J., & Bross, P. (2010). A cellular viability assay to monitor drug toxicity. *Methods Mol Biol, 648*, 303-311.

Hantz, E., Cao, A., Escaig, J., & Taillandier, E. (1986). The osmotic response of large unilamellar vesicles studied by quasielastic light scattering. *Biochim Biophys Acta, 862*(2), 379-386.

Harrigan, P. R., Madden, T. D., & Cullis, P. R. (1990). Protection of liposomes during dehydration or freezing. *Chemistry and Physics of Lipids, 52*(2), 139-149.

Hasan, A. S., Socha, M., Lamprecht, A., Ghazouani, F. E., Sapin, A., Hoffman, M., . . . Ubrich, N. (2007). Effect of the microencapsulation of nanoparticles on the reduction of burst release. *International Journal of Pharmaceutics, 344*(1), 53-61.

Heeremans, J. L. M., Gerrttsen, H. R., Meusen, S. P., Mijnheer, F. W., Gangaram Panday, R. S., Prevost, R., . . . Crommelin, D. J. A. (1995). The Preparation of Tissue-Type Plasminogen Activator (t-PA) Containing Liposomes: Entrapment Efficiency and Ultracentrifugation Damage. *Journal of Drug Targeting, 3*(4), 301-310.

Hua. (2014). Comparison of in vitro dialysis release methods of loperamide-encapsulated liposomal gel for topical drug delivery. *International Journal of Nanomedicine, 9*, 735-744.

Hua, Li, B.-G., Liu, Z.-J., & Sun, D.-W. (2003). Freeze-Drying of Liposomes with Cryoprotectants and Its Effect on Retention Rate of Encapsulated Ftorafur and Vitamin A. *Drying Technology, 21*(8), 1491-1505.

Huang, H., Zhao, G., Zhang, Y., Xu, J., Toth, T. L., & He, X. (2017). Predehydration and Ice Seeding in the Presence of Trehalose Enable Cell Cryopreservation. *ACS Biomaterials Science & Engineering, 3*(8), 1758-1768.

Huang, X., Li, M., Bruni, R., Messa, P., & Cellesi, F. (2017). The effect of thermosensitive liposomal formulations on loading and release of high molecular weight biomolecules. *International Journal of Pharmaceutics, 524*(1), 279-289.

Hubeek, I., Peters, G. J., Broekhuizen, R., Zwaan, C. M., Kaaijk, P., van Wering, E. S., . . . Kaspers, G. J. (2006). In vitro sensitivity and cross-resistance to deoxynucleoside analogs in childhood acute leukemia. *Haematologica, 91*(1), 17-23.

Hwang, & Chang. (2004). The Use of Cross-Flow Microfiltration in Purification of Liposomes. *Separation Science and Technology, 39*(11), 2557-2576.

Hwang, Lee, Hua, & Fang. (2007). Cisplatin encapsulated in phosphatidylethanolamine liposomes enhances the in vitro cytotoxicity and in vivo intratumor drug accumulation against melanomas. *J Dermatol Sci, 46*(1), 11-20.

Ingvarsson, P. T., Yang, M., Nielsen, H. M., Rantanen, J., & Foged, C. (2011). Stabilization of liposomes during drying. *Expert opinion on drug delivery, 8*(3), 375-388.

Innocenti, F., Schilsky, R. L., Ramírez, J., Janisch, L., Undevia, S., House, L. K., . . . Ratain, M. J. (2014). Dose-Finding and Pharmacokinetic Study to Optimize the Dosing of Irinotecan According to the UGT1A1 Genotype of Patients With Cancer. *Journal of Clinical Oncology, 32*(22), 2328-2334.

Institute for Public Health. (2011). *Report of the Global Adult Tobacco Survey (GATS) Malaysia*. Retrieved from Kuala Lumpur:

Iwasaki, Y., Nagata, K., Nakanishi, M., Natuhara, A., Kubota, Y., Ueda, M., . . . Hara, H. (2005). Double-cycle, high-dose ifosfamide, carboplatin, and etoposide followed by peripheral blood stem-cell transplantation for small cell lung cancer. *Chest, 128*(4), 2268-2273.

Jahn, A., Stavis, S., Hong, J., Vreeland, W., DeVoe, D., & Gaitan, M. (2010). Microfluidic Mixing and the Formation of Nanoscale Lipid Vesicles. *ACS Nano, 4*(4), 2077-2087.

Jahn, A., Vreeland, W., DeVoe, D., Locascio, L., & Gaitan, M. (2007). Microfluidic Directed Formation of Liposomes of Controlled Size. *Langmuir, 23*(11), 6289-6293.

Jahn, A., Vreeland, W., Gaitan, M., & Locascio, L. (2004). Controlled Vesicle Self-Assembly in Microfluidic Channels with Hydrodynamic Focusing. *Journal of the American Chemical Society, 126*(9), 2674-2675.

Järvå, M., Phan, T. K., Lay, F. T., Caria, S., Kvansakul, M., & Hulett, M. D. (2018). Human β-defensin 2 kills Candida albicans through phosphatidylinositol 4,5-bisphosphate–mediated membrane permeabilization. *Science Advances, 4*(7).

Jemal, A., Bray, F., Center, M., Ferlay, J., Ward, E., & Forman, D. (2011). Global cancer statistics. *CA: A Cancer Journal for Clinicians, 61*(2), 69-90.

Jiang, J., Liang, X., Zhou, X., Huang, L., Huang, R., Chu, Z., & Zhan, Q. (2010). A Meta-Analysis of Randomized Controlled Trials Comparing Irinotecan/Platinum with Etoposide/Platinum in Patients with Previously Untreated Extensive-Stage Small Cell Lung Cancer. *Journal of Thoracic Oncology, 5*(6), 867-873.

Jimah, J. R., Schlesinger, P. H., & Tolia, N. H. (2017). Liposome Disruption Assay to Examine Lytic Properties of Biomolecules. *Bio-protocol, 7*(15).

Jin, L., Engelhart, A. E., Adamala, K. P., & Szostak, J. W. (2018). Preparation, Purification, and Use of Fatty Acid-containing Liposomes. *Journal of Visualized Experiments : JoVE*(132), 57324.

Joseph, E., & Singhvi, G. (2019). Chapter 4 - Multifunctional nanocrystals for cancer therapy: a potential nanocarrier. In A. M. Grumezescu (Ed.), *Nanomaterials for Drug Delivery and Therapy* (pp. 91-116): William Andrew Publishing.

Junior, A., Vieira, F., De Melo, V., Lopes, M., Silveira, J., Ramaldes, G., . . . Oliveira, M. (2007). Preparation and cytotoxicity of cisplatin-containing liposomes. *Brazilian Journal of Medical and Biological Research, 40*(8), 1149-1157.

Kano, Y., Suzuki, K., Akutsu, M., Suda, K., Inoue, Y., Yoshida, M., . . . Miura, Y. (1992). Effects of CPT-11 in combination with other anti-cancer agents in culture. *Int J Cancer, 50*(4), 604-610.

Karbownik, A., Szałek, E., Urjasz, H., Głęboka, A., Mierzwa, E., & Grześkowiak, E. (2012). The physical and chemical stability of cisplatin (Teva) in concentrate and diluted in sodium chloride 0.9%. *Contemporary Oncology, 16*(5), 435-439.

Kastner, E., Kaur, R., Lowry, D., Moghaddam, B., Wilkinson, A., & Perrie, Y. (2014). High-throughput manufacturing of size-tuned liposomes by a new microfluidics method using enhanced statistical tools for characterization. *International Journal of Pharmaceutics, 477*(1-2), 361-368.

Kawashima, Y., Serigano, T., Hino, T., Yamamoto, H., & Takeuchi, H. (1998). A New Powder Design Method to Improve Inhalation Efficiency of Pranlukast Hydrate Dry Powder Aerosols by Surface Modification with Hydroxypropylmethylcellulose Phthalate Nanospheres. *Pharmaceutical research, 15*(11), 1748-1752.

Khan, I., Elhissi, A., Shah, M., Alhnan, M. A., & Ahmed, W. (2013). 9 - Liposome-based carrier systems and devices used for pulmonary drug delivery. In J. P. Davim (Ed.), *Biomaterials and Medical Tribology* (pp. 395-443): Woodhead Publishing.

Khoshneviszadeh, R., Fazly, B. B. S., Housaindokht, M. R., Ebrahim, H. A., & Rajabi, O. (2016). A Comparison of Explanation Methods of Encapsulation Efficacy of Hydroquinone in a Liposomal System.

Kim, Keam, B., Kim, T.-M., Kim, H.-G., Kim, J.-S., Lee, S. S., . . . Heo, D. S. (2017). Phase II Study of Irinotecan and Cisplatin Combination Chemotherapy in Metastatic, Unresectable Esophageal Cancer. *Cancer Research and Treatment : Official Journal of Korean Cancer Association, 49*(2), 416-422.

Kim, & Yoon, C. J. (1998). Roller pump induced tubing wear of polyvinylchloride and silicone rubber tubing: phase contrast and scanning electron microscopic studies. *Artif Organs, 22*(10), 892-897.

Kobayashi, T., Ishida, T., Okada, Y., & Ise, S. (2007). Effect of transferrin receptor-targeted liposomal doxorubicin in P-glycoprotein-mediated drug resistant tumor cells. *International Journal of Pharmaceutics, 329*, 94-102.

Komatsu, H., & Okada, S. (1997). Effects of ethanol on permeability of phosphatidylcholine/cholesterol mixed liposomal membranes. *Chemistry and Physics of Lipids, 85*(1), 67-74.

Konan, Y. N., Gurny, R., & Allémann, E. (2002). Preparation and characterization of sterile and freeze-dried sub-200 nm nanoparticles. *International Journal of Pharmaceutics, 233*(1), 239-252.

Kosmas, C., Tsavaris, N. B., Malamos, N. A., Vadiaka, M., & Koufos, C. (2001). Phase II study of paclitaxel, ifosfamide, and cisplatin as second-line treatment in relapsed small-cell lung cancer. *J Clin Oncol, 19*(1), 119-126.

Kudoh, S., Takada, M., Masuda, N., Nakagawa, K., Itoh, K., Kusunoki, Y., . . . Fukuoka, M. (1993). Enhanced Antitumor Efficacy of a Combination of CPT-11, a New Derivative of Camptothecin, and Cisplatin against Human Lung Tumor Xenografts. *Japanese Journal of Cancer Research, 84*(2), 203-207.

Kulma, M., Kacprzyk-Stokowiec, A., Kwiatkowska, K., Traczyk, G., Sobota, A., & Dadlez, M. (2017). R468A mutation in perfringolysin O destabilizes toxin structure and induces membrane fusion. *Biochimica et Biophysica Acta (BBA) - Biomembranes, 1859*(6), 1075-1088.

Kurup, A., & Hanna, N. (2004). Treatment of small cell lung cancer. *Critical Reviews in Oncology/Hematology, 52*(2), 117-126.

Labiris, N., & Dolovich, M. (2003a). Pulmonary drug delivery. Part I: Physiological factors affecting therapeutic effectiveness of aerosolized medications. *British Journal of Clinical Pharmacology*, *56*(6), 588-599.

Labiris, N., & Dolovich, M. (2003b). Pulmonary drug delivery. Part II: The role of inhalant delivery devices and drug formulations in therapeutic effectiveness of aerosolized medications. *British Journal of Clinical Pharmacology, 56*(6), 600-612.

LC Laboratories. (2018, June 1). Safety Data Sheet Irinotecan.

Leamon, C., & Low, P. (1992). Cytotoxicity of momordin–folate conjugates in cultured human cells. *The Journal of Biological Chemistry, 267*, 24966-24971.

Lee, R., & Low, P. (1994). Delivery of Liposomes into Cultured KB Cells via Folate. *The Journal of Biological Chemistry, 269*, 3198-3204.

Lehtonen, J. Y., & Kinnunen, P. K. (1994). Changes in the lipid dynamics of liposomal membranes induced by poly(ethylene glycol): free volume alterations revealed by inter- and intramolecular excimer-forming phospholipid analogs. *Biophysical Journal*, *66*(6), 1981-1990.

Li, X., Ding, L., Xu, Y., Wang, Y., & Ping, Q. (2009). Targeted delivery of doxorubicin using stealth liposomes modified with transferrin. *International Journal of Pharmaceutics, 373*, 116-123.

Liang, X., Mao, G., & Ng, K. (2004). Mechanical properties and stability measurement of cholesterol-containing liposome on mica by atomic force microscopy. *Journal of Colloid and Interface Science, 278*(1), 53-62.

Liu, Z.-L., Wang, B., Liu, J.-Z., & Liu, W.-W. (2018). Irinotecan plus cisplatin compared with etoposide plus cisplatin in patients with previously untreated extensive-stage small cell lung cancer: A meta-analysis. *Journal of Cancer Research and Therapeutics, 14*(12), 1076-1083.

MacGillivray, R., Moore, S., Chen, J., Anderson, B., Baker, H., Luo, Y., . . . Baker, E. (1998). Two high-resolution crystal structures of the recombinant N-lobe of human transferrin reveal a structural change implicated in iron release. *Biochemistry, 37*, 7919-7928.

Martín, M. C., Díaz, L. A., Manzanal, M. B., & Hardisson, C. (1986). Role of trehalose in the spores of Streptomyces. *FEMS microbiology letters, 35*(1), 49-54.

Mascaux, C., Paesmans, M., Berghmans, T., Branle, F., Lafitte, J. J., Lemaître, F., . . . Sculier, J. P. (2000). A systematic review of the role of etoposide and cisplatin in the chemotherapy of small cell lung cancer with methodology assessment and meta-analysis. *Lung Cancer, 30*(1), 23-36.

Masumoto, N., Nakano, S., Esaki, T., Fujishima, H., Tatsumoto, T., & Niho, Y. (1995). Inhibition of cis-diamminedichloroplatinum (II)-induced DNA interstrand cross-link removal by 7-ethyl-10-hydroxy-camptothecin in HST-1 human squamous-carcinoma cells. *Int J Cancer, 62*(1), 70-75.

Moh'd Atrouse, O. (2002). The effects of liposome composition and temperature on the stability of liposomes and the interaction of liposomes with human neutrophils. *Pakistan Journal of Biological Sciences, 5*(9), 948-951.

Mohamed, F., & van der Walle, C. (2006). PLGA microcapsules with novel dimpled surfaces. *International Journal of Pharmaceutics, 311*, 97-107.

Morton, S., Lee, M., J Deng, Z., Dreaden, E., Siouve, E., Shopsowitz, K., . . . T Hammond, P. (2014). *A Nanoparticle-Based Combination Chemotherapy Delivery System for Enhanced Tumor Killing by Dynamic Rewiring of Signaling Pathways* (Vol. 7).

Mura, S., Bui, D., Couvreur, P., & Nicolas, J. (2015). Lipid prodrug nanocarriers in cancer therapy. *Journal of Controlled Release*.

Nayar, R., Hope, M. J., & Cullis, P. R. (1989). Generation of large unilamellar vesicles from long-chain saturated phosphatidylcholines by extrusion technique. *Biochimica et Biophysica Acta (BBA) - Biomembranes, 986*(2), 200-206.

Nilsson, M., Trägårdh, G., & Östergren, K. (2008). The influence of pH, salt and temperature on nanofiltration performance. *Journal of Membrane Science, 312*(1), 97-106.

Nounou, M. M., El-Khordagui, L., Khalafallah, N., Khalil, S., & Rasheed, K. (2005). INFLUENCE OF DIFFERENT SUGAR CRYOPROTECTANTS ON THE STABILITY AND PHYSICO-CHEMICAL CHARACTERISTICS OF FREEZE-DRIED 5-FLUOROURACIL PLURILAMELLAR VESICLES. *DARU JOURNAL OF PHARMACEUTICAL SCIENCE*, *13*(4), 133-142.

Nugent, P. (2011). 18 - Rotational Molding. In M. Kutz (Ed.), *Applied Plastics Engineering Handbook* (pp. 311-332). Oxford: William Andrew Publishing.

O'Dowd, E., McKeever, T., Baldwin, D., Anwar, S., Powell, H., & Hubbard, R. (2014). *Risk Factors For Early Death From Lung Cancer*. Paper presented at the American Thoracic Society International Conference Abstracts.

Obeid, M. A., Gebril, A. M., Tate, R. J., Mullen, A. B., & Ferro, V. A. (2017). Comparison of the physical characteristics of monodisperse non-ionic surfactant vesicles (NISV) prepared using different manufacturing methods. *International Journal of Pharmaceutics, 521*(1), 54-60.

Obeid, M. A., Khadra, I., Mullen, A. B., Tate, R. J., & Ferro, V. A. (2017). The effects of hydration media on the characteristics of non-ionic surfactant vesicles (NISV) prepared by microfluidics. *International Journal of Pharmaceutics, 516*(1), 52-60.

Ohtake, S., Schebor, C., & de Pablo, J. J. (2006). Effects of trehalose on the phase behavior of DPPC–cholesterol unilamellar vesicles. *Biochimica et Biophysica Acta (BBA) - Biomembranes, 1758*(1), 65-73.

Ohtake, S., Schebor, C., Palecek, S. P., & de Pablo, J. J. (2005). Phase behavior of freeze-dried phospholipid–cholesterol mixtures stabilized with trehalose. *Biochimica et Biophysica Acta (BBA) - Biomembranes, 1713*(1), 57-64.

Omary, M., Trowbridge, I., & Minowada, J. (1980). Human cell surface glycoprotein with unusual properties. *Nature, 286*, 888-891.

Ong, S. G. M., Chitneni, M., Lee, K. S., Ming, L. C., & Yuen, K. H. (2016). Evaluation of extrusion technique for nanosizing liposomes. *Pharmaceutics, 8*(4), 36.

Ozer, A. Y., & Talsma, H. (1989). Preparation and stability of liposomes containing 5-fluorouracil. *International Journal of Pharmaceutics, 55*(2), 185-191.

Paszko, E., Vaz, G., Ehrhardt, C., & Senge, M. (2013). Transferrin conjugation does not increase the efficiency of liposomal Foscan during in vitro photodynamic therapy of oesophageal cancer. *European Journal of Pharmaceutical Sciences, 48*(1-2), 202-210.

Patel, Nail, S. L., Pikal, M. J., Geidobler, R., Winter, G., Hawe, A., . . . Rambhatla Gupta, S. (2017). Lyophilized Drug Product Cake Appearance: What Is Acceptable? *Journal of Pharmaceutical Sciences, 106*(7), 1706-1721.

Patel, Rathi, A., Mongayt, D., & Torchilin, V. P. (2011). Reversal of multidrug resistance by co-delivery of tariquidar (XR9576) and paclitaxel using long-circulating liposomes. *International Journal of Pharmaceutics, 416*(1), 296-299.

Patra, M., Salonen, E., Terama, E., Vattulainen, I., Faller, R., Lee, B. W., . . . Karttunen, M. (2006). Under the Influence of Alcohol: The Effect of Ethanol and Methanol on Lipid Bilayers. *Biophysical Journal, 90*(4), 1121-1135.

Pereira, C. S., Lins, R. D., Chandrasekhar, I., Freitas, L. C. G., & Hünenberger, P. H. (2004). Interaction of the disaccharide trehalose with a phospholipid bilayer: a molecular dynamics study. *Biophysical Journal, 86*(4), 2273-2285.

Petushkov, A., Intra, J., Graham, J. B., Larsen, S. C., & Salem, A. K. (2009). Effect of Crystal Size and Surface Functionalization on the Cytotoxicity of Silicalite-1 Nanoparticles. *Chemical Research in Toxicology, 22*(7), 1359-1368.

Pharmaceutical Service Division Ministry of Health Malaysia (Producer). (2015, May 20). Consumer Price Guide. *Official Portal of Pharmaceutical Service Division, Ministry of Health Malaysia*. Retrieved from http://www.pharmacy.gov.my/v2/ms/apps/drug-price

Pharmaceutical Services Division and Clinical Research Centre Ministry of Health Malaysia. (2014). *Malaysian Statistics on Medicine 2009 & 2010*. Retrieved from Kuala Lumpur:

Pignon, J.-P., Tribodet, H., Scagliotti, G. V., Douillard, J.-Y., Shepherd, F. A., Stephens, R. J., . . . Chevalier, T. L. (2008). Lung Adjuvant Cisplatin Evaluation: A Pooled Analysis by the LACE Collaborative Group. *Journal of Clinical Oncology, 26*(21), 3552-3559.

Pikal, M. J., & Shah, S. (1990). The collapse temperature in freeze drying: Dependence on measurement methodology and rate of water removal from the glassy phase. *International Journal of Pharmaceutics, 62*(2), 165-186.

Ponka, P., & Lok, C. (1999). The transferrin receptor: role in health and disease. *International Journal of Biochemistry & Cell Biology, 31*, 1111-1137.

Popova, A. V., & Hincha, D. K. (2007). Effects of cholesterol on dry bilayers: interactions between phosphatidylcholine unsaturation and glycolipid or free sugar. *Biophysical Journal, 93*(4), 1204-1214.

Ramachandran, S., Quist, A. P., Kumar, S., & Lal, R. (2006). Cisplatin Nanoliposomes for Cancer Therapy: AFM and Fluorescence Imaging of Cisplatin Encapsulation, Stability, Cellular Uptake, and Toxicity. *Langmuir, 22*(19), 8156-8162.

Ramalingam, S., Owonikoko, T., & Khuri, F. (2011). Lung cancer: New biological insights and recent therapeutic advances. *CA: A Cancer Journal for Clinicians, 61*(2), 91-112.

Redondo-Morata, L., Giannotti, M. I., & Sanz, F. (2012). Influence of Cholesterol on the Phase Transition of Lipid Bilayers: A Temperature-Controlled Force Spectroscopy Study. *Langmuir*, *28*(35), 12851-12860.

Robson, A.-L., Dastoor, P. C., Flynn, J., Palmer, W., Martin, A., Smith, D. W., . . . Hua, S. (2018). Advantages and Limitations of Current Imaging Techniques for Characterizing Liposome Morphology. *Frontiers in pharmacology, 9*, 80-80.

Rodrigues, J. P., Paraguassú-Braga, F. H., Carvalho, L., Abdelhay, E., Bouzas, L. F., & Porto, L. C. (2008). Evaluation of trehalose and sucrose as cryoprotectants for hematopoietic stem cells of umbilical cord blood. *Cryobiology, 56*(2), 144-151.

Rothenberg, M. L. (2001). Irinotecan (CPT-11): Recent Developments and Future Directions–Colorectal Cancer and Beyond. *The Oncologist, 6*(1), 66-80.

Rougier, P., Van Cutsem, E., Bajetta, E., Niederle, N., Possinger, K., Labianca, R., . . . Jacques, C. (1998). Randomised trial of irinotecan versus fluorouracil by continuous infusion after fluorouracil failure in patients with metastatic colorectal cancer. *The Lancet, 352*(9138), 1407-1412.

Ruozi, B., Belletti, D., Tombesi, A., Tosi, G., Bondioli, L., Forni, F., & Vandelli, M. A. (2011). AFM, ESEM, TEM, and CLSM in liposomal characterization: a comparative study. *International Journal of Nanomedicine, 6*, 557-563.

Ruozi, B., Tosi, G., Forni, F., Fresta, M., & Vandelli, M. (2005). Atomic force microscopy and photon correlation spectroscopy: Two techniques for rapid characterization of liposomes. *European Journal of Pharmaceutical Sciences, 25*(1), 81-89.

Ruozi, B., Tosi, G., Leo, E., & Vandelli, M. (2007). Application of atomic force microscopy to characterize liposomes as drug and gene carriers. *Talanta, 73*(1), 12-22.

Sadhukha, T., & Prabha, S. (2014). Encapsulation in nanoparticles improves anti-cancer efficacy of carboplatin. *AAPS PharmSciTech, 15*(4), 1029-1038.

Saliba, F., Hagipantelli, R., Misset, J. L., Bastian, G., Vassal, G., Bonnay, M., . . . Cvitkovic, E. (1998). Pathophysiology and therapy of irinotecan-induced delayed-onset diarrhea in patients with advanced colorectal cancer: a prospective assessment. *Journal of Clinical Oncology, 16*(8), 2745-2751.

Salvati, A., Pitek, A., Monopoli, M., Prapainop, K., Bombelli, F., Hristov, D., . . . Dawson, K. (2013). Transferrin-functionalized nanoparticles lose their targeting capabilities when a biomolecule corona adsorbs on the surface. *Nature Nanotechnology, 8*, 137-143.

Samad, A., Sultana, Y., & Aqil, M. (2007). Liposomal Drug Delivery Systems: An Update Review. *Current Drug Delivery, 4*(4), 297-305.

Samimi, S., Maghsoudnia, N., Eftekhari, R. B., & Dorkoosh, F. (2019). Chapter 3 - Lipid-Based Nanoparticles for Drug Delivery Systems. In S. S. Mohapatra, S. Ranjan, N. Dasgupta, R. K. Mishra, & S. Thomas (Eds.), *Characterization and Biology of Nanomaterials for Drug Delivery* (pp. 47-76): Elsevier.

Sandler, A., Gray, R., Perry, M., Brahmer, J., Schiller, J., Dowlati, A., . . . Johnson, D. (2006). Paclitaxel-carboplatin alone or with bevacizumab for non-small-cell lung cancer. *The New England Journal of Medicine, 355*(24), 2542-2550.

Sarfraz, M., Afzal, A., Yang, T., Gai, Y., Raza, S. M., Khan, M. W., . . . Xiang, G. (2018). Development of Dual Drug Loaded Nanosized Liposomal Formulation by A Reengineered Ethanolic Injection Method and Its Pre-Clinical Pharmacokinetic Studies. *Pharmaceutics, 10*(3), 151.

Scagliotti, G., Hanna, N., Fossella, F., Sugarman, K., Blatter, J., Peterson, P., . . . Shepherd, F. (2009). The differential efficacy of pemetrexed according to NSCLC histology: a review of two Phase III studies. *Oncologist, 14*(3), 253-263.

Schneider, T., Sachse, A., Leike, J., Röβling, G., Schmidtgen, M., Drechsler, M., & Brandl, M. (1996). Surface modification of continuously extruded contrast-carrying liposomes: Effect on their physical properties. *International Journal of Pharmaceutics, 132*(1), 9-21.

Schneider, T., Sachse, A., Röβling, G., & Brandl, M. (1995). Generation of contrast-carrying liposomes of defined size with a new continuous high pressure extrusion method. *International Journal of Pharmaceutics, 117*(1), 1-12.

Sen, K., Banerjee, S., & Mandal, M. (2019). Dual drug loaded liposome bearing apigenin and 5-Fluorouracil for synergistic therapeutic efficacy in colorectal cancer. *Colloids and Surfaces B: Biointerfaces, 180*, 9-22.

Sewell, G. (2010). Physical and chemical stability of cisplatin infusions in PVC containers. *European Journal of Oncology Pharmacy, 4*, 11-13.

Shah, V. M., Nguyen, D. X., Patel, P., Cote, B., Al-Fatease, A., Pham, Y., . . . Alani, A. W. G. (2019). Liposomes produced by microfluidics and extrusion: A comparison for scale-up purposes. *Nanomedicine: Nanotechnology, Biology and Medicine, 18*, 146-156.

Shaji, J., & Iyer, S. (2014). Double-loaded liposomes encapsulating Quercetin and Quercetin beta-cyclodextrin complexes: Preparation, characterization and evaluation. *Asian Journal of Pharmaceutics (AJP): Free full text articles from Asian J Pharm, 6*(3).

Sham, J., Zhang, Y., Finlay, W., Roa, W., & Loebenberg, R. (2004). Formulation and characterization of spray-dried powders containing nanoparticles for aerosol delivery to the lung. *International Journal of Pharmaceutics, 269*(2), 457-467.

Shao-Yu, C., Bing, Y., Jacobson, K., & Sulik, K. K. (1996). The membrane disordering effect of ethanol on neural crest cells in vitro and the protective role of GM1 ganglioside. *Alcohol, 13*(6), 589-595.

Siegel, R., Naishadham, D., & Jemal, A. (2013). Cancer statistics, 2013. *CA: A Cancer Journal for Clinicians, 63*(1), 11-30.

Snow, M. J. H., de Winter, D., Buckingham, R., Campbell, J., & Wagner, J. (1996). New techniques for extreme conditions: high temperature reverse osmosis and nanofiltration. *Desalination, 105*(1), 57-61.

Socaciu, C., Jessel, R., & Diehl, H. A. (2000). Competitive carotenoid and cholesterol incorporation into liposomes: effects on membrane phase transition, fluidity, polarity and anisotropy. *Chemistry and Physics of Lipids, 106*(1), 79-88.

Stayner, L., Bena, J., Sasco, A., Smith, R., Steenland, K., Kreuzer, M., & Straif, K. (2007). Lung Cancer Risk and Workplace Exposure to Environmental Tobacco Smoke. *American Journal Of Public Health, 97*(3), 545-551.

Stroock, A. D., Dertinger, S. K. W., Ajdari, A., Mezić, I., Stone, H. A., & Whitesides, G. M. (2002). Chaotic Mixer for Microchannels. *Science, 295*(5555), 647.

Sułkowski, W. W., Pentak, D., Nowak, K., & Sułkowska, A. (2005). The influence of temperature, cholesterol content and pH on liposome stability. *Journal of Molecular Structure, 744-747*, 737-747.

Sun, W. Q., Leopold, A. C., Crowe, L. M., & Crowe, J. H. (1996). Stability of dry liposomes in sugar glasses. *Biophys J, 70*(4), 1769-1776. doi:10.1016/s0006-3495(96)79740-0

Surianarayanan, R., Shivakumar, H. G., Vegesna, N. S. K. V., & Srivastava, A. (2016). Effect of sample Concentration on the Characterization of Liposomes using Dynamic light Scattering Technique. *Pharmaceutical Methods*, *7*(1), 70.

Sylvester, B., Porfire, A., Van Bockstal, P.-J., Porav, S., Achim, M., Beer, T. D., & Tomuţă, I. (2018). Formulation Optimization of Freeze-Dried Long-Circulating Liposomes and In-Line Monitoring of the Freeze-Drying Process Using an NIR Spectroscopy Tool. *Journal of Pharmaceutical Sciences, 107*(1), 139-148.

Tardi, P., Dos Santos, N., Harasym, T. O., Johnstone, S. A., Zisman, N., Tsang, A. W., . . . Mayer, L. D. (2009). Drug ratio–dependent antitumor activity of irinotecan and cisplatin combinations in vitro and in vivo. *Molecular Cancer Therapeutics, 8*(8), 2266.

Thiele, J., Steinhaus, D., Pfohl, T., & Förster, S. (2010). Preparation of Monodisperse Block Copolymer Vesicles via Flow Focusing in Microfluidics. *Langmuir, 26*(9), 6860-6863.

Thun, M., Hannan, L., Adams-Campbell, L., Boffetta, P., Buring, J., Feskanich, D., . . . Samet, J. (2008). Lung cancer occurrence in never-smokers: an analysis of 13 cohorts and 22 cancer registry studies. *PLoS Medicine, 5*(9), 1357-1371.

Tiwari, G., Tiwari, R., Sriwastawa, B., Bhati, L., Pandey, S., Pandey, P., & Bannerjee, S. K. (2012). Drug delivery systems: An updated review. *International journal of pharmaceutical investigation, 2*(1), 2-11.

Tomita, Y., Rikimaru-Kaneko, A., Hashiguchi, K., & Shirotake, S. (2011). Effect of anionic and cationic n-butylcyanoacrylate nanoparticles on NO and cytokine production in Raw264.7 cells. *Immunopharmacol Immunotoxicol, 33*(4), 730-737.

Tomoko, N., & Fumiyoshi, I. (2005). Encapsulation efficiency of water-soluble and insoluble drugs in liposomes prepared by the microencapsulation vesicle method. *International Journal of Pharmaceutics, 298*(1), 198-205.

Toro-Cordova, A., Flores-Cruz, M., Santoyo-Salazar, J., Carrillo-Nava, E., Jurado, R., Figueroa-Rodriguez, P. A., . . . Garcia-Lopez, P. (2018). Liposomes Loaded with Cisplatin and Magnetic Nanoparticles: Physicochemical Characterization, Pharmacokinetics, and In-Vitro Efficacy. *Molecules, 23*(9).

Travis, W. (2011). Pathology of Lung Cancer. *Clinics in Chest Medicine, 32*(4), 669-692.

Travis, W., Brambilla, E., Muller-Hermelink, H., & Harris, C. (2004). *World Health Organization Classification of Tumours. Pathology and Genetics of Tumours of the Lung, Pleura, Thymus and Heart*. Lyon: IARC Press.

Travis, W., Brambilla, E., Nicholson, A. G., Yatabe, Y., Austin, J. H. M., Beasley, M. B., . . . Wistuba, I. (2015). The 2015 World Health Organization Classification of Lung Tumors: Impact of Genetic, Clinical and Radiologic Advances Since the 2004 Classification. *Journal of Thoracic Oncology, 10*(9), 1243-1260.

Tsapis, N., Bennett, D., Jackson, B., Weitz, D., & Edwards, D. (2002). Trojan particles: Large porous carriers of nanoparticles for drug delivery. *Proceedings of the National Academy of Sciences of the United States of America*, *99*(19), 12001-12005.

Tsunoda, T., Tanimura, H., Hotta, T., Tani, M., Iwahashi, M., Ishimoto, K., . . . Yamaue, H. (2000). In vitro augmentation of antitumor effect in combination with CPT-11 and CDDP for human colorectal cancer. *Journal of Surgical Oncology, 73*(1), 6-11.

Uhumwangho, M., & Okor, R. (2005). Current trends in the production and biomedical applications of liposomes: a review.

Valencia, P. M., Pridgen, E. M., Perea, B., Gadde, S., Sweeney, C., Kantoff, P. W., . . . Farokhzad, O. C. (2013). Synergistic cytotoxicity of irinotecan and cisplatin in dual-drug targeted polymeric nanoparticles. *Nanomedicine (London, England), 8*(5), 687-698.

van Meerbeeck, J., Fennell, D., & De Ruysscher, D. (2011). Small-cell lung cancer. *The Lancet, 378*(9804), 1741-1755.

van Meerloo, J., Kaspers, G. J., & Cloos, J. (2011). Cell sensitivity assays: the MTT assay. *Methods Mol Biol, 731*, 237-245.

van Winden, E. C. A. (2003). Freeze-Drying of Liposomes: Theory and Practice. In *Methods in Enzymology* (Vol. 367, pp. 99-110): Academic Press.

Verschraegen, C., Gilbert, B., Loyer, E., Huaringa, A., Walsh, G., Newman, R., & Knight, V. (2004). Clinical Evaluation of the Delivery and Safety of Aerosolized Liposomal 9-Nitro-20(S)-Camptothecin in Patients with Advanced Pulmonary Malignancies. *Clinical Cancer Research, 10*, 2319-2326.

Vincourt, V., Nguyen, L., Chaumeil, J.-C., & Dumortier, G. (2010). Freeze-drying of ATP entrapped in cationic, low lipid liposomes. *Cryobiology, 60*(3), 262-270.

Wagner, A., Vorauer-Uhl, K., & Katinger, H. (2002). Liposomes produced in a pilot scale: production, purification and efficiency aspects. *European Journal of Pharmaceutics and Biopharmaceutics, 54*(2), 213-219.

Weitman, S., Lark, R., Coney, L., Fort, D., Frasca, V., & Zurawski, V. (1992). Distribution of the folate receptor GP38 in normal and malignant cell lines and tissues. *Cancer Research, 52*, 3396-3401.

Win, K., & Feng, S. (2005). Effects of particle size and surface coating on cellular uptake of polymeric nanoparticles for oral delivery of anticancer drugs. *Biomaterials, 26*(15), 2713-2722.

Wittgen, B., Kunst, P., van der Born, K., van Wijk, A., Perkins, W., Pilkiewicz, F., . . . Postmus, P. (2007). Phase I Study of Aerosolized SLIT Cisplatin in the Treatment of Patients with Carcinoma of the Lung. *Clinical Cancer Research, 13*, 2414-2421.

Wolfe, J., & Bryant, G. (1999). Freezing, Drying, and/or Vitrification of Membrane–Solute–Water Systems. *Cryobiology, 39*(2), 103-129.

Wolfram, J., Suri, K., Huang, Y., Molinaro, R., Borsoi, C., Scott, B., . . . Shen, H. (2014). Evaluation of anticancer activity of celastrol liposomes in prostate cancer cells. *Journal of microencapsulation, 31*.

World Health Organization. (1992). *The ICD-10 classification of mental and behavioural disorders: clinical descriptions and diagnostic guidelines 6th edition*. Geneva: World Health Organization.

Wyatt, G. R., & Kalf, G. F. (1957). THE CHEMISTRY OF INSECT HEMOLYMPH. *The Journal of General Physiology, 40*(6), 833.

Xu, Liu, Y., Tai, H., Zhu, J., Ding, H., & Lee, R. (2011). Synthesis of transferrin (Tf) conjugated liposomes via Staudinger ligation. *International Journal of Pharmaceutics, 404*, 205-210.

Xu, Ren, X., Chen, Y., Li, Q., Li, R., Chen, Y., & Xia, S. (2018). Irinotecan-platinum combination therapy for previously untreated extensive-stage small cell lung cancer patients: a meta-analysis. *BMC cancer, 18*(1), 808-808.

Xu, & Villalona-Calero, M. A. (2002). Irinotecan: mechanisms of tumor resistance and novel strategies for modulating its activity. *Annals of Oncology, 13*(12), 1841-1851.

Xu, Yao, M., Xu, G., Ying, J., Ma, W., Li, B., & Y, J. (2012). A physical model for the size-dependent cellular uptake of nanoparticles modified with cationic surfactants. *International Journal of Nanomedicine, 7*, 3547-3554.

Yamada, A., Taniguchi, Y., Kawano, K., Honda, T., Hattori, Y., & Maitani, Y. (2008). Design of Folate-Linked Liposomal Doxorubicin to its Antitumor Effect in Mice. *Clinical Cancer Research, 14*, 8161-8168.

Yang, J., Zeng, J., Kong, T., Wang, X., Roa, W., El-Bialy, T., . . . Chen, J. (2007). The Effect of Surface Properties of Gold Nanoparticles on Cellular Uptake *IEEE/NIH Life Science Systems and Applications Workshop*, 92-95.

Yin, X., Zhou, J., Jie, C., Xing, D., & Zhang, Y. (2004). Anticancer activity and mechanism of Scutellaria barbata extract on human lung cancer cell line A549. *Life Sciences, 75*(18), 2233-2244.

Zaru, M., Mourtas, S., Klepetsanis, P., Fadda, A. M., & Antimisiaris, S. G. (2007). Liposomes for drug delivery to the lungs by nebulization. *European Journal of Pharmaceutics and Biopharmaceutics, 67*(3), 655-666.

Zentella, R., Mascorro-Gallardo, J. O., Van Dijck, P., Folch-Mallol, J., Bonini, B., Van Vaeck, C., . . . Iturriaga, G. (1999). A Selaginella lepidophylla trehalose-6-phosphate synthase complements growth and stress-tolerance defects in a yeast tps1 mutant. *Plant physiology, 119*(4), 1473-1482.

Zhang, Xuan, T., Parmar, M., Ma, L., Ugwu, S., Ali, S., & Ahmad, I. (2004). Development and characterization of a novel liposome-based formulation of SN-38. *International Journal of Pharmaceutics, 270*(1), 93-107.

Zhang, Zhai, M., Chen, Z., Han, X., Yu, F., Li, Z., . . . Mei, X. (2017). Dual-modified liposome codelivery of doxorubicin and vincristine improve targeting and therapeutic efficacy of glioma. *Drug Delivery, 24*(1), 1045-1055.

Zhang, Z., & Yao, J. (2012). Preparation of irinotecan-loaded folate-targeted liposome for tumor targeting delivery and its antitumor activity. *AAPS PharmSciTech, 13*(3), 802-810.

Zieske, P. A., Koberda, M., Hines, J. L., Knight, C. C., Sriram, R., Raghavan, N. V., & Rabinow, B. E. (1991). Characterization of cisplatin degradation as affected by pH and light. *Am J Hosp Pharm*, *48*(7), 1500-1506.

Zook, J., & Vreeland, W. (2010). Effects of temperature, acyl chain length, and flow-rate ratio on liposome formation and size in a microfluidic hydrodynamic focusing device. *Soft Matter*(6), 1352-1360.